

Hazard Mapping of the Philippines Using LIDAR ( Phil-LiDAR 1 )

# **LiDAR Surveys and Flood Mapping of Ulot River**



University of the Philippines Training Center  
for Applied Geodesy and Photogrammetry  
Visayas State University







© University of the Philippines and Visayas State University 2017

Published by the UP Training Center for Applied Geodesy and Photogrammetry (TCAGP)  
College of Engineering  
University of the Philippines – Diliman  
Quezon City  
1101 PHILIPPINES

This research project is supported by the Department of Science and Technology (DOST) as part of its Grant-in-Aid Program and is to be cited as:

E.C. Paringit, and F.F. Morales, (Eds.). (2017), LiDAR Surveys and Flood Mapping of Ulot River. Quezon City: University of the Philippines Training Center for Applied Geodesy and Photogrammetry. 159 pp.

The text of this information may be copied and distributed for research and educational purposes with proper acknowledgement. While every care is taken to ensure the accuracy of this publication, the UP TCAGP disclaims all responsibility and all liability (including without limitation, liability in negligence) and costs which might incur as a result of the materials in this publication being inaccurate or incomplete in any way and for any reason.

For questions/queries regarding this report, contact:

**Engr. Florentino Morales, Jr.**  
Project Leader, PHIL-LiDAR 1 Program  
Visayas State University  
Baybay, Leyte, Philippines 6521  
ffmorales\_jr@yahoo.com

**Enrico C. Paringit, Dr. Eng.**  
Program Leader, DREAM Program  
University of the Philippines Diliman  
Quezon City, Philippines 1101  
E-mail: ecparingit@up.edu.ph

National Library of the Philippines  
ISBN: 978-621-430-219-2

## TABLE OF CONTENTS

<b>LIST OF TABLES</b> .....	<b>5</b>
-----------------------------	----------



<b>LIST OF FIGURES</b> .....	6
<b>LIST OF ACRONYMS AND ABBREVIATIONS</b> .....	8
<b>CHAPTER 1: OVERVIEW OF THE PROGRAM AND ULOT RIVER</b> .....	9
<b>1.1 Background of the Phil-LiDAR 1 Program</b> .....	9
<b>1.2 Overview of the Ulot River Basin</b> .....	9
<b>CHAPTER 2: LIDAR ACQUISITION IN ULOT FLOODPLAIN</b> .....	11
<b>2.1 Flight Plans</b> .....	11
<b>2.2 Ground Base Station</b> .....	12
<b>2.3 Flight Missions</b> .....	14
<b>2.4 Survey Coverage</b> .....	15
<b>CHAPTER 3: LIDAR DATA PROCESSING FOR ULOT FLOODPLAIN</b> .....	17
<b>3.1 Overview of the LiDAR Data Pre-Processing</b> .....	17
<b>3.2 Transmittal of Acquired LiDAR Data</b> .....	18
<b>3.3 Trajectory Computation</b> .....	18
<b>3.4 LiDAR Point Cloud Computation</b> .....	20
<b>3.5 LiDAR Data Quality Checking</b> .....	20
<b>3.6 LiDAR Point Cloud Classification and Rasterization</b> .....	25
<b>3.7 LiDAR Image Processing and Orthophotograph Rectification</b> .....	27
<b>3.8 DEM Editing and Hydro-Correction</b> .....	28
<b>3.9 Mosaicking of Blocks</b> .....	29
<b>3.10 Calibration and Validation of Mosaicked LiDAR Digital Elevation Model</b> .....	30
<b>3.11 Integration of Bathymetric Data into the LiDAR Digital Terrain Model</b> .....	34
<b>3.12 Feature Extraction</b> .....	35
3.12.1 Quality Checking of Digitized Features' Boundary .....	36
3.12.2 Final Quality Checking of Extracted Features .....	37
<b>CHAPTER 4: LIDAR VALIDATION SURVEY AND MEASUREMENTS IN THE ULOT RIVER BASIN</b> .....	39
<b>4.1 Summary of Activities</b> .....	39
<b>4.2 Control Survey</b> .....	41
<b>4.3 Baseline Processing</b> .....	45
<b>4.4 Network Adjustment</b> .....	46
<b>4.5 Bridge Cross-section and As-built Survey, and Water Level Marking</b> .....	48
<b>4.6 Validation Points Acquisition Survey</b> .....	53
<b>4.7 River Bathymetric Survey</b> .....	56
<b>CHAPTER 5: FLOOD MODELING AND MAPPING</b> .....	61
<b>5.1 Data Used for Hydrologic Modeling</b> .....	61
5.1.1 Hydrometry and Rating Curves .....	61
5.1.2 Precipitation .....	61
5.1.3 Rating Curves and River Outflow .....	61
<b>5.2 RIDF Station</b> .....	63
<b>5.3 HMS Model</b> .....	64
<b>5.4 Cross-section Data</b> .....	68
<b>5.5 FLO-2D Model</b> .....	69
<b>5.6 Results of HMS Calibration</b> .....	70
<b>5.7 Calculated Outflow Hydrographs and Discharge Values for Different Rainfall Return Periods</b> ...	72
5.7.1 Hydrograph Using the Rainfall Runoff Model .....	72
5.7.2 Discharge Data Using Dr. Horritts's Recommended Hydrologic Method .....	73
<b>5.8 River Analysis Model Simulation</b> .....	74
<b>5.9 Flood Hazard and Flow Depth Map</b> .....	74
<b>5.10 Inventory of Areas Exposed to Flooding</b> .....	81
<b>5.11 Flood Validation</b> .....	95
<b>REFERENCES</b> .....	98
<b>ANNEXES</b> .....	99
<b>ANNEX 1. OPTTECH Technical Specification of the Aquarius Sensor</b> .....	99
<b>Annex 2. NAMRIA Certificates of Reference Points Used in the LiDAR Survey</b> .....	100
<b>Annex 3. Baseline Processing Reports of Reference Points Used in the LiDAR Survey</b> .....	101
<b>Annex 4. The LiDAR Survey Team Composition</b> .....	102
<b>Annex 5. Data Transfer Sheet for Ulot Floodplain</b> .....	103
<b>Annex 6. Flight Logs for the Flight Missions</b> .....	104
<b>Annex 7. Flight Status Reports</b> .....	106

<b><u>Annex 8. Mission Summary Reports</u></b> .....	<b>108</b>
<b><u>Annex 9. Ulot Model Basin Parameters</u></b> .....	<b>113</b>
<b><u>Annex 10. Ulot Model Reach Parameters</u></b> .....	<b>117</b>
<b><u>Annex 11. Ulot Field Validation Points</u></b> .....	<b>119</b>

## **LIST OF TABLES**

<b><u>Table 1. Flight planning parameters for Aquarius LiDAR system</u></b> .....	<b>11</b>
<b><u>Table 2. Details of the recovered NAMRIA horizontal control point SME-3139 used as base station for the</u></b>	

<u>LiDAR acquisition</u> .....	13
<u>Table 3. Details of the recovered NAMRIA horizontal control point SE-16 used as base station for the LiDAR acquisition</u> .....	14
<u>Table 4. Ground control points used during LiDAR data acquisition</u> .....	14
<u>Table 5. Flight missions for LiDAR data acquisition nearest Ulot Floodplain</u> .....	14
<u>Table 6. Actual parameters used during LiDAR data acquisition</u> .....	14
<u>Table 7. List of municipalities and cities surveyed during LiDAR survey nearest Ulot Floodplain</u> .....	15
<u>Table 8. Self-calibration results values for Ulot flights</u> .....	20
<u>Table 9. List of LiDAR blocks for Ulot Floodplain</u> .....	21
<u>Table 10. Ulot classification results in TerraScan</u> .....	25
<u>Table 11. LiDAR block with its corresponding area</u> .....	28
<u>Table 12. Shift values of each IFSAR Block of Ulot Floodplain and the nearby LiDAR block</u> .....	29
<u>Table 13. Calibration statistical measures</u> .....	33
<u>Table 14. Validation statistical measures</u> .....	34
<u>Table 15. Building features extracted for Ulot Floodplain</u> .....	36
<u>Table 16. Total length of extracted roads for Ulot Floodplain</u> .....	37
<u>Table 17. Number of extracted water bodies for Ulot Floodplain</u> .....	37
<u>Table 18. List of reference and control points used during the survey in Ulot River (Source: NAMRIA, UP-TCAGP)</u> .....	41
<u>Table 19. Baseline processing report for Ulot River static survey</u> .....	46
<u>Table 20. Control point constraints</u> .....	46
<u>Table 21. Adjusted grid coordinates</u> .....	47
<u>Table 22. Adjusted geodetic coordinates</u> .....	48
<u>Table 23. Reference and control points used and their location (Source: NAMRIA, UP-TCAGP)</u> .....	48
<u>Table 24. RIDF values for Borongan Rain Gauge computed by PAGASA</u> .....	52
<u>Table 25. Range of calibrated values for Ulot</u> .....	63
<u>Table 26. Summary of the efficiency test of Ulot HMS Model</u> .....	71
<u>Table 27. Peak values of the Ulot HEC-HMS model outflow using the Borongan RIDF</u> .....	72
<u>Table 28. Summary of Ulot River (1) discharge generated in HEC-HMS</u> .....	73
<u>Table 29. Validation of river discharge estimates</u> .....	73
<u>Table 30. Municipalities affected in Ulot Floodplain</u> .....	73
<u>Table 31. Affected areas in Can-avid, Eastern Samar during a 5-year rainfall return period</u> .....	74
<u>Table 32. Affected areas in Can-avid, Eastern Samar during a 5-year rainfall return period</u> .....	81
<u>Table 33. Affected areas in Can-avid, Eastern Samar during a 5-year rainfall return period</u> .....	81
<u>Table 34. Affected areas in Taft, Eastern Samar during a 5-year rainfall return period</u> .....	82
<u>Table 35. Affected areas in Can-avid, Eastern Samar during a 25-year rainfall return period</u> .....	84
<u>Table 36. Affected areas in Can-avid, Eastern Samar during a 25-year rainfall return period</u> .....	86
<u>Table 37. Affected areas in Can-avid, Eastern Samar during a 25-year rainfall return period</u> .....	86
<u>Table 38. Affected areas in Taft, Eastern Samar during a 25-year rainfall return period</u> .....	87
<u>Table 39. Affected areas in Can-avid, Eastern Samar during a 100-year rainfall return period</u> .....	89
<u>Table 40. Affected areas in Can-avid, Eastern Samar during a 100-year rainfall return period</u> .....	91
<u>Table 41. Affected areas in Can-avid, Eastern Samar during a 100-year rainfall return period</u> .....	91
<u>Table 42. Affected areas in Taft, Eastern Samar during a 100-year rainfall return period</u> .....	92
<u>Table 43. Actual flood depth vs. simulated flood depth in Ulot</u> .....	97
<u>Table 44. Summary of accuracy assessment in Ulot</u> .....	97

## **LIST OF FIGURES**

<u>Figure 1. Map of the Ulot River Basin (in brown)</u> .....	10
<u>Figure 2. Flight plan and base stations used nearest Ulot Floodplain</u> .....	12
<u>Figure 3. GPS set-up over SME-3139 located along the highway in Brgy. Sto. Nino, Ulot, Eastern Samar (a) and NAMRIA reference point SME-3139 (b) as recovered by the field team</u> .....	13

Figure 4. Actual LiDAR survey coverage nearest Ulot Floodplain .....	16
Figure 5. Schematic diagram for Data Pre-Processing Component .....	17
Figure 6. Smoothed Performance Metric parameters of Ulot Flight 1560A .....	18
Figure 7. Solution Status parameters of Ulot Flight 1560A .....	19
Figure 8. Best estimated trajectory of LiDAR missions conducted over Ulot Floodplain.....	20
Figure 9. Boundary of the processed LiDAR data over Ulot Floodplain.....	21
Figure 10. Image of data overlap for Ulot Floodplain.....	22
Figure 11. Pulse density map of merged LiDAR data for Ulot Floodplain.....	23
Figure 12. Elevation difference map between flight lines for Ulot Floodplain .....	24
Figure 13. Quality checking for a Ulot flight 1560A using the Profile Tool of QT Modeler .....	24
Figure 14. Tiles for Ulot Floodplain (a) and classification results (b) in TerraScan.....	25
Figure 15. Point cloud before (a) and after (b) classification .....	26
Figure 16. The production of last return DSM (a) and DTM (b); first return DSM (c) and secondary DTM (d) in some portion near Ulot Floodplain.....	26
Figure 17. Available orthophotographs near Ulot Floodplain .....	27
Figure 18. Sample orthophotograph tiles near Ulot Floodplain .....	28
Figure 19. Portions in the DTM of nearby block—a bridge before (a) and after (b) manual editing; a paddy field before (c) and after (d) data retrieval; and a building before (a) and after (b) manual editing .....	29
Figure 20. Map of IFSAR Data for Ulot Floodplain .....	30
Figure 21. Map of Ulot Floodplain with validation survey points in green.....	32
Figure 22. Correlation plot between calibration survey points and LiDAR data .....	33
Figure 23. Correlation plot between validation survey points and IFSAR data .....	34
Figure 24. Map of Ulot Floodplain with bathymetric survey points shown in blue.....	35
Figure 25. Ulot building features extracted from Google Earth images .....	36
Figure 26. Extracted features for Ulot Floodplain .....	38
Figure 27. Extent of the bathymetric survey (in blue) in Ulot River and the LiDAR data validation survey (in red).....	40
Figure 28. Ulot River Basin control survey extent .....	42
Figure 29. GNSS receiver set-up, Trimble® SPS 882 at SMR-41, located at Bagacay Elementary School in Brgy. Bagacay, Hinabangan, Eastern Samar .....	43
Figure 30. GNSS receiver set-up, Trimble® SPS 855, at SME-18, located inside San Jose Elementary School in Brgy. San Jose, Hernani, Eastern Samar.....	43
Figure 31. GNSS receiver set-up, Trimble® SPS 855, at SE-172, located inside Nato Elementary School in Brgy. Nato, Taft, Eastern Samar .....	44
Figure 32. GNSS receiver set-up, Trimble® SPS 855, at UP_ULO-2, located at the approach of Can-Avid Bridge in Brgy. Canteros, Can-Avid, Eastern Samar .....	44
Figure 33. GNSS receiver set-up, Trimble® SPS 985, at UP-SUL, located at the approach of Sulat Bridge in Brgy. Maramara, Sulat, Eastern Samar.....	45
Figure 34. GNSS receiver set-up, Trimble® SPS 855, at UP-BOR, located at the approach of Can-Obing Bridge in Brgy. Can-Abong, Borongan City, Eastern Samar .....	45
Figure 35. Upstream/downstream side of Can-Avid Bridge .....	49
Figure 36. As-built survey of Can-Avid Bridge .....	49
Figure 37. Can-Avid bridge location map .....	50
Figure 38. Can-Avid Bridge cross-section diagram .....	51
Figure 39. Can-Avid bridge data sheet.....	52
Figure 40. Water-level markings on Can-Avid Bridge .....	53
Figure 41. Validation points acquisition survey set-up for Ulot River.....	54
Figure 42. Validation points acquisition covering the Ulot River Basin area .....	55
Figure 43. Bathymetric survey of ABSD at Ulot River using Hi-Target® echo sounder .....	56
Figure 44. Gathering of random bathymetric points along Ulot River .....	57
Figure 45. Bathymetric survey of Ulot River.....	58
Figure 46. Quality checking points gathered along Ulot River by DVBC .....	59
Figure 47. Ulot riverbed profile .....	60
Figure 48. The location map of Ulot HEC-HMS model used for calibration.....	61
Figure 49. Cross-section plot of Can-Avid Bridge .....	62
Figure 50. Rating curve at Can-Avid Bridge .....	62
Figure 51. Rainfall and outflow data at Can-Avid Bridge used for modeling .....	63
Figure 52. Location of Borongan RIDF station relative to Ulot River Basin .....	64

Figure 53. Synthetic storm generated for a 24-hour period rainfall for various return periods ..... 64

Figure 54. Soil map of Ulot River Basin ..... 65

Figure 55. Land cover map of Ulot River Basin ..... 66

Figure 56. Slope map of the Ulot River Basin ..... 67

Figure 57. Stream delineation map of the Ulot River Basin ..... 67

Figure 58. The Ulot River Basin model generated using HEC-HMS ..... 68

Figure 59. River cross-section of Ulot River generated through ArcMap HEC GeoRAS tool ..... 69

Figure 60. Screenshot of subcatchment with the computational area to be modeled in  
FLO-2D GDS Pro ..... 70

Figure 61. Outflow hydrograph of Ulot Bridge generated in HEC-HMS model compared with  
observed outflow ..... 71

Figure 62. Outflow hydrograph at Ulot Station generated using Borongan RIDF simulated in  
HEC-HMS ..... 72

Figure 63. Ulot River (1) generated discharge using 5-, 25-, and 100-year Catbalogan RIDF in  
HEC-HMS ..... 73

Figure 64. Sample output Ulot RAS Model ..... 74

Figure 65. 100-year flood hazard map for Ulot Floodplain ..... 75

Figure 66. 100-year flow depth map for Ulot Floodplain ..... 76

Figure 67. 25-year flood hazard map for Ulot Floodplain ..... 77

Figure 68. 25-year flow depth map for Ulot Floodplain ..... 78

Figure 69. 5-year flood hazard map for Ulot Floodplain ..... 79

Figure 70. 5-year flow depth map for Ulot Floodplain ..... 80

Figure 71. Affected areas in Can-avid, Eastern Samar during a 5-year rainfall return period ..... 83

Figure 72. Affected areas in Can-avid, Eastern Samar during a 5-year rainfall return period ..... 83

Figure 73. Affected areas in Can-avid, Eastern Samar during a 5-year rainfall return period ..... 84

Figure 74. Affected areas in Taft, Eastern Samar during a 5-year rainfall return period ..... 84

Figure 75. Affected areas in Can-avid, Eastern Samar during a 25-year rainfall return period ..... 88

Figure 76. Affected areas in Can-avid, Eastern Samar during a 25-year rainfall return period ..... 88

Figure 77. Affected areas in Can-avid, Eastern Samar during a 25-year rainfall return period ..... 89

Figure 78. Affected areas in Taft, Eastern Samar during a 25-year rainfall return period ..... 90

Figure 79. Affected areas in Can-avid, Eastern Samar during a 100-year rainfall return period ..... 93

Figure 80. Affected areas in Can-avid, Eastern Samar during a 100-year rainfall return period ..... 93

Figure 81. Affected areas in Can-avid, Eastern Samar during a 100-year rainfall return period ..... 94

Figure 82. Affected areas in Taft, Eastern Samar during a 100-year rainfall return period ..... 95

Figure 83. Validation points for 100-year Flood Depth Map of Ulot Floodplain ..... 96

## LIST OF ACRONYMS AND ABBREVIATIONS

AAC	Asian Aerospace Corporation	LAS	LiDAR Data Exchange File format
Ab	abutment	LC	Low Chord
ALTM	Airborne LiDAR Terrain Mapper	LGU	local government unit

ARG	automatic rain gauge	LiDAR	Light Detection and Ranging
ATQ	Antique	LMS	LiDAR Mapping Suite
AWLS	Automated Water Level Sensor	m AGL	meters Above Ground Level
BA	Bridge Approach	MMS	Mobile Mapping Suite
BM	benchmark	MSL	mean sea level
CAD	Computer-Aided Design	NAMRIA	National Mapping and Resource Information Authority
CN	Curve Number	NSTC	Northern Subtropical Convergence
CSRS	Chief Science Research Specialist	PAF	Philippine Air Force
DAC	Data Acquisition Component	PAGASA	Philippine Atmospheric Geophysical and Astronomical Services Administration
DEM	Digital Elevation Model	PDOP	Positional Dilution of Precision
DENR	Department of Environment and Natural Resources	PPK	Post-Processed Kinematic [technique]
DOST	Department of Science and Technology	PRF	Pulse Repetition Frequency
DPPC	Data Pre-Processing Component	PTM	Philippine Transverse Mercator
DREAM	Disaster Risk and Exposure Assessment for Mitigation [Program]	QC	Quality Check
DRRM	Disaster Risk Reduction and Management	QT	Quick Terrain [Modeler]
DSM	Digital Surface Model	RA	Research Associate
DTM	Digital Terrain Model	RIDF	Rainfall-Intensity-Duration-Frequency
DVBC	Data Validation and Bathymetry Component	RMSE	Root Mean Square Error
FMC	Flood Modeling Component	SAR	Synthetic Aperture Radar
FOV	Field of View	SCS	Soil Conservation Service
GiA	Grants-in-Aid	SRTM	Shuttle Radar Topography Mission
GCP	Ground Control Point	SRS	Science Research Specialist
GNSS	Global Navigation Satellite System	SSG	Special Service Group
GPS	Global Positioning System	TBC	Thermal Barrier Coatings
H E C - HMS	Hydrologic Engineering Center - Hydrologic Modeling System	U P - TCAGP	University of the Philippines – Training Center for Applied Geodesy and Photogrammetry
H E C - RAS	Hydrologic Engineering Center - River Analysis System	UTM	Universal Transverse Mercator
HC	High Chord	VSU	Visayas State University
IDW	Inverse Distance Weighted [interpolation method]	WGS	World Geodetic System
IMU	Inertial Measurement Unit	UTM	Universal Transverse Mercator
kts	knots	WGS	World Geodetic System

## CHAPTER 1: OVERVIEW OF THE PROGRAM AND ULOT RIVER

*Engr. Florentino Morales, Jr., and Enrico C. Paringit, Dr. Eng.*



## **1.1 Background of the Phil-LiDAR 1 Program**

The University of the Philippines Training Center for Applied Geodesy and Photogrammetry (UP-TCAGP) launched a research program in 2014 entitled “Nationwide Hazard Mapping using LiDAR” or Phil-LiDAR 1, supported by the Department of Science and Technology (DOST) Grants-in-Aid (GiA) Program. The program was primarily aimed at acquiring a national elevation and resource dataset at sufficient resolution to produce information necessary to support the different phases of disaster management. Particularly, it targeted to operationalize the development of flood hazard models that would produce updated and detailed flood hazard maps for the major river systems in the country.

The program was also aimed at producing an up-to-date and detailed national elevation dataset suitable for 1:5,000 scale mapping, with 50 cm and 20 cm horizontal and vertical accuracies, respectively. These accuracies were achieved through the use of the state-of-the-art Light Detection and Ranging (LiDAR) airborne technology procured by the project through DOST. The methods applied in this report are thoroughly described in a separate publication titled *Flood Mapping of Rivers in the Philippines Using Airborne LiDAR: Methods* (Paringit et al., 2017) available separately.

The implementing partner university for the Phil-LiDAR 1 Program is the Visayas State University (VSU). VSU is in charge of processing LiDAR data and conducting data validation reconnaissance, cross section, bathymetric survey, validation, river flow measurements, flood height and extent data gathering, flood modeling, and flood map generation for the 28 river basins in the Eastern Visayas Region. The university is located in Baybay City in the province of Leyte.

## **1.2 Overview of the Ulot River Basin**

The Ulot River Basin traverses the barangays of Canteros, Guibuangan, Malogo, Mabuhay, Jepaco, Baruk, Camantang, Can-Ilay, and Salvacion in the municipality of Can-Avid. The DENR River Basin Control Office (RBCO) states that the Ulot River Basin has a drainage area of 903 km<sup>2</sup> and an estimated annual run-off of 1,716 m (MCM) (RBCO, 2015).

Its main stem, Ulot River, is part of the twenty-eight (28) river systems in Eastern Visayas Region. According to the 2015 national census of PSA, a total of 6885 persons are residing in the barangays that are within the immediate vicinity of the river. The economy of the province of Eastern Samar largely rests on fishery and agriculture which include production of coconut, cacao, rice, tobacco, root crops and corn. (Lancion, C.M., 2002). On December 25, 2016, a flood advisory was release by the National Disaster Risk Reduction and Management Council due to the heavy rains brought by Typhoon “Nina” affecting provinces in Central Luzon, and Visayas, including the province of Eastern Samar. (NDRRCM, 2016).

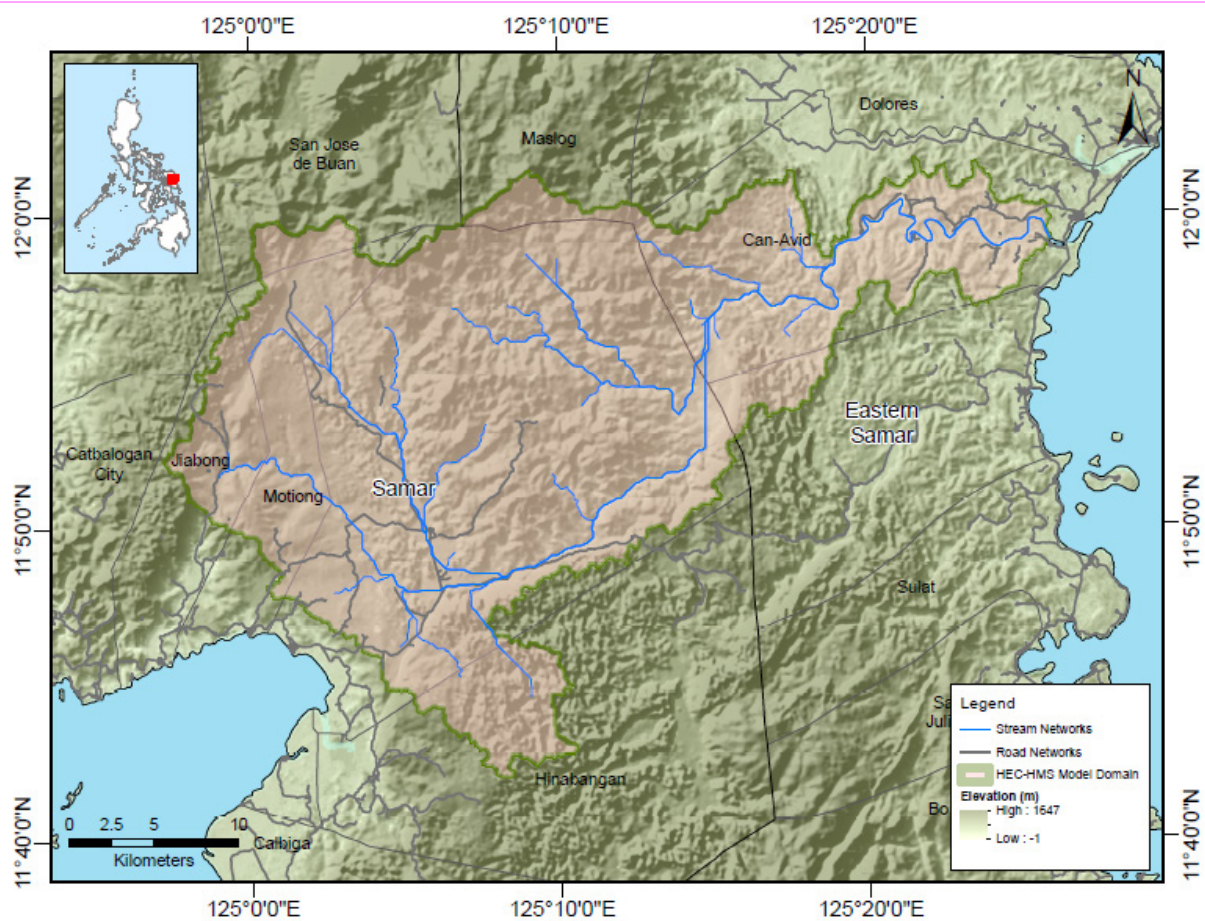


Figure 1. Map of the Ulot River Basin (in brown)

## CHAPTER 2: LIDAR ACQUISITION IN ULOT FLOOD-PLAIN

*Engr. Louie P. Balicanta, Engr. Christopher Cruz, Lovely Gracia Acuña, Engr. Gerome Hipolito, Ms. Jasmine T. Alviar, Engr. Brylle Adam G. De Castro*

The methods applied in this chapter were based on the DREAM methods manual (Sarmiento et al., 2014) and further enhanced and updated in Paringit et al. (2017).

## 2.1 Flight Plans

Plans were made to acquire LiDAR data nearest the delineated priority area for Ulot Floodplain in Eastern Samar. These missions were planned for 17 lines that run for at most four and a half (4.5) hours including take-off, landing and turning time. However, the acquisition flight over Ulot Floodplain did not push through because of inclement weather condition in the area. This report shows the LiDAR data nearest Ulot Floodplain. The flight planning parameters for the LiDAR system are found in Table 1. Figure 2 shows the flight plan for the LiDAR survey nearest Ulot Floodplain.

Table 1. Flight planning parameters for Aquarius LiDAR system

Block Name	Flying Height (m AGL)	Overlap (%)	Field of View ( $\theta$ )	Pulse Repetition Frequency (PRF) (kHz)	Scan Frequency (Hz)	Average Speed (kts)	Average Turn Time (Minutes)
BLK33J	500	20	44	50	45	120	5

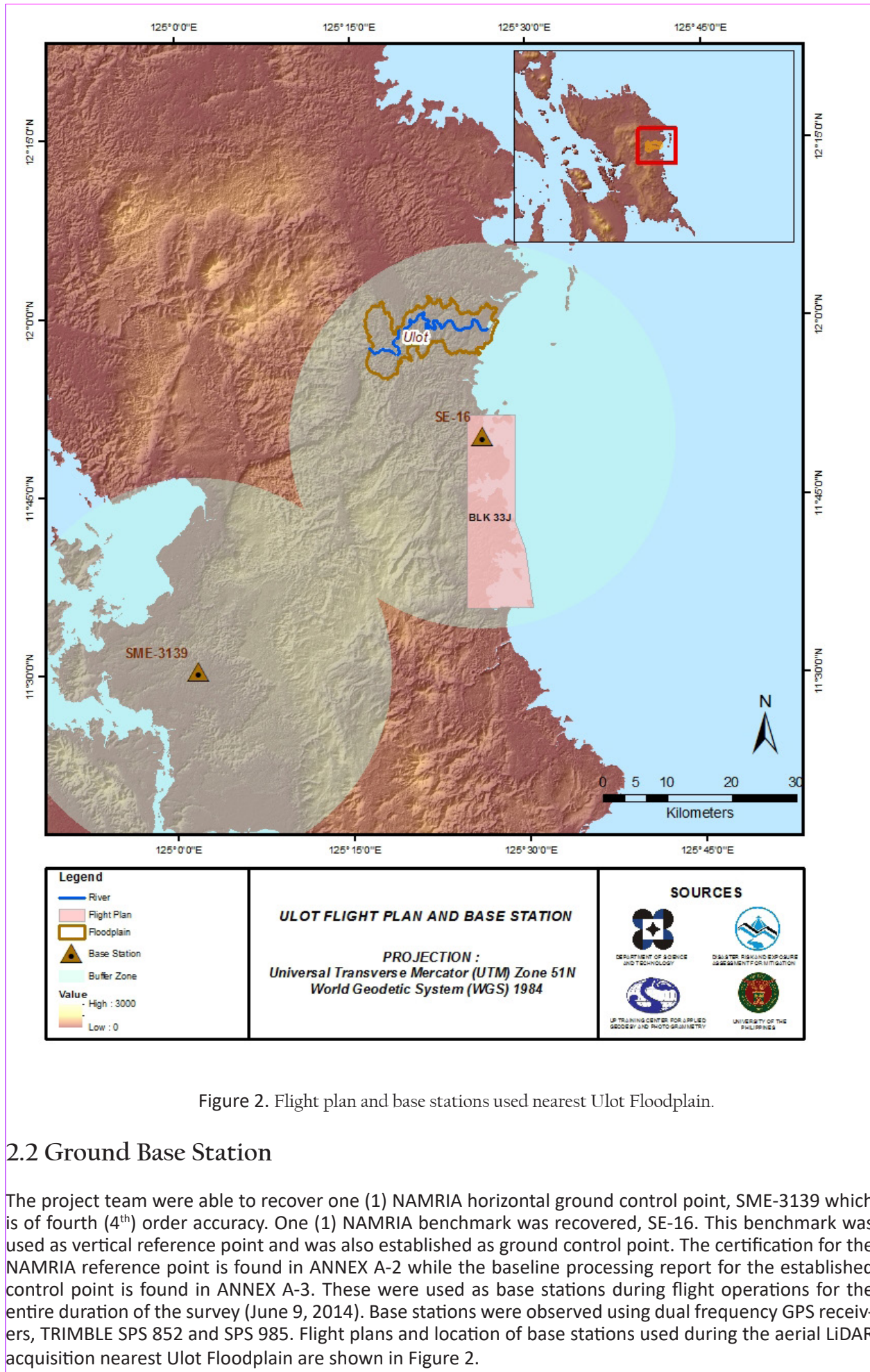


Figure 2. Flight plan and base stations used nearest Ulot Floodplain.

## 2.2 Ground Base Station

The project team were able to recover one (1) NAMRIA horizontal ground control point, SME-3139 which is of fourth (4<sup>th</sup>) order accuracy. One (1) NAMRIA benchmark was recovered, SE-16. This benchmark was used as vertical reference point and was also established as ground control point. The certification for the NAMRIA reference point is found in ANNEX A-2 while the baseline processing report for the established control point is found in ANNEX A-3. These were used as base stations during flight operations for the entire duration of the survey (June 9, 2014). Base stations were observed using dual frequency GPS receivers, TRIMBLE SPS 852 and SPS 985. Flight plans and location of base stations used during the aerial LiDAR acquisition nearest Ulot Floodplain are shown in Figure 2.



Figure 3 shows the recovered NAMRIA reference points within the area. Table 2 to Table 3 shows the details about the following NAMRIA control stations and established point, while Table 11 shows the list of all ground control points occupied during the acquisition with the corresponding dates of utilization.



Figure 3. GPS set-up over SME-3139 located along the highway in Brgy. Sto. Nino, Ulot, Eastern Samar (a) and NAMRIA reference point SME-3139 (b) as recovered by the field team.

Table 2. Details of the recovered NAMRIA horizontal control point SME-3139 used as base station for the LiDAR acquisition.

Station Name	SME-3139	
Order of Accuracy	4 <sup>th</sup> Order	
Relative Error (horizontal positioning)	1:10,000	
Geographic Coordinates, Philippine Reference of 1992 Datum (PRS 92)	Latitude	11° 30' 17.85657" North
	Longitude	125° 1' 29.837339" East
	Ellipsoidal Height	26.13400 meters
Grid Coordinates, Philippine Transverse Mercator Zone 5 (PTM Zone 5 PRS 92)	Easting	502722.403 meters
	Northing	1272180.079 meters
Geographic Coordinates, World Geodetic System 1984 Datum (WGS 84)	Latitude	11° 30' 13.52495" North
	Longitude	125° 1' 34.96980" East
	Ellipsoidal Height	87.78700 meters
Grid Coordinates, Universal Transverse Mercator Zone 51 North (UTM 51N WGS 1984)	Easting	720874.14 meters
	Northing	1272513.40 meters

Table 3. Details of the recovered NAMRIA horizontal control point SE-16 used as base station for the LiDAR acquisition.

Station Name	SE-16	
Order of Accuracy	4 <sup>th</sup>	
Relative Error (horizontal positioning)	1:10,000	
Geographic Coordinates, Philippine Reference of 1992 Datum (PRS 92)	Latitude	11° 50' 03.05106" North
	Longitude	125° 26' 03.03429" East
	Ellipsoidal Height	0.472 meters
Geographic Coordinates, World Geodetic System 1984 Datum (WGS 84)	Latitude	11° 49' 58.67117" North
	Longitude	125° 26' 08.13400" East
	Ellipsoidal Height	62.301 meters
Grid Coordinates, Universal Transverse Mercator Zone 51 North (UTM 51N WGS 1984)	Easting	765219.942 meters
	Northing	1309292.154 meters

Table 4. Ground control points used during LiDAR data acquisition.

Date surveyed	Flight Number	Mission Name	Ground Control Points
9 JUN 14	1558A	3 B L K - 33J160A	SE-16,SME-3139
9 JUN 14	1560A	3 B L K - 33JS160B	SE-16,SME-3139

### 2.3 Flight Missions

Two (2) missions were conducted to complete LiDAR data acquisition nearest Ulot Floodplain, for a total of eight hours and thirty-four minutes (8+34) of flying time for RP-9122. The missions were acquired using Aquarius LiDAR systems. Table 5 shows the total area of actual coverage and the corresponding flying hours per mission, while Table 6 presents the actual parameters used during the LiDAR data acquisition.

Table 5. Flight missions for LiDAR data acquisition nearest Ulot Floodplain.

Date Surveyed	Flight Number	Flight Plan Area (km <sup>2</sup> )	Surveyed Area (km <sup>2</sup> )	Area Surveyed within the Floodplain (km <sup>2</sup> )	Area Surveyed Outside the Floodplain (km <sup>2</sup> )	No. of Images (Frames)	Flying Hours	
							hr	Min
9 JUN 14	1558A	225.57	117.98	NA	117.98	98	4	41
9 JUN 14	1560A	225.57	127.54	NA	127.54	1294	3	53
TOTAL		451.14	245.52	NA	245.52	1392	8	34

Table 6. Actual parameters used during LiDAR data acquisition

Flight Number	Flying Height (m AGL)	Overlap (%)	FOV (θ)	PRF (khz)	Scan Frequency (Hz)	Average Speed (kts)	Average Turn Time (Minutes)
1558A	500	30	44	50	45	120	5
1560A	500	20	44	50	45	120	5

## 2.4 Survey Coverage

Ulot Floodplain is located in the province of Eastern Samar. The list of municipalities and cities surveyed, with at least one (1) square kilometer coverage, is shown in Table 7. The actual coverage of the LiDAR acquisition nearest Ulot Floodplain is presented in Figure 4.

Table 7. List of municipalities and cities surveyed during LiDAR survey nearest Ulot Floodplain.

Province	Municipality/City	Area of Municipality/City (km <sup>2</sup> )	Total Area Surveyed (km <sup>2</sup> )	Percentage of Area Surveyed
Eastern Samar	Sulat	150.05	39.95	26.63%
	San Julian	127.43	22.72	17.83%
	Borongan City	596.08	69.2	11.61%
	Taft	230.27	1.95	0.85%
	Total	1,103.83	133.82	12.12%

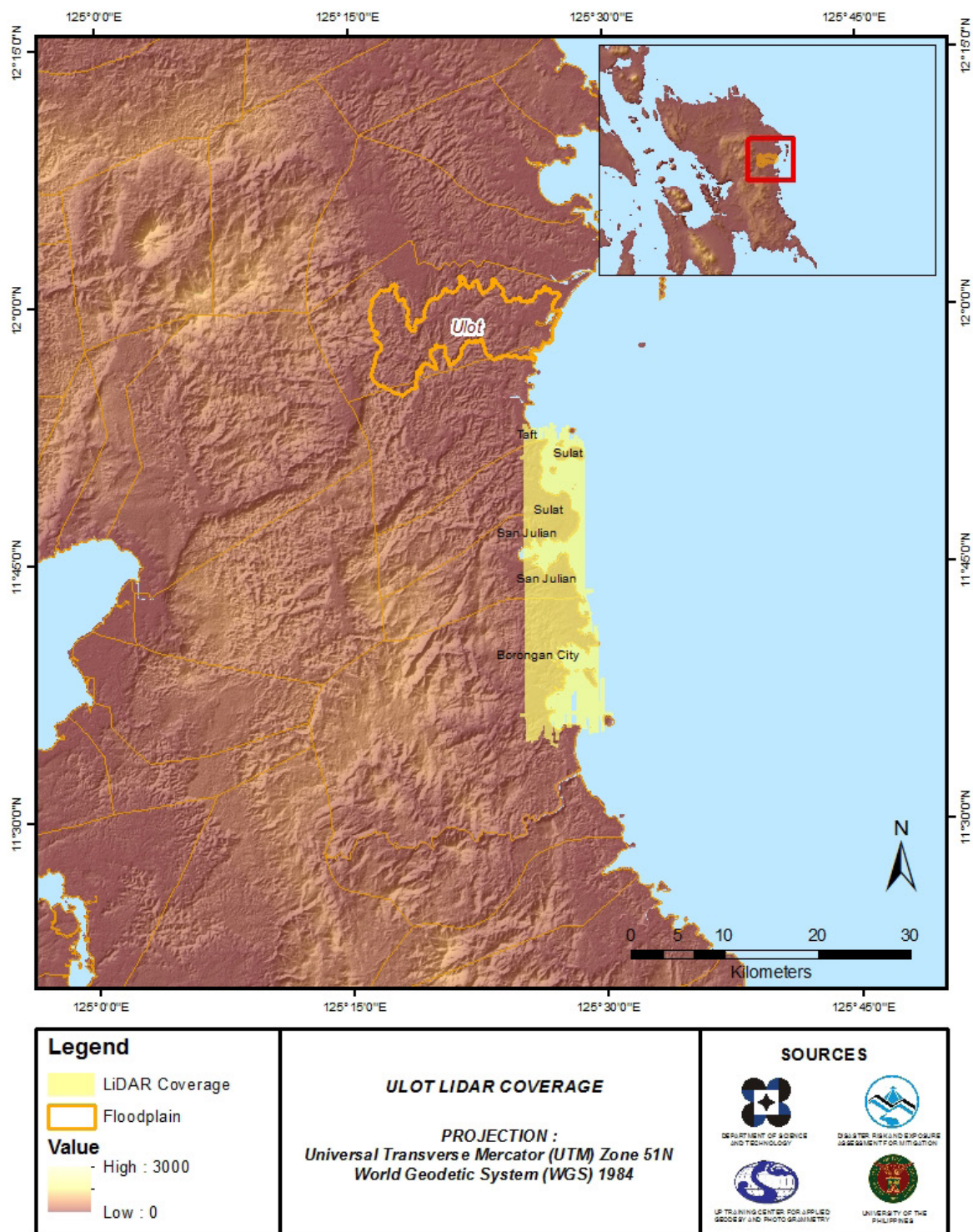


Figure 4. Actual LiDAR survey coverage nearest Ulot Floodplain



## CHAPTER 3: LIDAR DATA PROCESSING FOR ULOT FLOODPLAIN

*Engr. Ma. Ailyn L. Olanda, Engr. Jovelle Anjeanette S. Canlas, Jovy Anne S. Narisma,  
Engr. Vincent Louise DL. Azucena*

The methods applied in this chapter were based on the DREAM methods manual (Ang et al., 2014) and further enhanced and updated in Paringit et al. (2017).

### 3.1 Overview of the LiDAR Data Pre-Processing

The data transmitted by the Data Acquisition Component are checked for completeness based on the list of raw files required to proceed with the pre-processing of the LiDAR data. Upon acceptance of the LiDAR field data, georeferencing of the flight trajectory is done in order to obtain the exact location of the LiDAR sensor when the laser was shot. Point cloud georectification is performed to incorporate correct position and orientation for each point acquired. The georectified LiDAR point clouds are subject for quality checking to ensure that the required accuracies of the program, which are the minimum point density, vertical and horizontal accuracies, are met. The point clouds are then classified into various classes before generating Digital Elevation Models such as Digital Terrain Model and Digital Surface Model.

Using the elevation of points gathered in the field, the LiDAR-derived digital models are calibrated. Portions of the river that are barely penetrated by the LiDAR system are replaced by the actual river geometry measured from the field by the Data Validation and Bathymetry Component. LiDAR acquired temporally are then mosaicked to completely cover the target river systems in the Philippines. Orthorectification of images acquired simultaneously with the LiDAR data is done through the help of the georectified point clouds and the metadata containing the time the image was captured.

These processes are summarized in the flowchart shown in Figure 5.

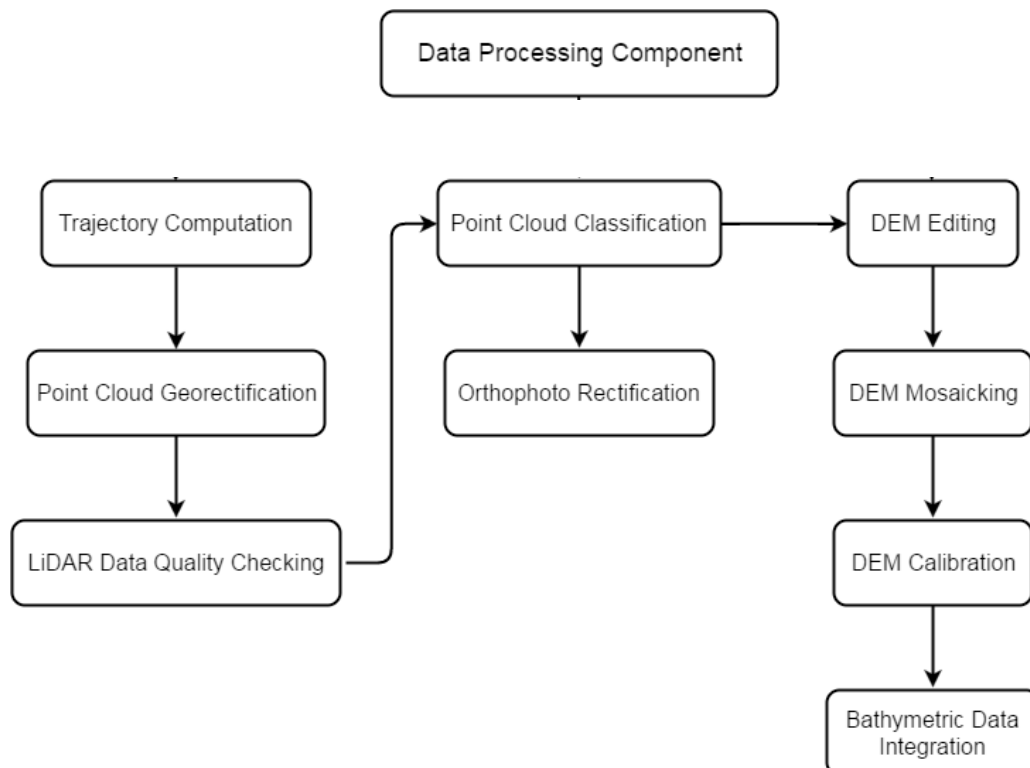


Figure 5. Schematic diagram for Data Pre-Processing Component

### 3.2 Transmittal of Acquired LiDAR Data

Data transfer sheets for all the LiDAR missions for Ulot Floodplain can be found in ANNEX A-5. Missions flown during the first survey conducted on June 2014 used the Airborne LiDAR Terrain Mapper (ALTM™ Optech Inc.) Aquarius system Can- Avid, Eastern Samar. The Data Acquisition Component (DAC) transferred a total of 26.3 Gigabytes of Range data, 500 Megabytes of POS data, 32.2 Megabytes of GPS base station data, and 167.9 Gigabytes of raw image data to the data server on June 19, 2014. The Data Pre-Processing Component (DPPC) verified the completeness of the transferred data. The whole dataset for Ulot was fully transferred on June 19, 2014, as indicated on the data transfer sheets for Ulot Floodplain.

### 3.3 Trajectory Computation

The Smoothed Performance Metric parameters of the computed trajectory for flight 1560A, one of the Ulot flights, which is the North, East, and Down position RMSE values are shown in Figure 6. The x-axis corresponds to the time of flight, which is measured by the number of seconds from the midnight of the start of the GPS week, which on that week fell on June 9, 2014 00:00AM. The y-axis is the RMSE value for that particular position.

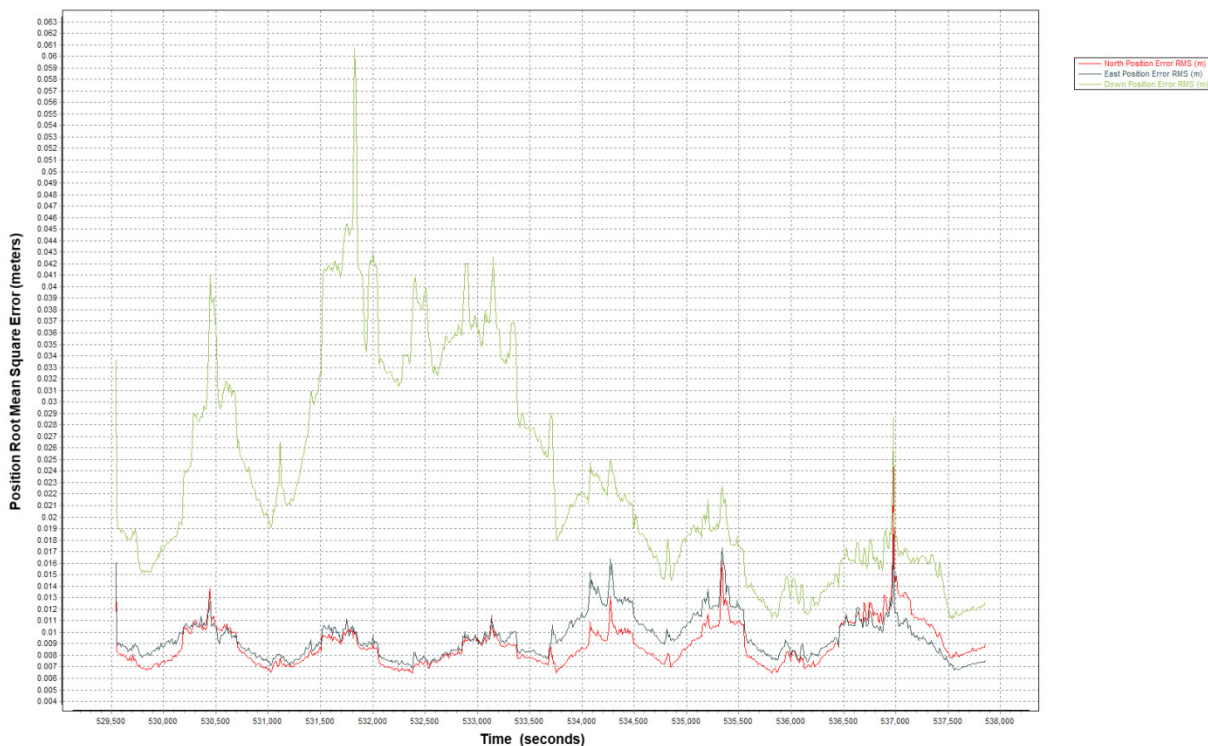


Figure 6. Smoothed Performance Metric parameters of a Ulot Flight 1560A.

The time of flight was from 529,500 seconds to 538,000 seconds, which corresponds to afternoon of June 9, 2014. The initial spike that is seen on the data corresponds to the time that the aircraft was getting into position to start the acquisition, and the POS system starts computing for the position and orientation of the aircraft. Redundant measurements from the POS system quickly minimized the RMSE value of the positions. The periodic increase in RMSE values from an otherwise smoothly curving RMSE values correspond to the turn-around period of the aircraft, when the aircraft makes a turn to start a new flight line. Figure 6 shows that the North position RMSE peaks at 2.40 centimeters, the East position RMSE peaks at 1.80 centimeters, and the Down position RMSE peaks at 6.00 centimeters, which are within the prescribed accuracies described in the methodology.

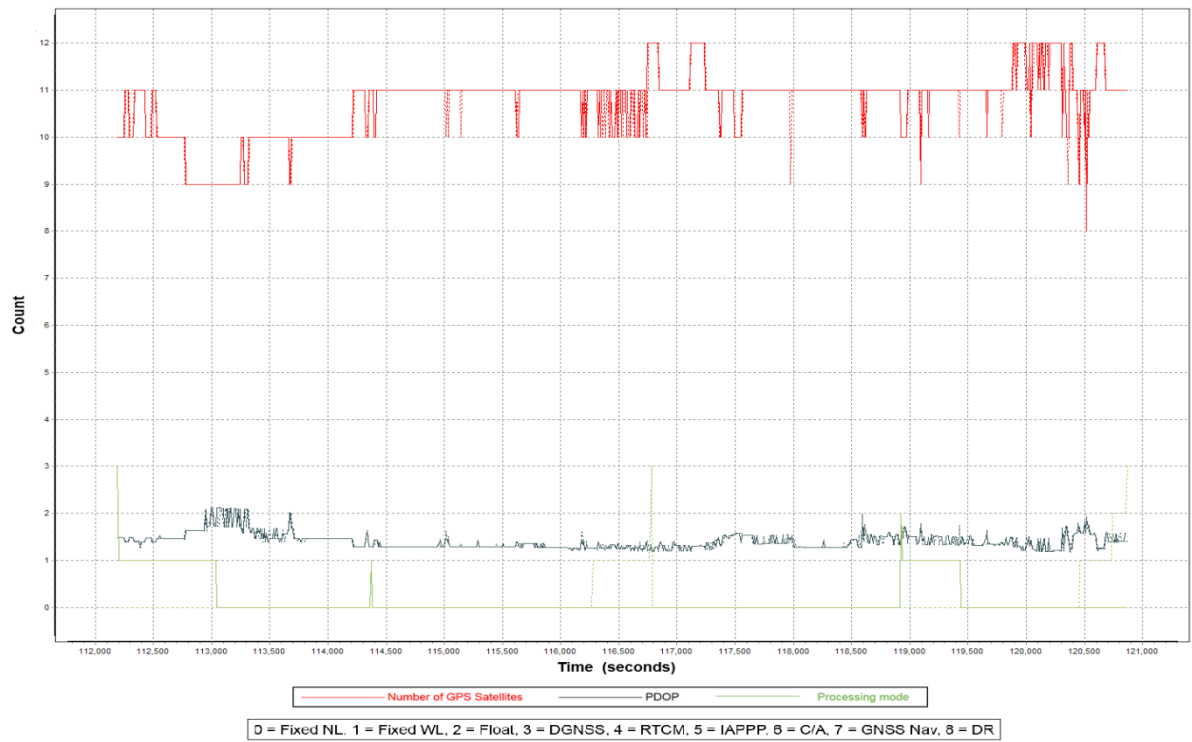


Figure 7. Solution Status parameters of Ulot Flight 1560A.

The Solution Status parameters of flight 1560A, one of the Ulot flights, which are the number of GPS satellites, Positional Dilution of Precision (PDOP), and the GPS processing mode used, are shown in Figure 7. The graphs indicate that the number of satellites during the acquisition did not go down to 9. Majority of the time, the number of satellites tracked was between 9 and 12. The PDOP value also did not go above the value of 3, which indicates optimal GPS geometry. The processing mode stayed at the value of 0 for majority of the survey with some peaks up to 1 attributed to the turns performed by the aircraft. The value of 0 corresponds to a Fixed, Narrow-Lane mode, which is the optimum carrier-cycle integer ambiguity resolution technique available for POSPAC MMS. All of the parameters adhered to the accuracy requirements for optimal trajectory solutions, as indicated in the methodology. The computed best estimated trajectory for all Ulot flights is shown in Figure 8.

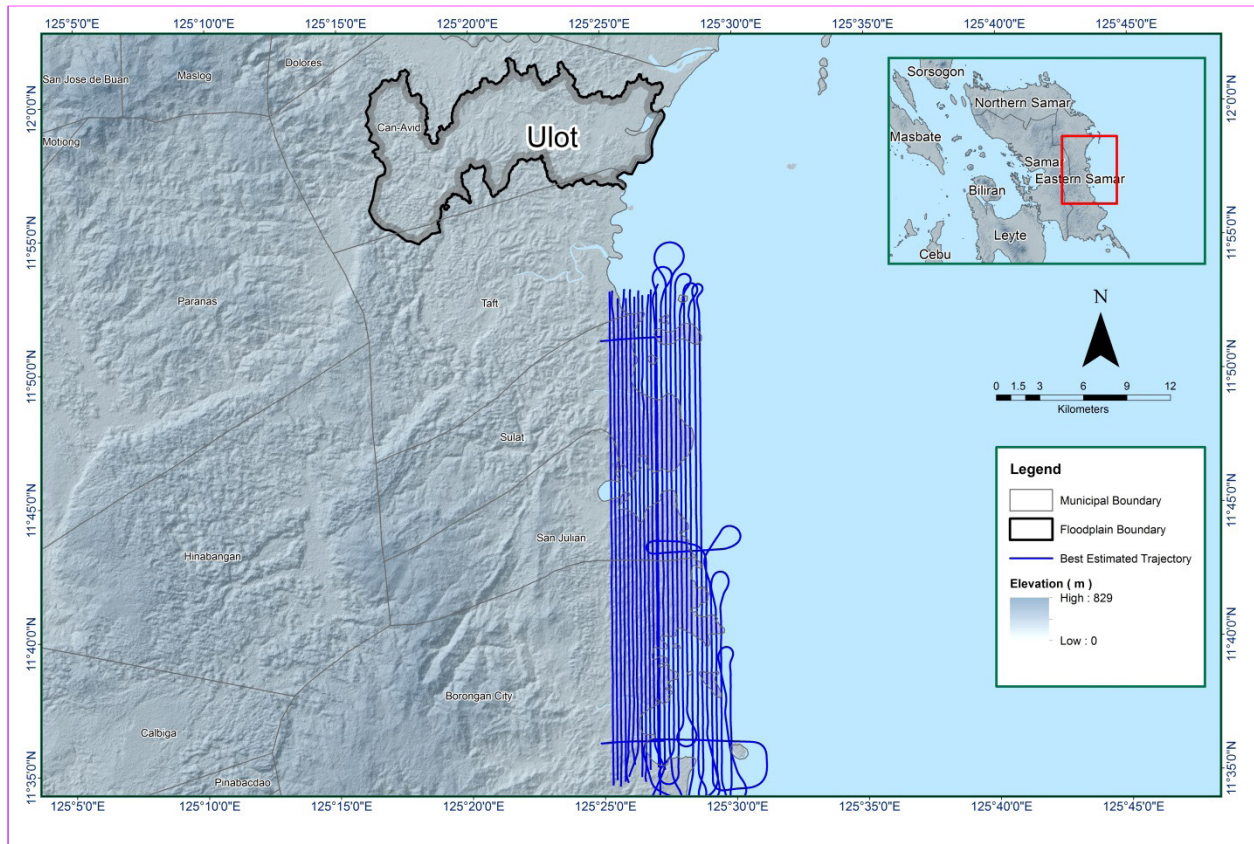


Figure 8. Best estimated trajectory of LiDAR missions conducted over Ulot Floodplain

### 3.4 LiDAR Point Cloud Computation

The produced LAS data contains 28 flight lines, with each flight line containing one channel, since Aquarius system contains one channel only. The summary of the self-calibration results obtained from LiDAR processing in LiDAR Mapping Suite (LMS) software for all flights over Ulot Floodplain are given in Table 8.

Table 8. Self-calibration results values for Ulot flights.

Parameter	Computed Value
Boresight Correction stdev (<0.001degrees)	0.000327
IMU Attitude Correction Roll and Pitch Corrections stdev (<0.001degrees)	0.000909
GPS Position Z-correction stdev (<0.01meters)	0.0098

The optimum accuracy is obtained for all Ulot flights based on the computed standard deviations of the corrections of the orientation parameters. Standard deviation values for individual blocks are available in the ANNEX B-1. Mission Summary Reports.

### 3.5 LiDAR Data Quality Checking

The boundary of the processed LiDAR data on top of a SAR Elevation Data over Ulot Floodplain is shown in Figure 9. The map shows gaps in the LiDAR coverage that are attributed to cloud coverage.



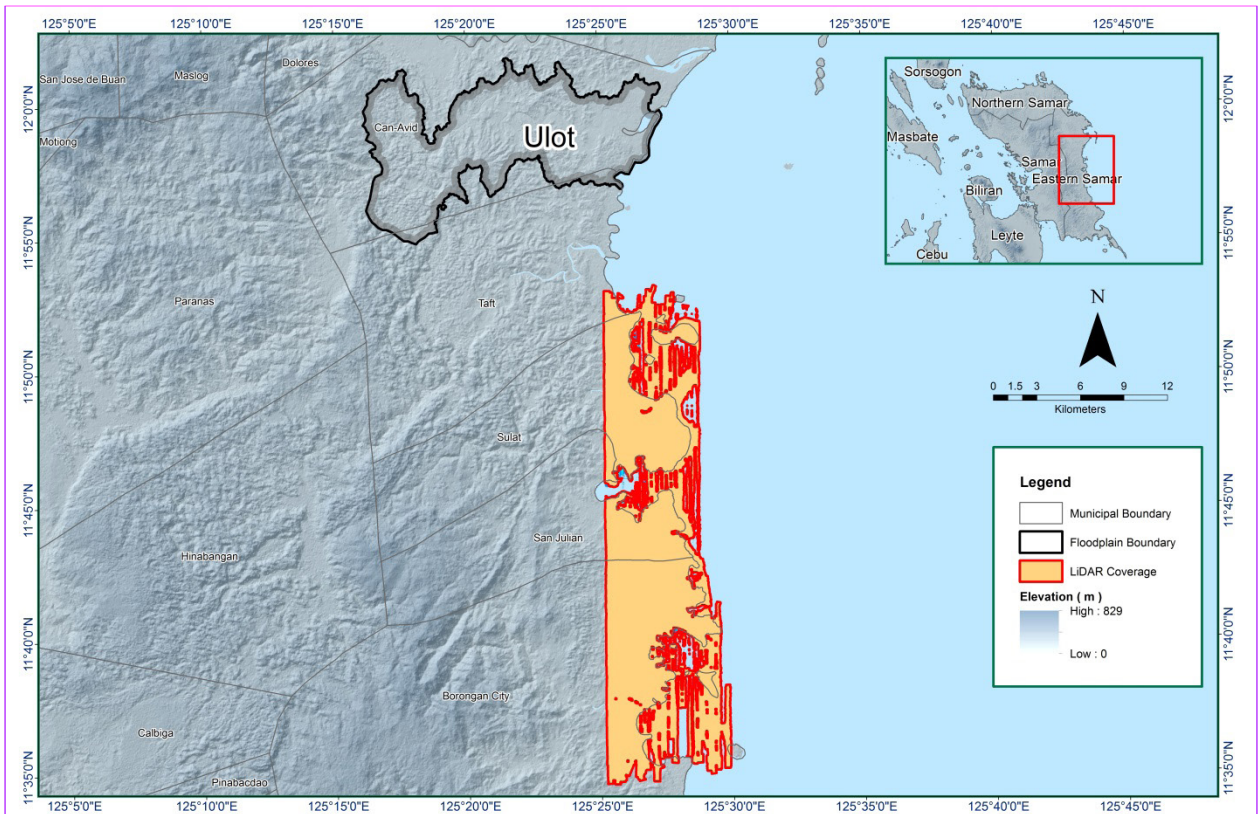


Figure 9. Boundary of the processed LiDAR data over Ulot Floodplain

The total area covered by the Ulot missions is 174.99 sq km that is comprised of two (2) flight acquisitions grouped and merged into one (1) block as shown in Table 9.

Table 9. List of LiDAR blocks for Ulot Floodplain.

LiDAR Blocks	Flight Numbers	Area (sq km)
Samar_Leyte_Bl33J	1558A	174.99
	1560A	
<b>TOTAL</b>		<b>174.99 sq km</b>

The overlap data for the merged LiDAR blocks, showing the number of channels that pass through a particular location is shown in Figure 10. Since the Aquarius system employs one channel, we would expect an average value of 1 (blue) for areas where there is limited overlap, and a value of 2 (yellow) or more (red) for areas with three or more overlapping flight lines.

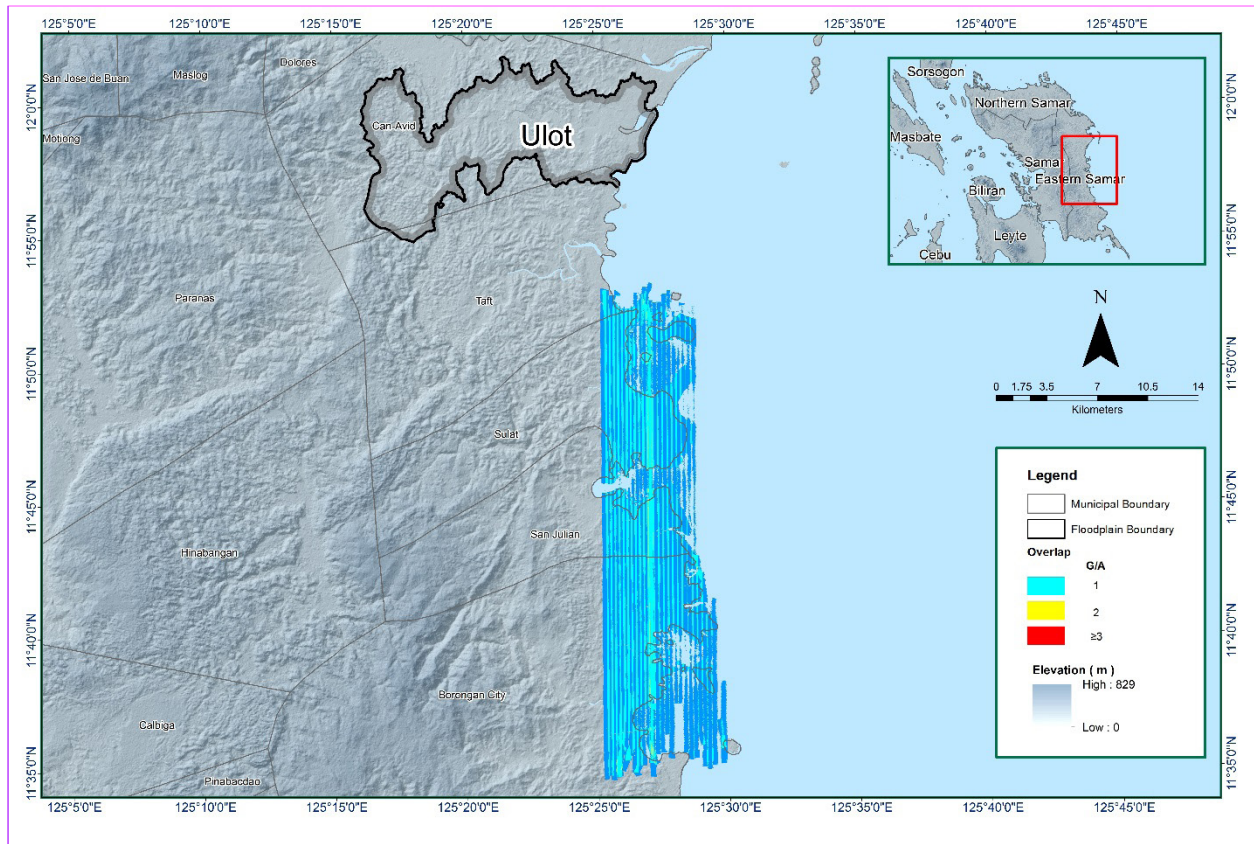


Figure 10. Image of data overlap for Ulot Floodplain.

The overlap statistics per block for the Ulot Floodplain can be found in ANNEX B-1. One pixel corresponds to 25.0 square meters on the ground. For this area, the percent overlap 36.01%, which passed the 25% requirement.

The pulse density map for the merged LiDAR data, with the red parts showing the portions of the data that satisfy the 2 points per square meter criterion is shown in Figure 11. It was determined that all LiDAR data for Ulot Floodplain satisfy the point density requirement, and the average density for the entire survey area is 2.71 points per square meter.

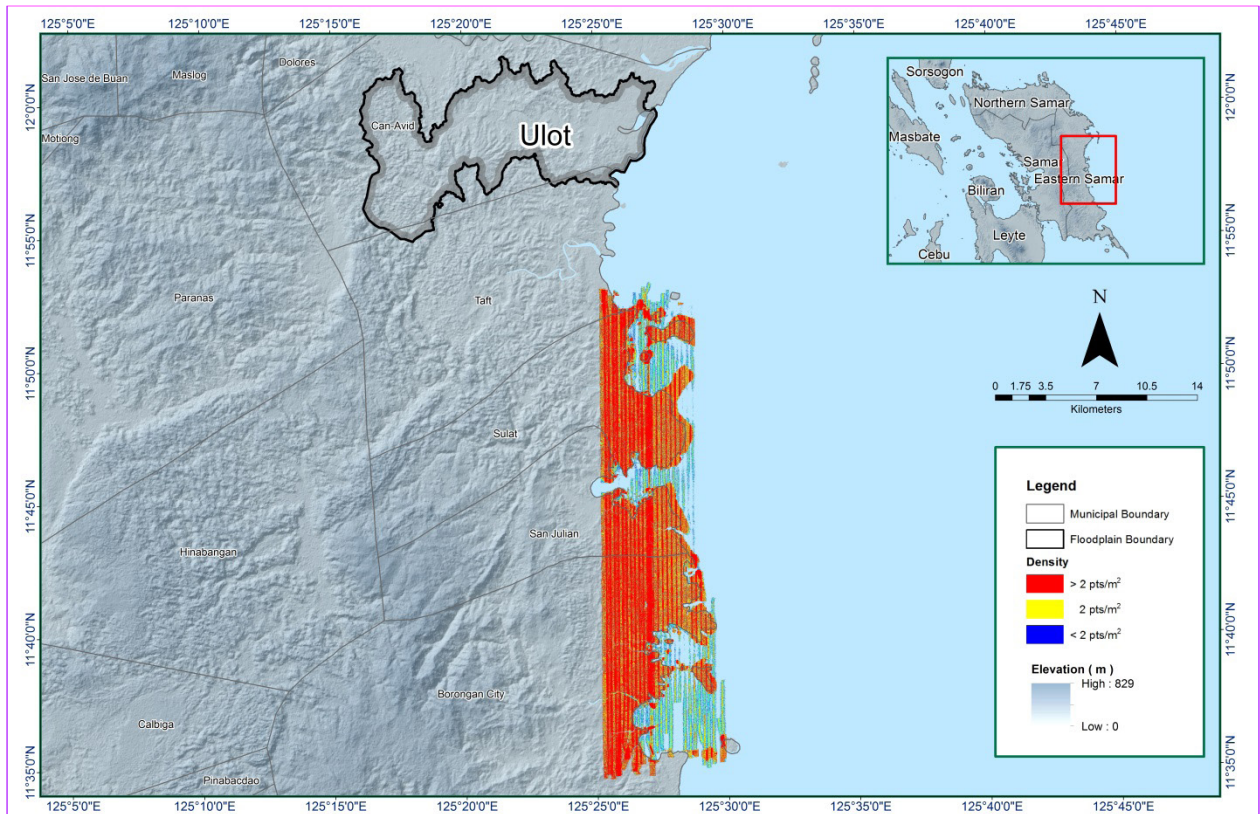


Figure 11. Pulse density map of merged LiDAR data for Ulot Floodplain.

The elevation difference between overlaps of adjacent flight lines is shown in Figure 12. The default color range is from blue to red, where bright blue areas correspond to portions where elevations of a previous flight line, identified by its acquisition time, are higher by more than 0.20m relative to elevations of its adjacent flight line. Bright red areas indicate portions where elevations of a previous flight line are lower by more than 0.20m relative to elevations of its adjacent flight line. Areas with bright red or bright blue need to be investigated further using Quick Terrain Modeler software.



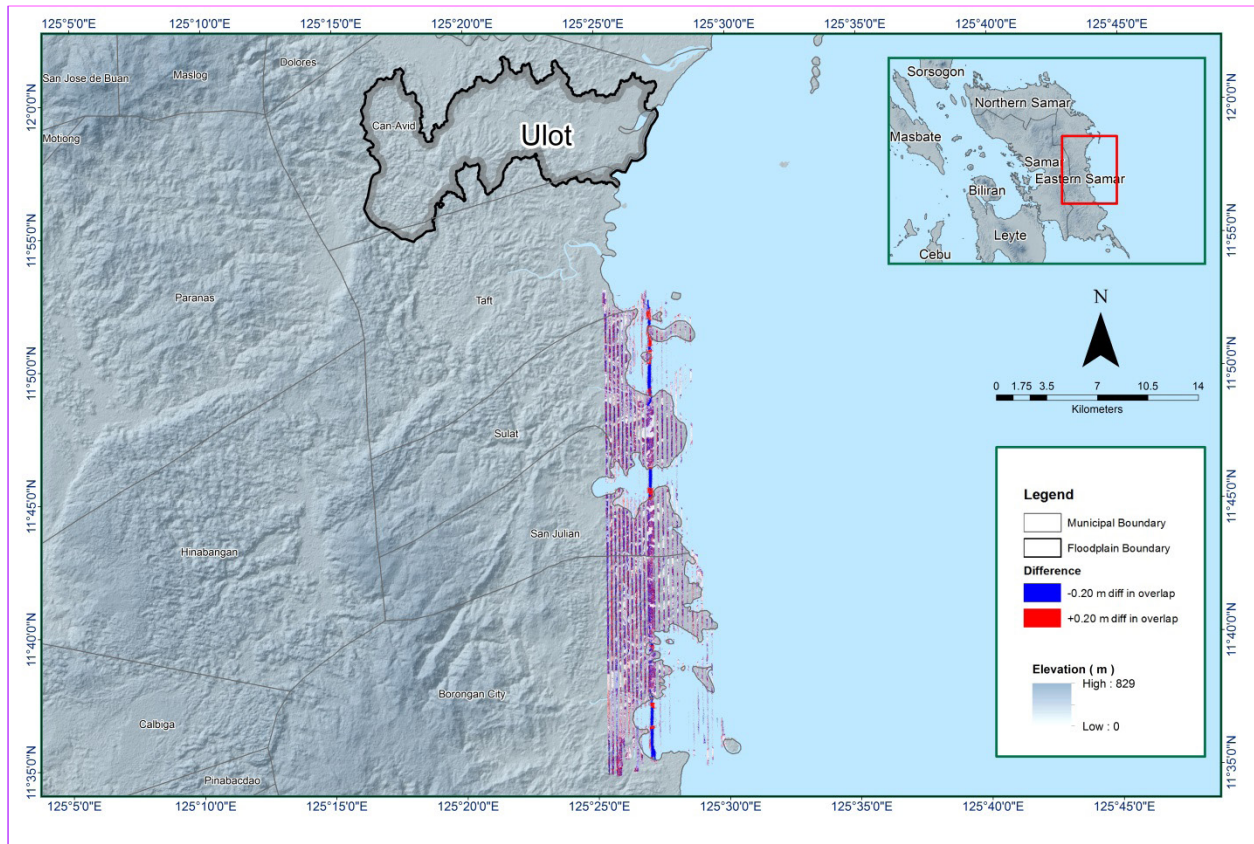


Figure 12. Elevation difference map between flight lines for Ulot Floodplain.

A screen capture of the processed LAS data from a Ulot flight 1560A loaded in QT Modeler is shown in Figure B-9. The upper left image shows the elevations of the points from two overlapping flight strips traversed by the profile, illustrated by a dashed red line. The x-axis corresponds to the length of the profile. It is evident that there are differences in elevation, but the differences do not exceed the 20-centimeter mark. This profiling was repeated until the quality of the LiDAR data becomes satisfactory. No reprocessing was done for this LiDAR dataset.

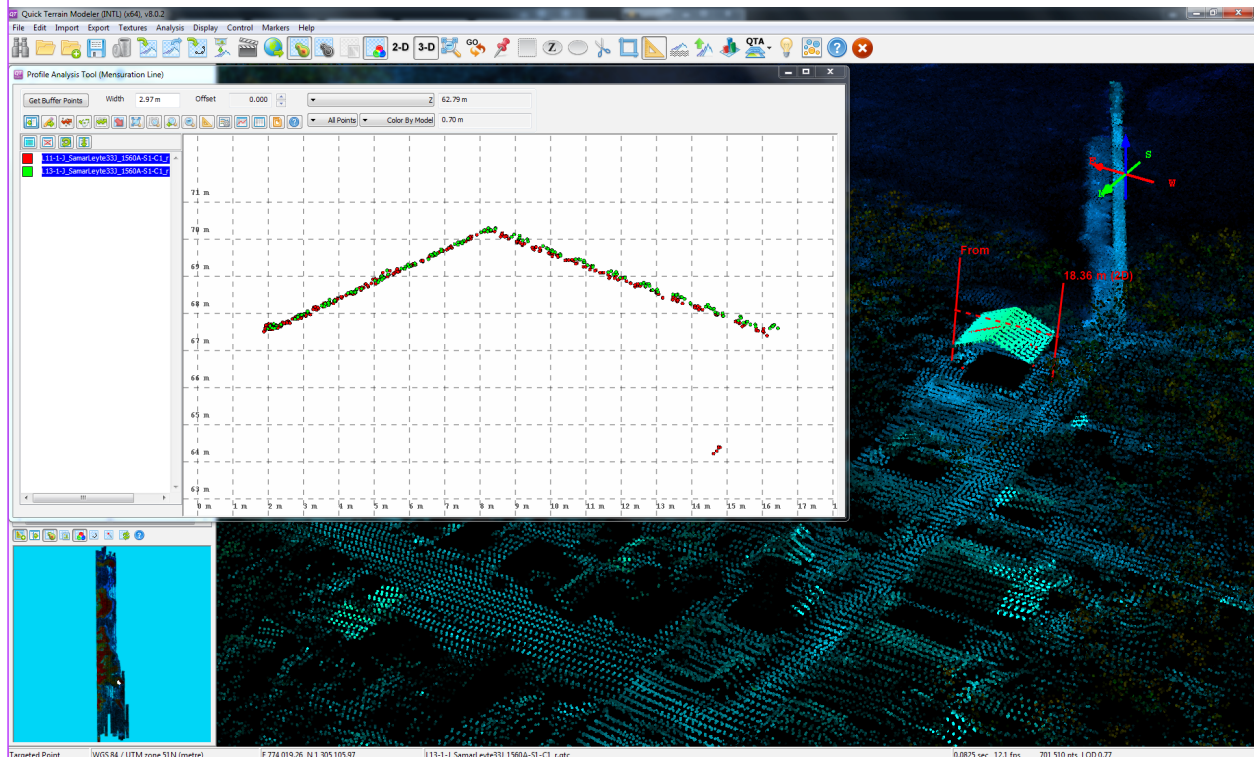


Figure 13. Quality checking for a Ulot flight 1560A using the Profile Tool of QT Modeler.



### 3.6 LiDAR Point Cloud Classification and Rasterization

Table 10. Ulot classification results in TerraScan.

Pertinent Class	Total Number of Points
Ground	110,486,647
Low Vegetation	51,277,620
Medium Vegetation	61,095,498
High Vegetation	151,119,077
Building	2,518,830

The tile system that TerraScan employed for the LiDAR data and the final classification image for a block near Ulot Floodplain is shown in Figure 14. A total of 291 1km by 1km tiles were produced. The number of points classified to the pertinent categories is illustrated in Table 10. The point cloud has a maximum and minimum height of 248.48 meters and 49.30 meters respectively.

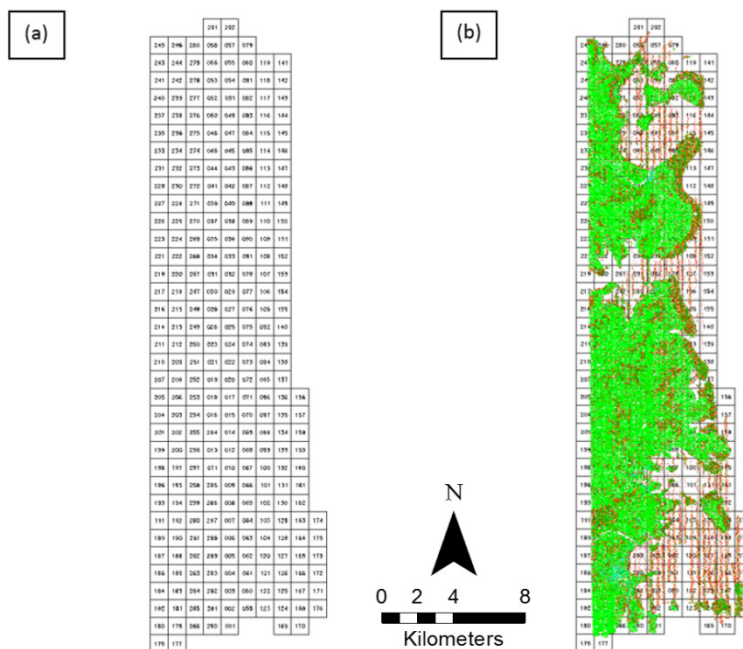


Figure 14. Tiles for Ulot Floodplain (a) and classification results (b) in TerraScan

An isometric view of an area before and after running the classification routines is shown in Figure 15. The ground points are in orange, the vegetation is in different shades of green, and the buildings are in cyan. It can be seen that residential structures adjacent or even below canopy are classified correctly, due to the density of the LiDAR data.



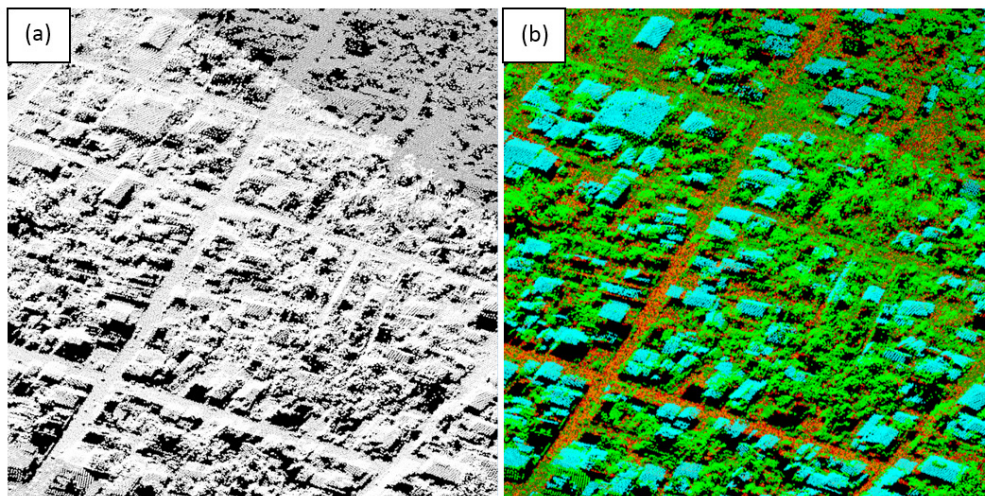


Figure 15. Point cloud before (a) and after (b) classification.

The production of last return (V\_ASCII) and the secondary (T\_ASCII) DTM, first (S\_ASCII) and last (D\_ASCII) return DSM of the area in top view display are shown in Figure 16. It shows that DTMs are the representation of the bare earth while on the DSMs, all features are present such as buildings and vegetation.

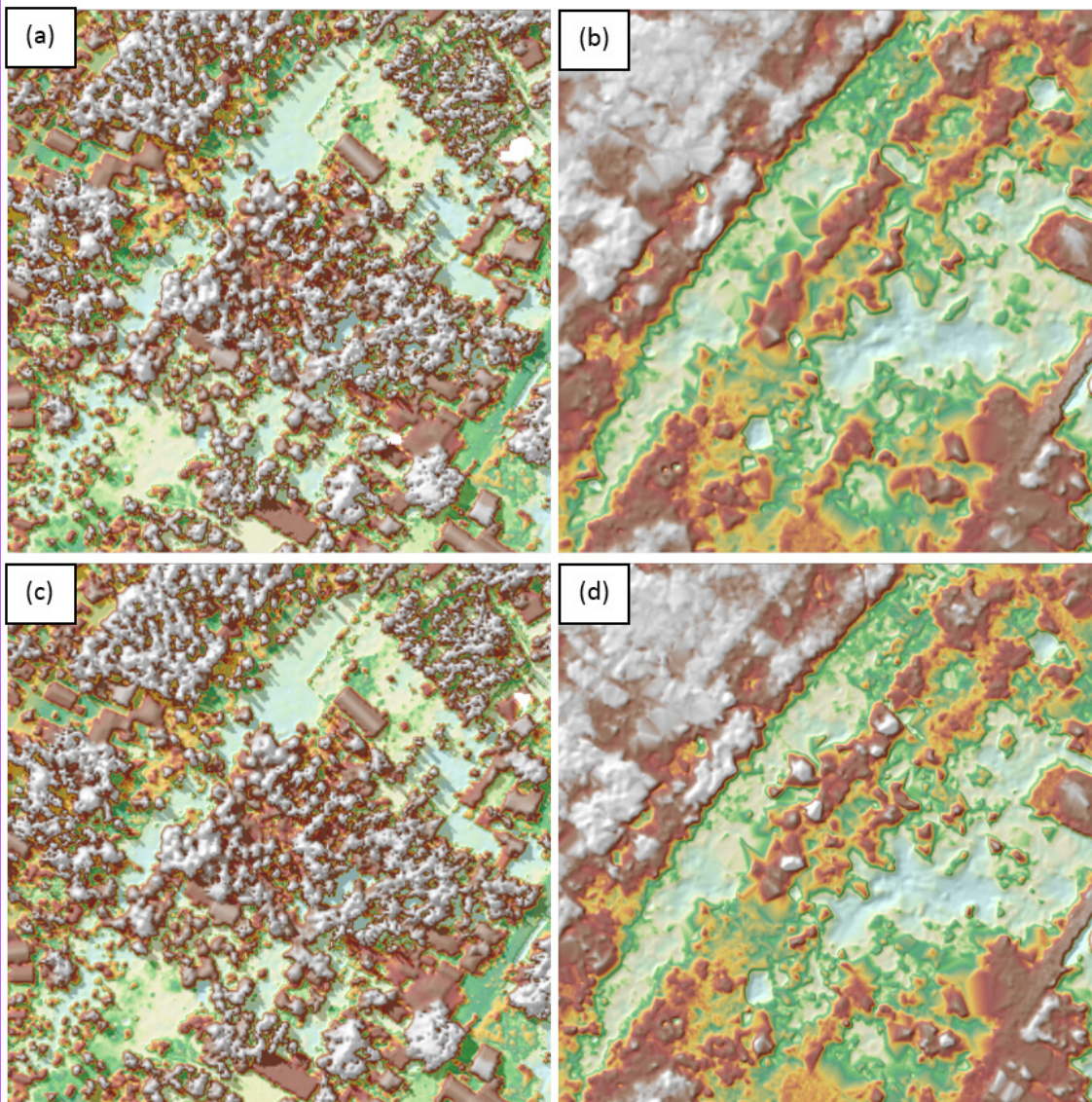


Figure 16. The production of last return DSM (a) and DTM (b), first return DSM (c) and secondary DTM (d) in some portion near Ulot Floodplain.



### 3.7 LiDAR Image Processing and Orthophotograph Rectification

The 292 1km by 1km tiles of the block covering the Ulot Floodplain is shown in Figure 17. After tie point selection to fix photo misalignments, color points were added to smoothen out visual inconsistencies along the seamlines where photos overlap. The block covering the Ulot Floodplain has a total of 219.66 sq km orthophotograph coverage comprised of 2,657 images. However, the block does not have a complete set of orthophotographs and no orthophotographs cover the area of the Ulot Floodplain. A zoomed in version of sample orthophotographs named in reference to its tile number is shown in Figure 18.

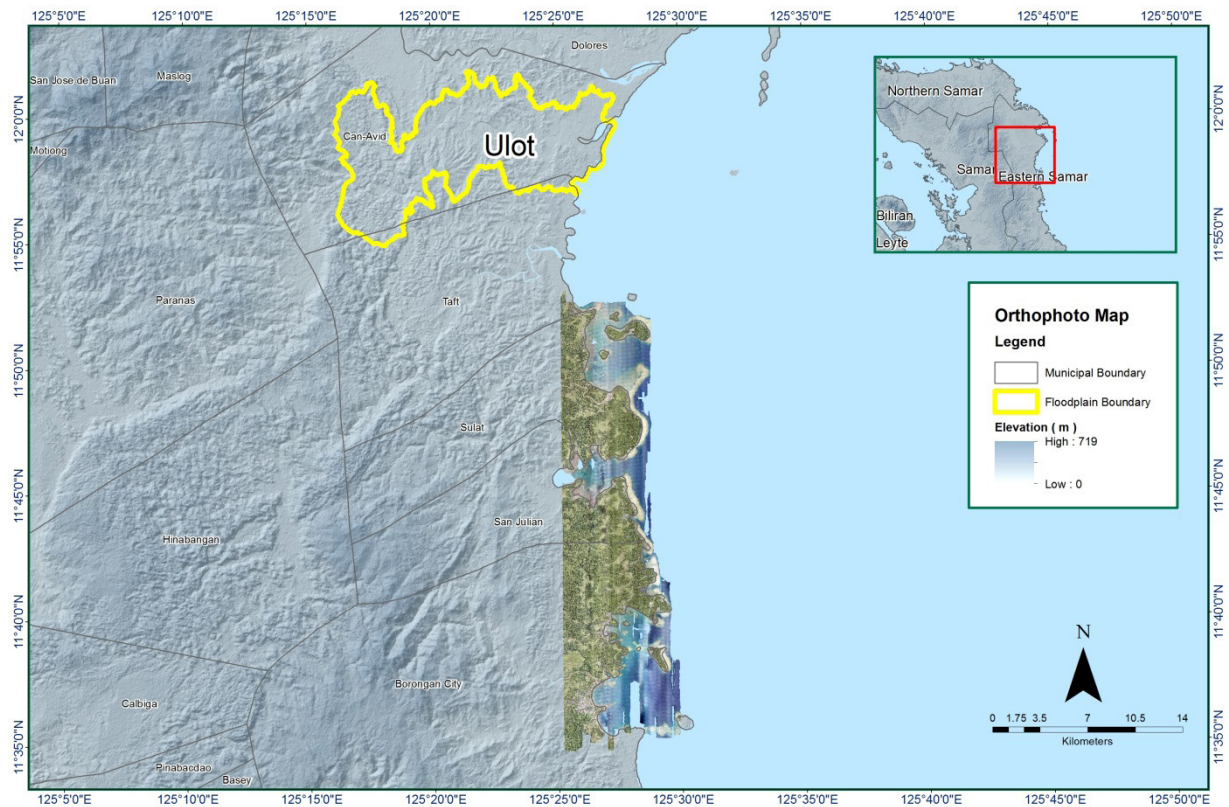


Figure 17. Available orthophotographs near Ulot Floodplain.

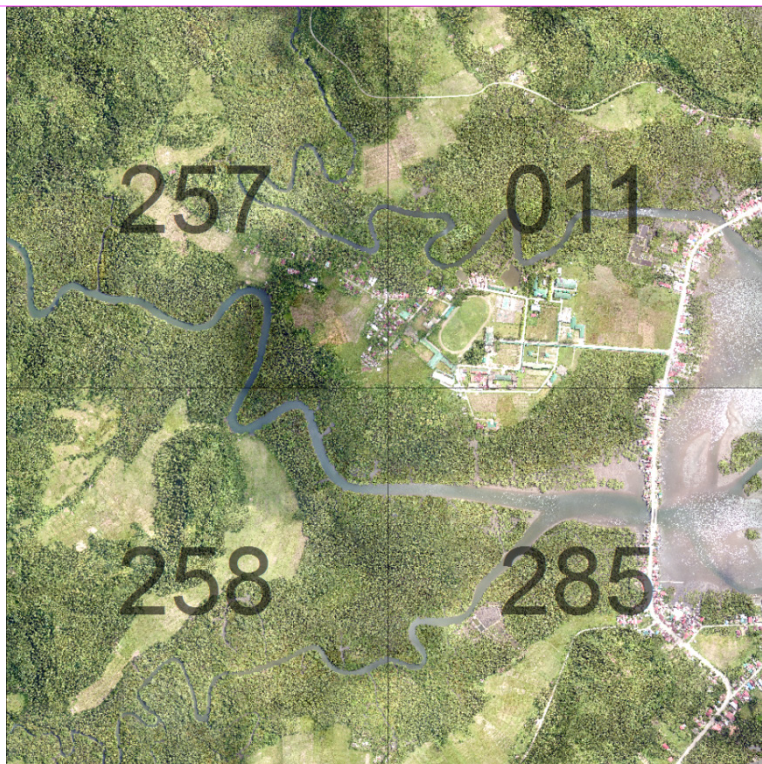


Figure 18. Sample orthophotograph tiles near Ulot Floodplain.

### 3.8 DEM Editing and Hydro-Correction

SamarLeyte\_Bl33J is the nearby block to the Ulot Floodplain. It was processed in order to produce DEMs covering municipalities neighboring the Ulot Floodplain. It has an area of 174.99 square kilometers. Table 11 shows the LiDAR block/s and their corresponding area in square kilometers.

Table 11. LiDAR block/s with its corresponding area.

LiDAR Blocks	Area (sq km)
Samar_Leyte_Bl33J	174.99

Portions of DTM before and after manual editing are shown in Figure 19. The bridge (Figure 19a) is also considered to be an impedance to the flow of water along the river and has to be removed (Figure 19b) in order to hydrologically correct the river. The paddy field (Figure 19c) has been misclassified and removed during classification process and has to be retrieved to complete the surface (Figure 19d) to allow the correct flow of water.



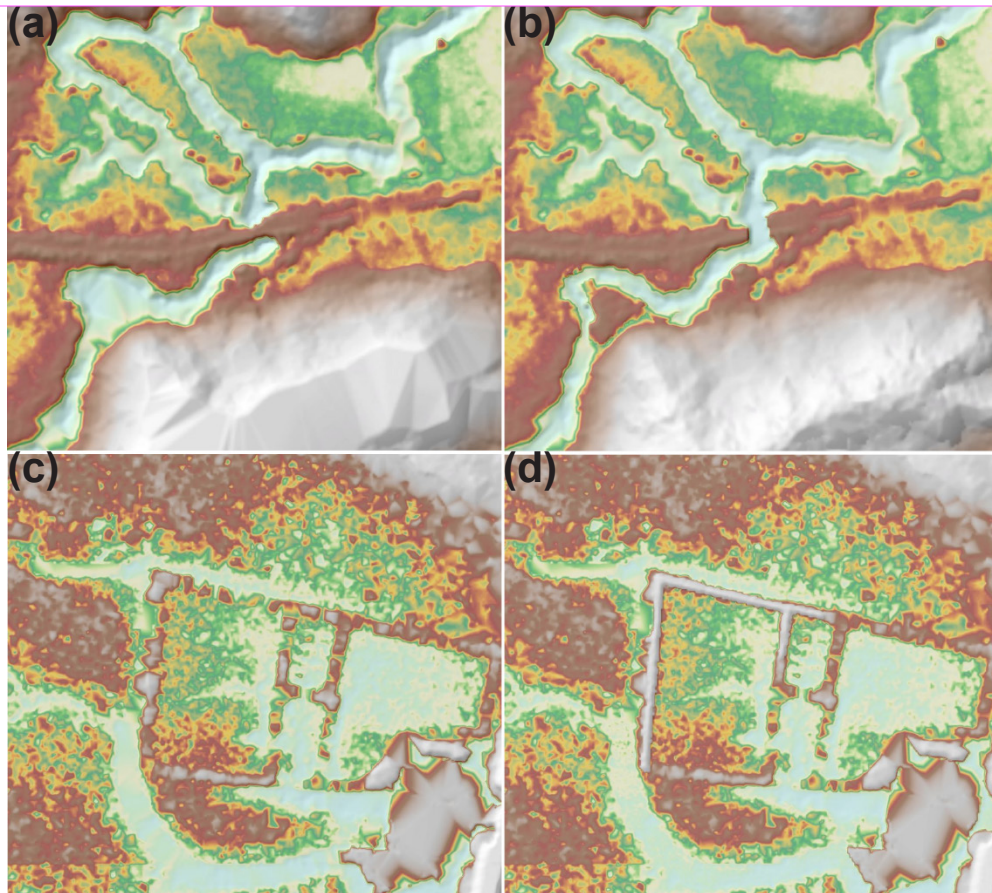


Figure 19. Portions in the DTM of nearby block – a bridge before (a) and after (b) manual editing; a paddy field before (c) and after (d) data retrieval; and a building before (a) and after (b) manual editing

### 3.9 Mosaicking of Blocks

The IFSAR data covering all floodplains located in Eastern Samar such as Ulot, Ulot and Oras and the processed LiDAR data Samar Leyte Blk 33J were mosaicked to the calibrated Tacloban LiDAR data. Table 12 shows the shift values applied to the LiDAR/IFSAR during mosaicking.

IFSAR data for Ulot Floodplain is shown in Figure B-16.

Table 12. Shift values of each IFSAR Block of Ulot Floodplain and the nearby LiDAR block.

Mission Blocks	Shift Values (meters)		
	x	y	z
4024-I-1-5, 6-9	0.06482	-0.00238	-1.00
4025-II-21-25	0.22093	0.05265	-1.00
SamarLeyte_Bl33J	-1.00	2.00	-1.00

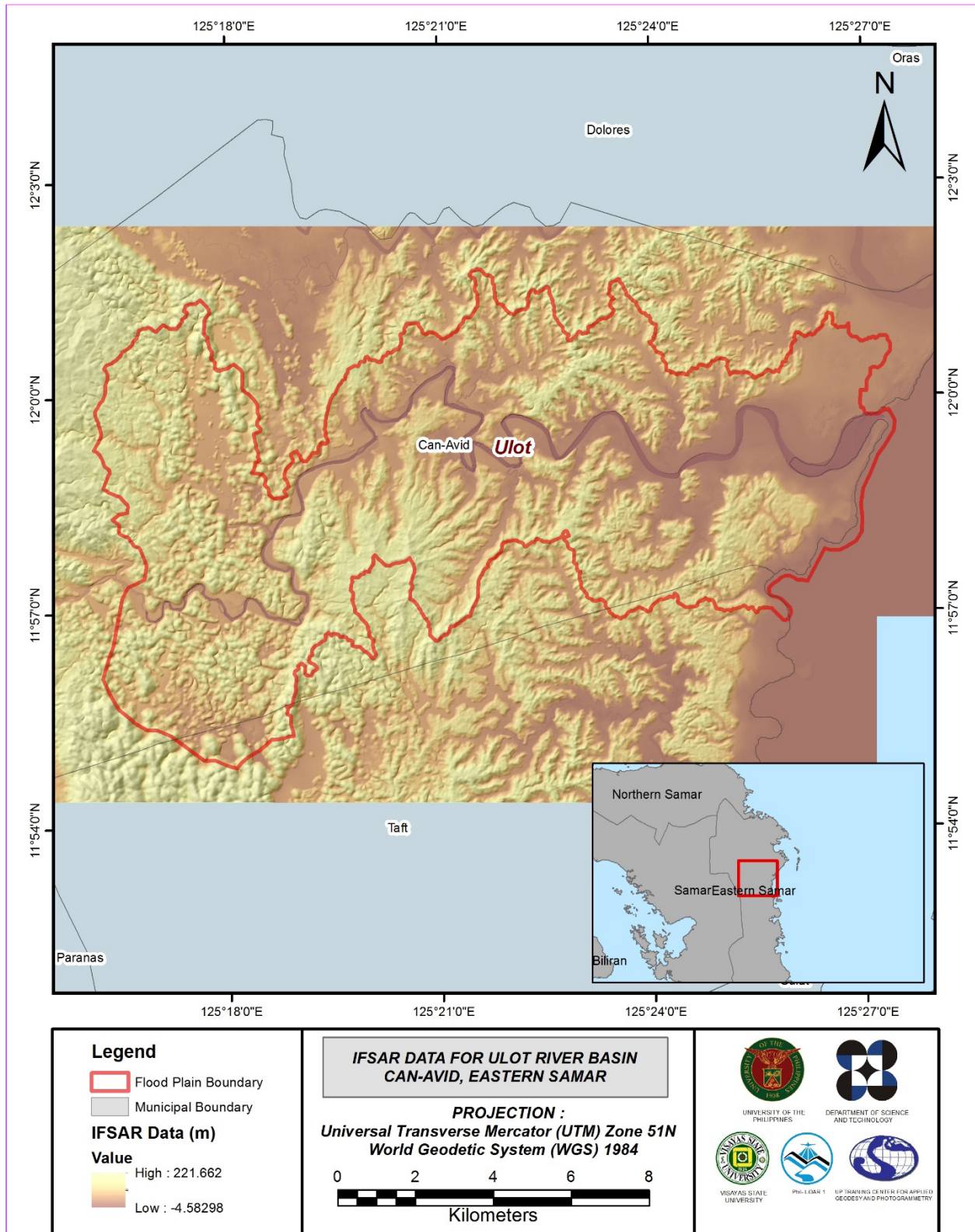


Figure 20. Map of IFSAR Data for Ulot Floodplain.

### 3.10 Calibration and Validation of Mosaicked LiDAR Digital Elevation Model

The extent of the validation survey done by the Data Validation and Bathymetry Component (DVBC) in Ulot to collect points with which the LiDAR dataset is validated is shown in Figure 21. A total of 3,574 survey points were gathered for the Ulot Floodplain. However, the point dataset was not used for the calibration of the LiDAR data for Ulot because during the mosaicking process, the IFSAR was referred to the calibrated Tacloban DEM. Therefore, the IFSAR DEM of Ulot can already be considered as a calibrated DEM.

A good correlation between the uncalibrated Tacloban LiDAR DTM and ground survey elevation values is shown in Figure 22. Statistical values were computed from extracted LiDAR values using the selected points to assess the quality of data and obtain the value for vertical adjustment. The computed height difference between the LiDAR DTM and calibration points is 0.14 meters with a standard deviation of 0.13 meters. Calibration of Tacloban LiDAR data was done by subtracting the height difference value, 0.14 meters, to Tacloban mosaicked LiDAR data. Table 13 shows the statistical values of the compared elevation values between Tacloban LiDAR data and calibration data. These values were also applicable to the Ulot DEM.



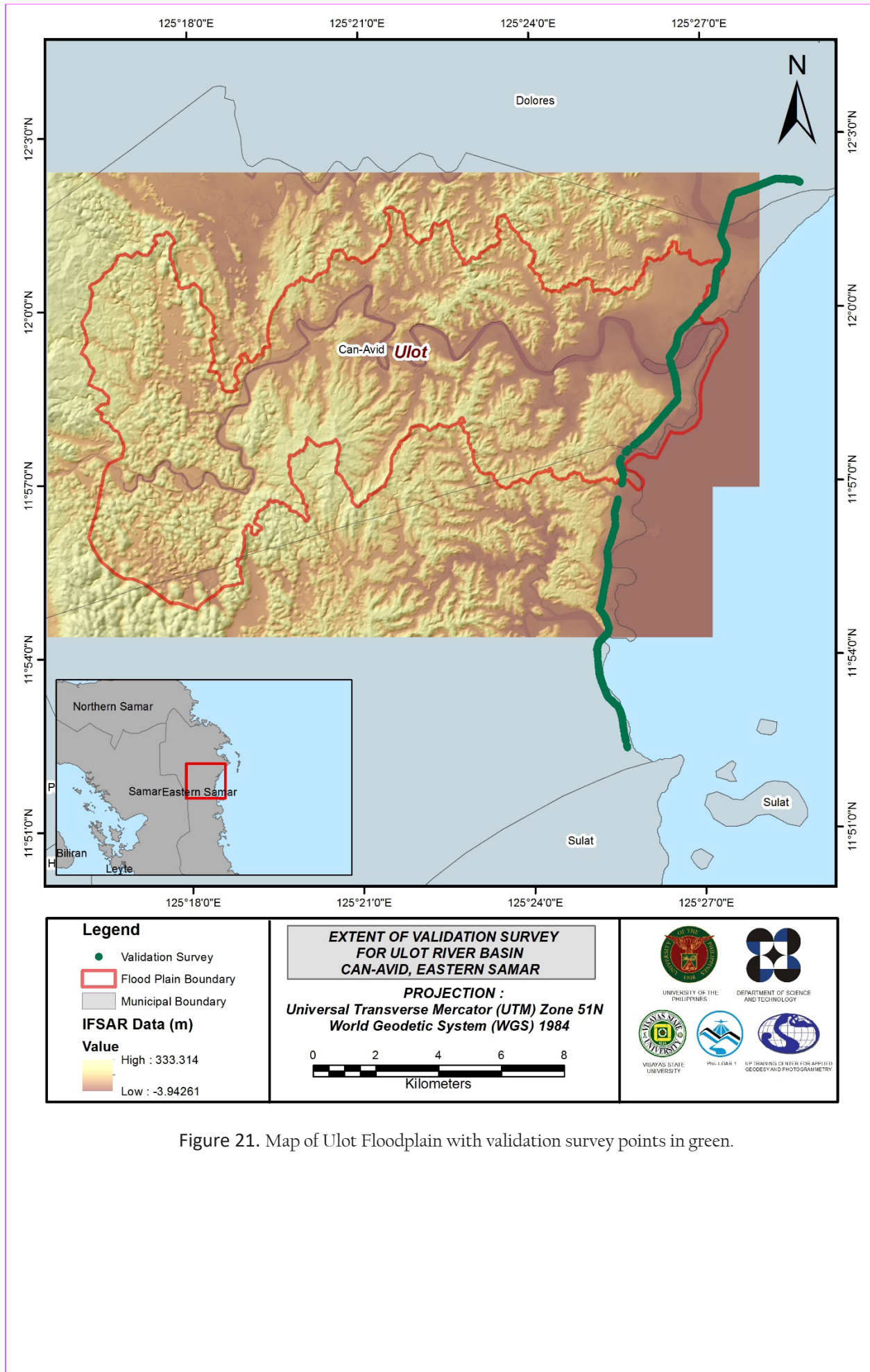


Figure 21. Map of Ulot Floodplain with validation survey points in green.



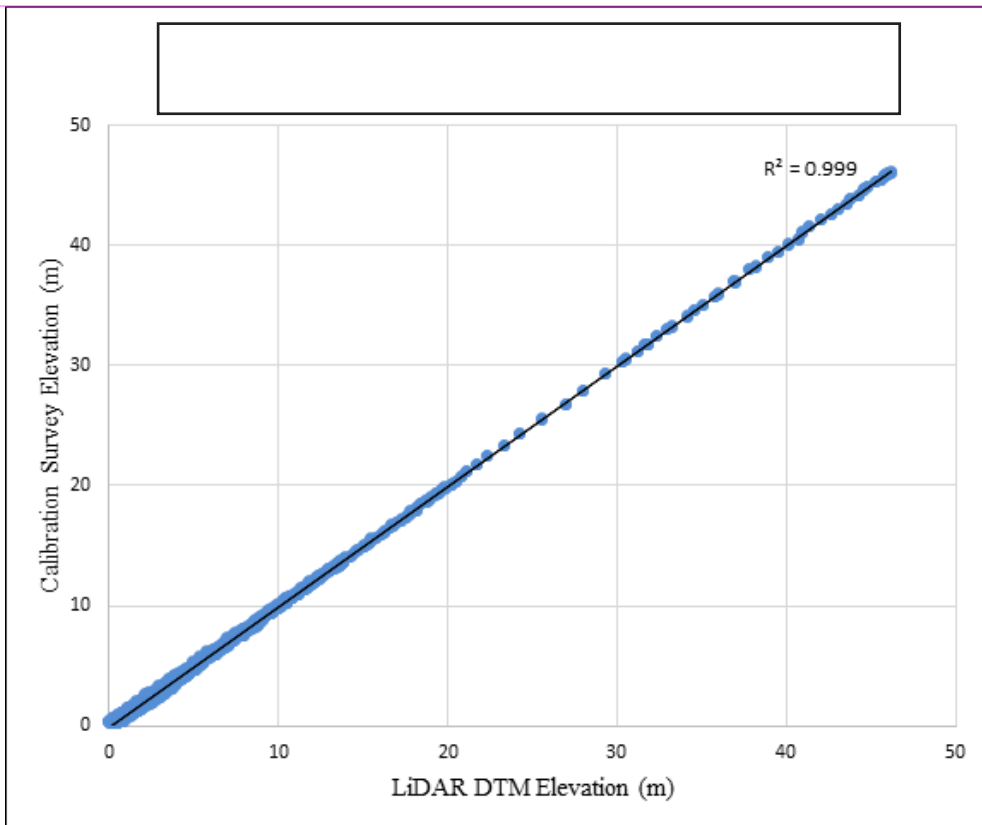


Figure 22. Correlation plot between calibration survey points and LiDAR data

Table 13. Calibration statistical measures.

Calibration Statistical Measures	Value (meters)
Height Difference	0.14
Standard Deviation	0.13
Average	-0.05
Minimum	-0.32
Maximum	0.22

A total of 384 survey points were used for the validation of the calibrated Ulot DTM. A good correlation between the calibrated mosaicked IFSAR elevation values and the ground survey elevation, which reflects the quality of the IFSAR DTM is shown in Figure 23. The computed RMSE between the calibrated IFSAR DTM and validation elevation values is 2.00 meters with a standard deviation of 0.89 meters, as shown in Table 14.

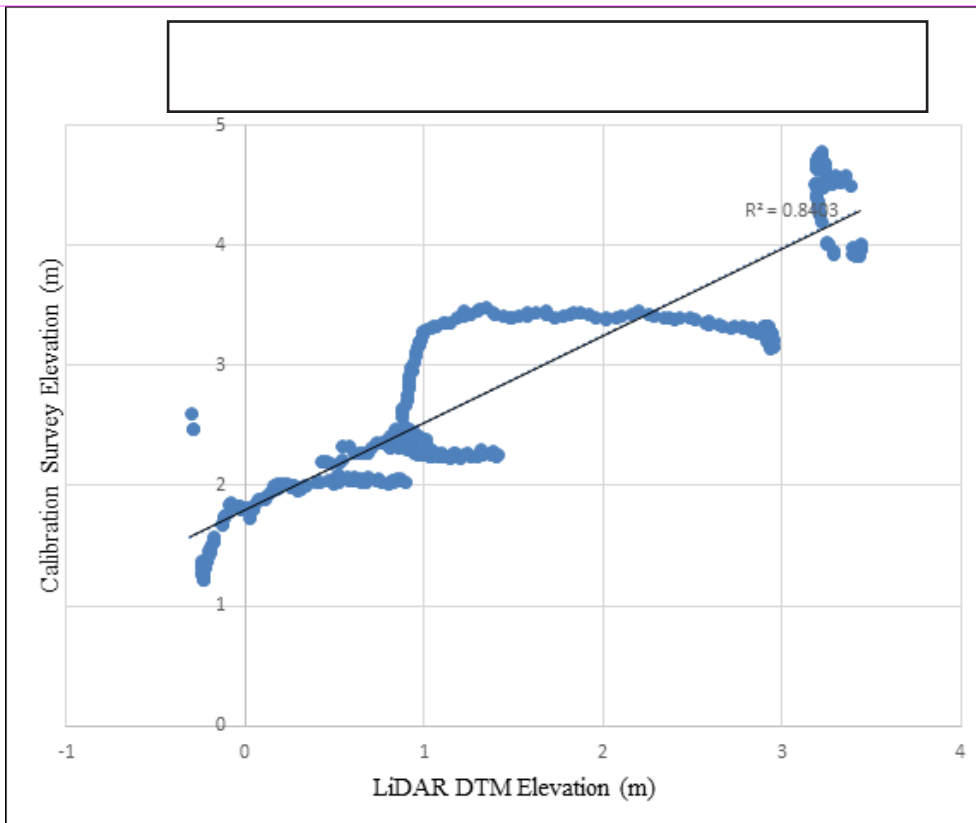


Figure 23. Correlation plot between validation survey points and IFSAR data

Table 14. Validation statistical measures.

Validation Statistical Measures	Value (meters)
RMSE	1.46
Standard Deviation	0.51
Average	1.37
Minimum	0.22
Maximum	2.90

Note: Validation points lie within the IFSAR data, thus, the RMSE and Standard Deviation values are obtained are still acceptable.

### 3.11 Integration of Bathymetric Data into the LiDAR Digital Terrain Model

For bathy integration, centerline and zigzag are the available data for Ulot with 49,742 bathymetric survey points. The resulting raster surface was obtained using the Kernel Interpolation with Barriers method. After burning the bathymetric data to the calibrated DTM, assessment of the interpolated surface is represented by the computed RMSE value of 0.46 meters. The extent of the bathymetric data surveyed by the Data Validation and Bathymetry Component (DVBC) in Ulot integrated with the processed IFSAR DEM is shown in Figure 24.

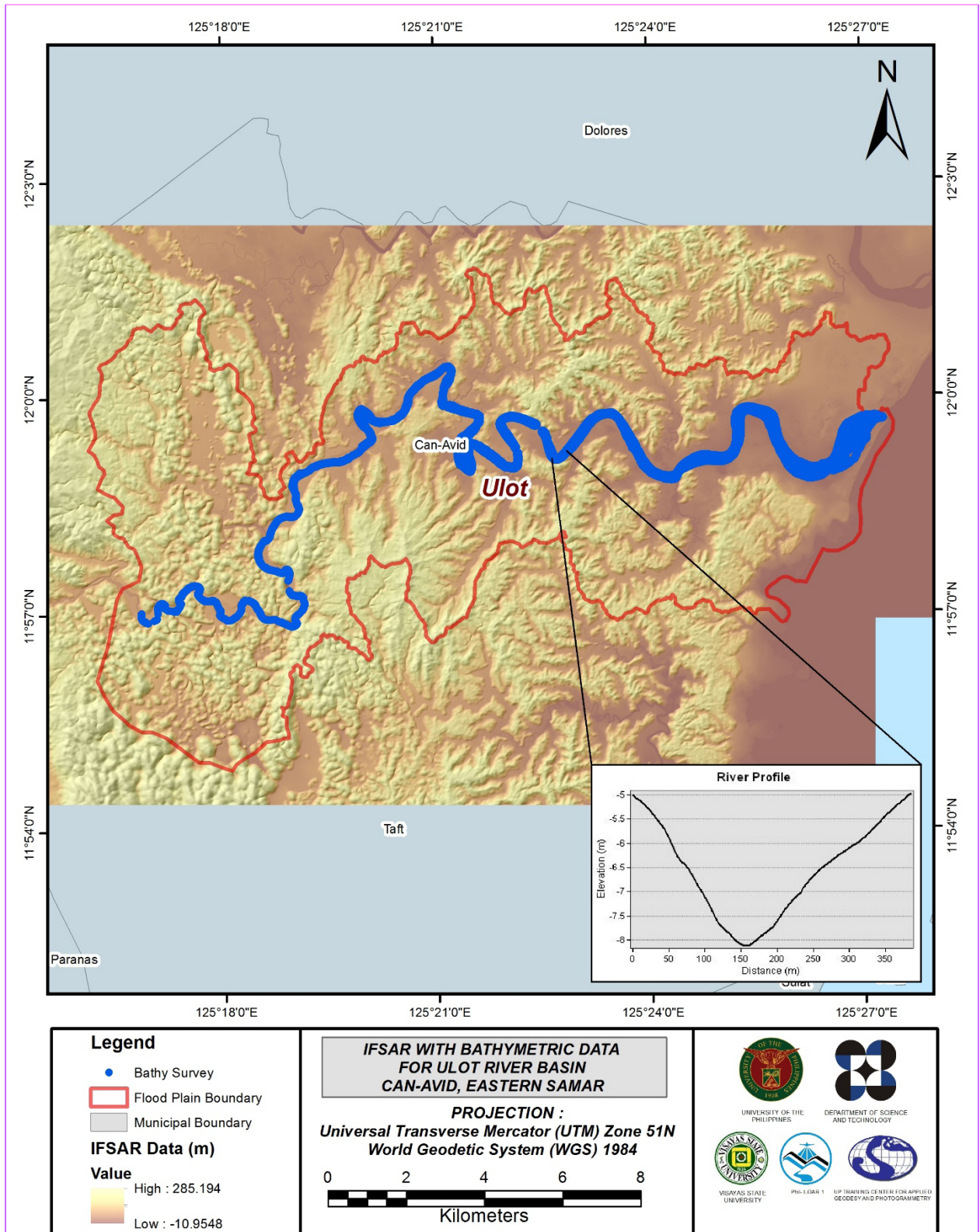


Figure 24. Map of Ulot Floodplain with bathymetric survey points shown in blue.

### 3.12 Feature Extraction

The features salient in flood hazard exposure analysis include buildings, road networks, bridges, and water bodies within the floodplain area with a 200-meter buffer zone. Due to unavailability of LiDAR data in Ulot Floodplain, Google Earth images taken on July 12, 2014, May 10, 2015, and July 17, 2015 were used as bases for the extraction of exposed features.

Ulot Floodplain, including its 200 m buffer, has a total area of 157.15 sq km. Figure X shows the extent of

the floodplain with buffer (in white) and the extracted building features (in red).

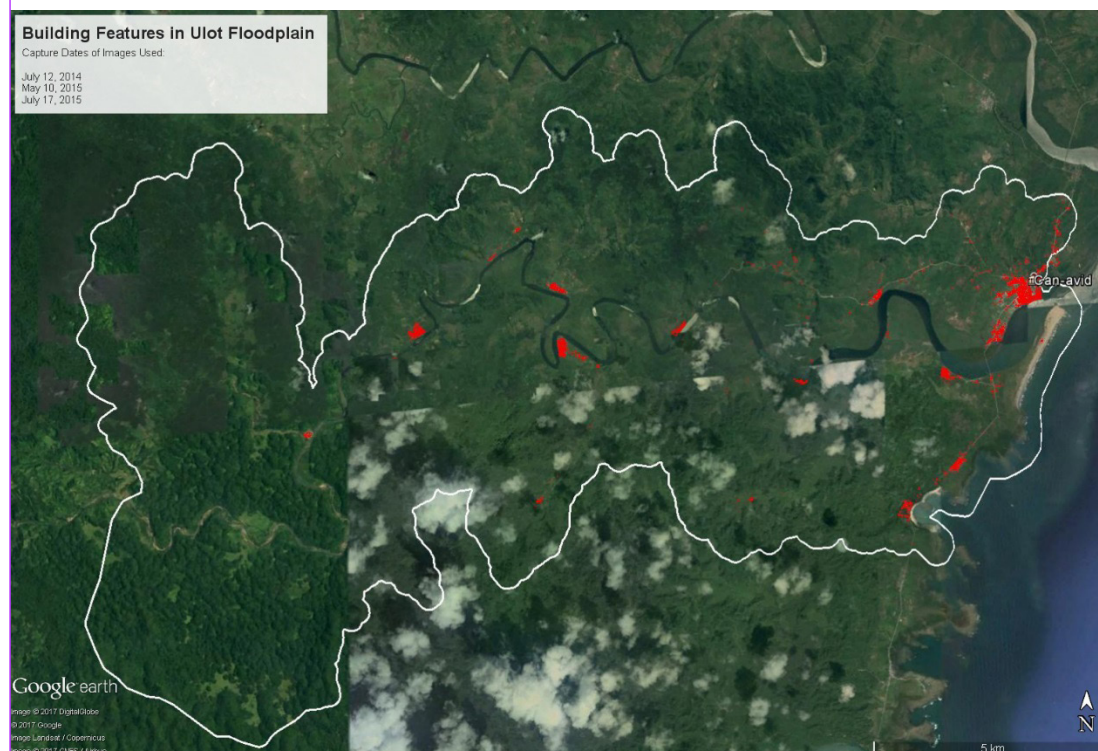


Figure 25. Ulot building features extracted from Google Earth images.

### 3.12.1 Quality Checking of Digitized Features' Boundary

For feature attribution, the digitized features were marked and coded in the field using handheld GPS receivers. The attributes of non-residential buildings were first identified; all other buildings were then coded as residential. Table 15 summarizes the number of building features per type. On the other hand, Table 16 shows the total length of each road type, while Table 17 shows the number of water features extracted per type.

Table 15. Building features extracted for Ulot Floodplain.

Facility Type	No. of Features
Residential	4,930
School	70
Market	3
Agricultural/Agro-Industrial Facilities	0
Medical Institutions	3
Barangay Hall	12
Military Institution	0
Sports Center/Gymnasium/Covered Court	6
Telecommunication Facilities	2
Transport Terminal	0
Warehouse	1
Power Plant/Substation	0
NGO/CSO Offices	1
Police Station	1
Water Supply/Sewerage	0
Religious Institutions	7

Bank	0
Factory	0
Gas Station	1
Fire Station	1
Other Government Offices	6
Other Commercial Establishments	31
<b>Total</b>	<b>5,075</b>

Table 16. Total length of extracted roads for Ulot Floodplain.

Floodplain	Road Network Length (km)					Total
	Barangay Road	City/Municipal Road	Provincial Road	National Road	Others	
Ulot	56.03	5.70	0.00	8.76	0.00	<b>70.50</b>

Table 17. Number of extracted water bodies for Ulot Floodplain.

Floodplain	Water Body Type					Total
	Rivers/Streams	Lakes/Ponds	Sea	Dam	Fish Pen	
Ulot	50	1	0	0	0	<b>51</b>

A total of 17 bridges and culverts over small channels that are part of the river network were also extracted for the floodplain.

### 3.12.2 Final Quality Checking of Extracted Features

All extracted ground features were completely given the required attributes. All these output features comprise the flood hazard exposure database for the floodplain. This completes the feature extraction phase of the project.

Figure 26 shows the Interferometric Synthetic Aperture Radar Digital Elevation Model (IFSAR DEM) of Ulot Floodplain overlaid with its ground features.



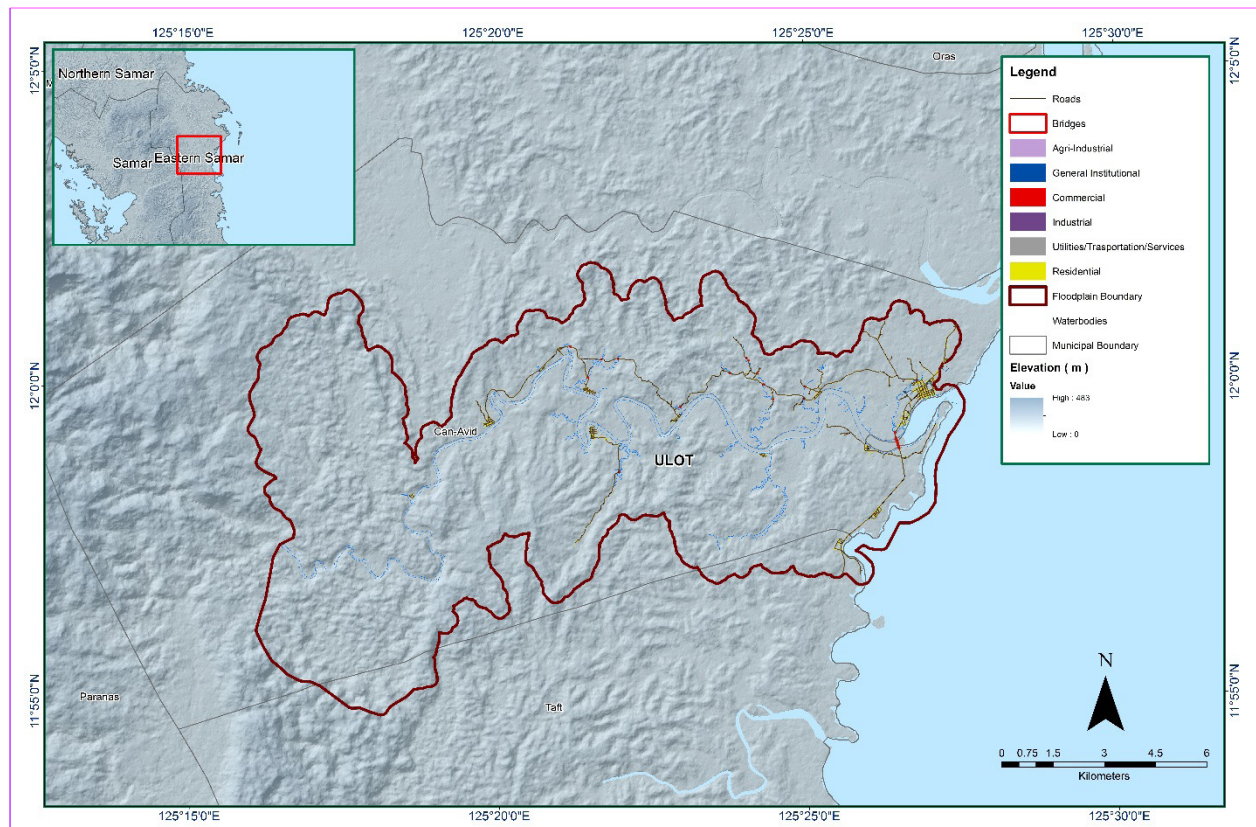


Figure 26. Extracted features for Ulot Floodplain.

## **CHAPTER 4: LIDAR VALIDATION SURVEY AND MEASUREMENTS IN THE ULOT RIVER BASIN**

*Engr. Louie P. Balicanta, Engr. Joemarie S. Caballero, Ms. Patrizia Mae. P. dela Cruz, Engr. Kristine Ailene B. Borromeo Mr. Michael Anthony C. Labrador, Mr. Erlan Patrick T. Mendoza, Engr. Romalyn Francis P. Boado, For. Maridel P. Miras, For. Rodel C. Alberto, Engr. Caren Joy S. Ordoña*

The methods applied in this chapter were based on the DREAM methods manual (Balicanta et al., 2014) and further enhanced and updated in Paringit et al. (2017).

### **4.1 Summary of Activities**

AB Surveying and Development (ABSD) conducted a field survey in Ulot River on April 7, 11, 12, to 14, 19 to 23 and 27, 2016, May 8 to 10, 13, 14 and 16, 2016 with the following scope: reconnaissance; control survey; and cross-section and as-built survey at Can-Avid Bridge in Brgy. Canteros, Municipality of Can-Avid, Eastern Samar. Random checking points for the contractor's cross-section and bathymetry data were gathered by DVBC on August 11, 2016 using a Trimble® SPS 882 GNSS PPK survey technique. In addition to this, validation points acquisition survey was conducted covering the Ulot River Basin area. The entire survey extent is illustrated in Figure 27.

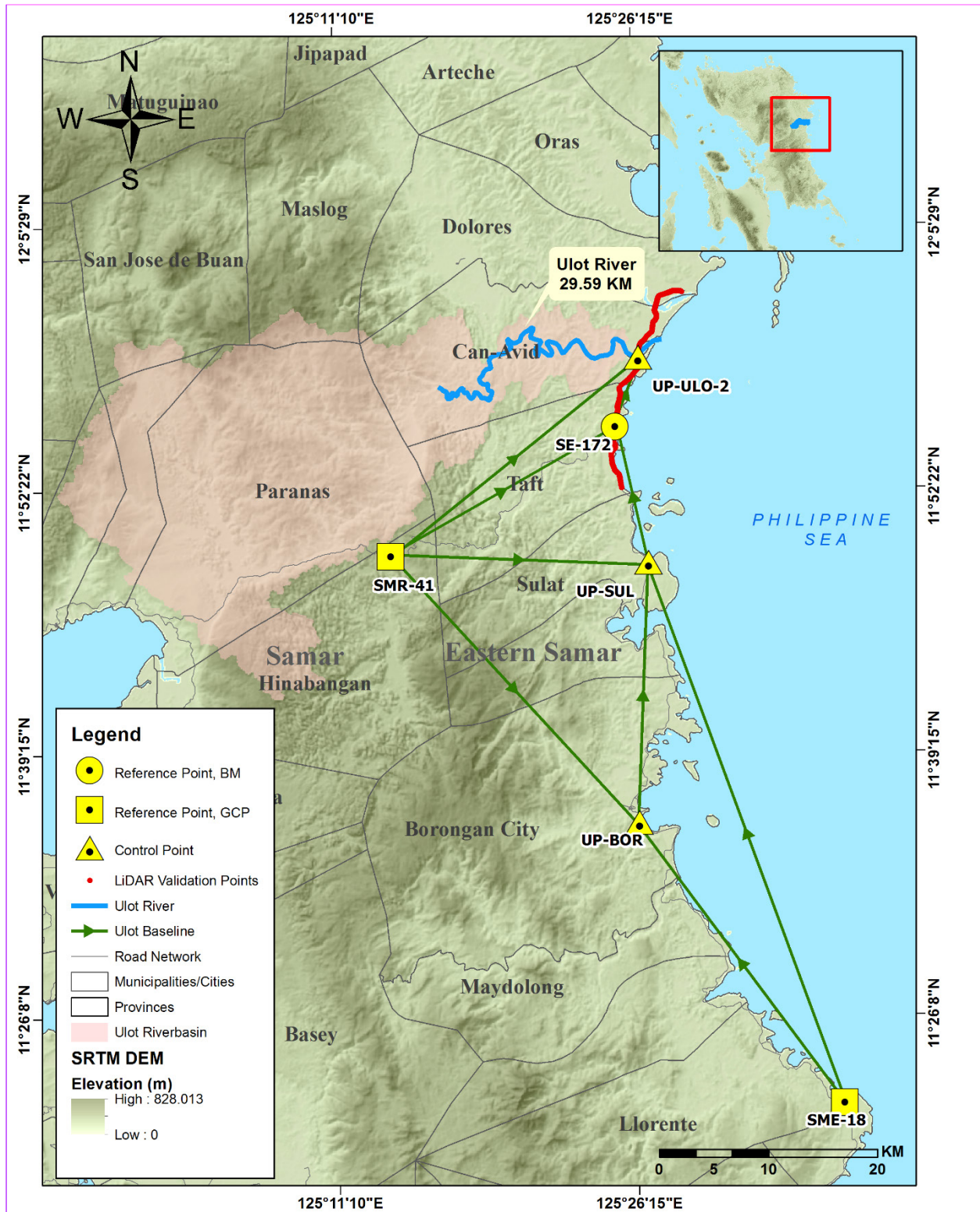


Figure 27. Ulot River Survey Extent



## 4.2 Control Survey

The GNSS network used for Ulot River is composed of four (4) loops established on December 6, 2016 occupying the following reference points: SMR-41, a second-order GCP, in Brgy. Bagacay, Municipality of Hinabanga, Eastern Samar; SE-142, a first-order BM, in Brgy. Nato, Municipality of Taft, Eastern Samar; and SME-18, a second-order GCP, in Brgy. San Jose, Municipality of Hernani, Eastern Samar.

Three (3) control points established in the area were also occupied: UP\_ULO-2, located at the approach of Can-Avid Bridge in Brgy. Canteros, Municipality of Can-Avid, Province of Eastern Samar; UP-SUL, located at the approach of Sulat Bridge in Brgy. Maramara, Municipality of Sulat, Province of Eastern Samar; and UP-BOR, located at the approach of Can-Obing Bridge in Brgy. Can-Abong, Borongan City, Province of Eastern Samar.

The summary of reference and control points and its location is summarized in Table 18 while GNSS network established is illustrated in Figure 28.

Table 18. List of reference and control points used during the survey in Ulot River (Source: NAMRIA, UP-TCAGP)

Control Point	Order of Accuracy	Geographic Coordinates (WGS 84)				
		Latitude	Longitude	Ellipsoid Height (m)	Elevation (MSL) (m)	Date of Establishment
SMR-41	2nd order, GCP	11°49' 03.09527 "N	125°13'56.04672"E	232.562	171.203	2007
SME-18	2nd order, GCP	11°21' 43.08128 "N	125°36'37.41861"E	78.216	17.659	2007
SE-172	1st order, BM	11°55'25.95794" N	125° 25' 18.96211"E	61.761	3.155	2007
UP_ULO-2	Established	11°58'54.06226" N	125°26'29.62952"E	63.770	5.912	05-02-16
UP-SUL	Established	11°48'41.00280" N	125°26'56.90219"E	64.565	5.374	12-06-2016
UP-BOR	Established	11°35'44.89710" N	125°26'23.64085"E	67.048	5.989	12-06-2016

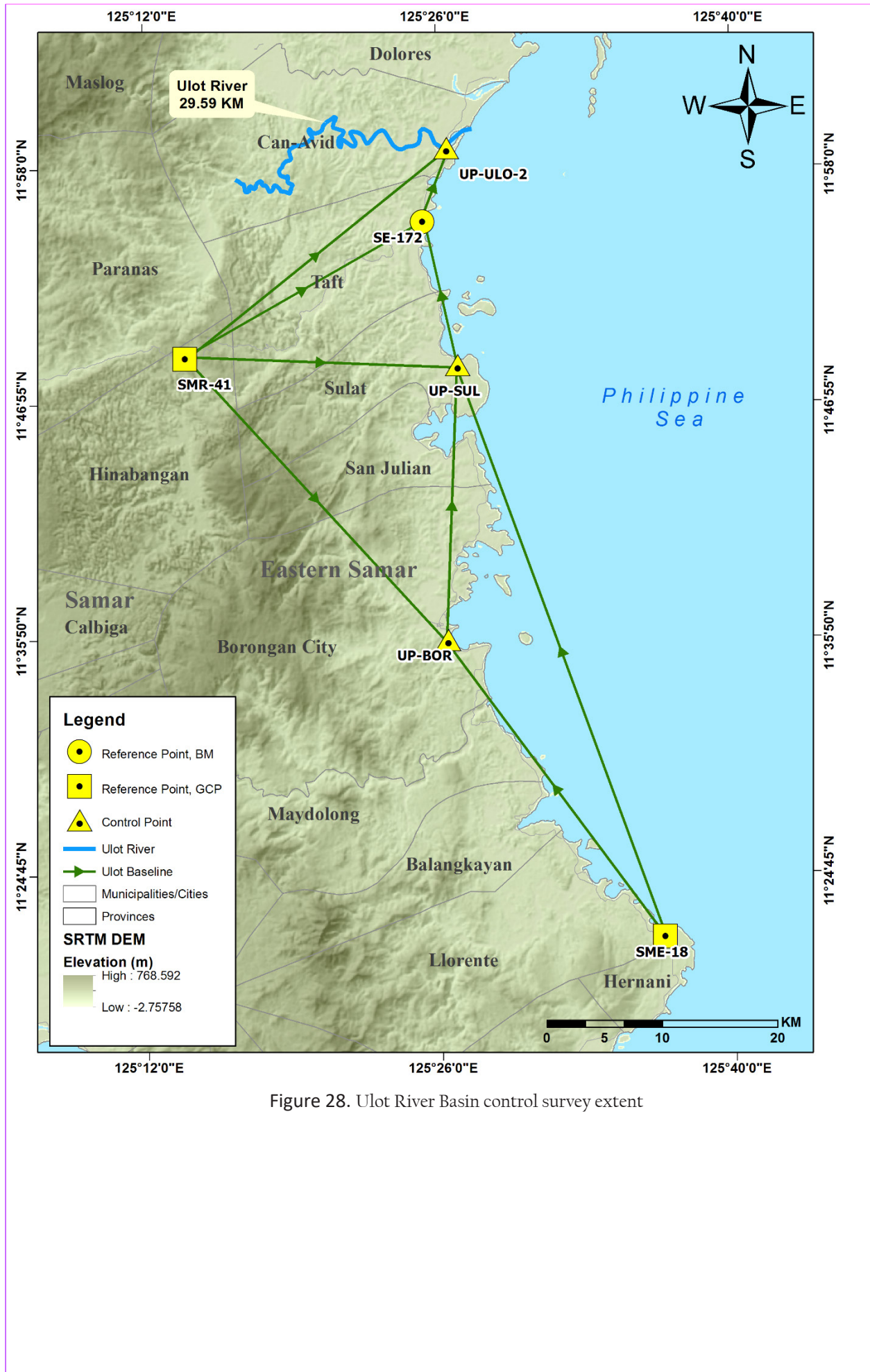


Figure 28. Ulot River Basin control survey extent

The GNSS set-ups on recovered reference points and established control points in Ulot River are shown from Figure 29 to Figure 34.



Figure 29. GNSS receiver setup, Trimble® SPS 882 at SMR-41, located at Bagacay Elementary School in Brgy. Bagacay, Hinabangan, Eastern Samar

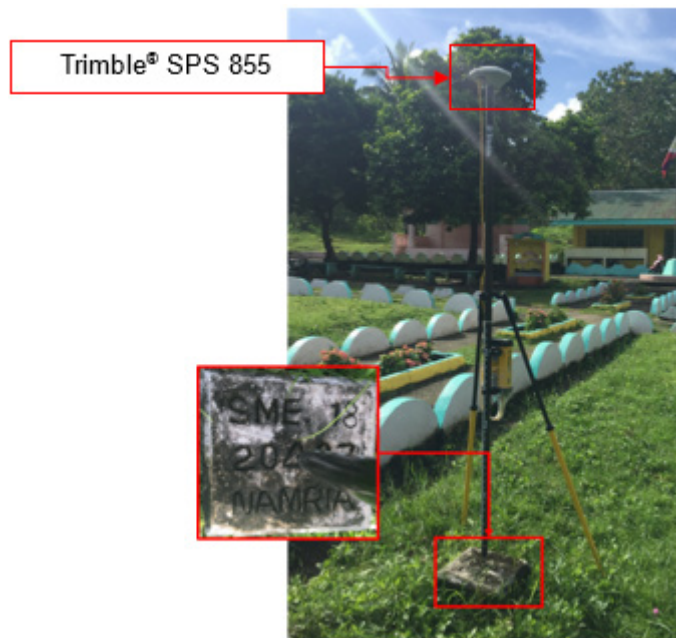


Figure 30. GNSS receiver set up, Trimble® SPS 855, at SME-18, located inside San Jose Elementary School in Brgy. San Jose, Hernani, Eastern Samar



Figure 31. GNSS receiver set up, Trimble® SPS 855, at SE-172, located inside Nato Elementary School in Brgy. Nato, Taft, Eastern Samar

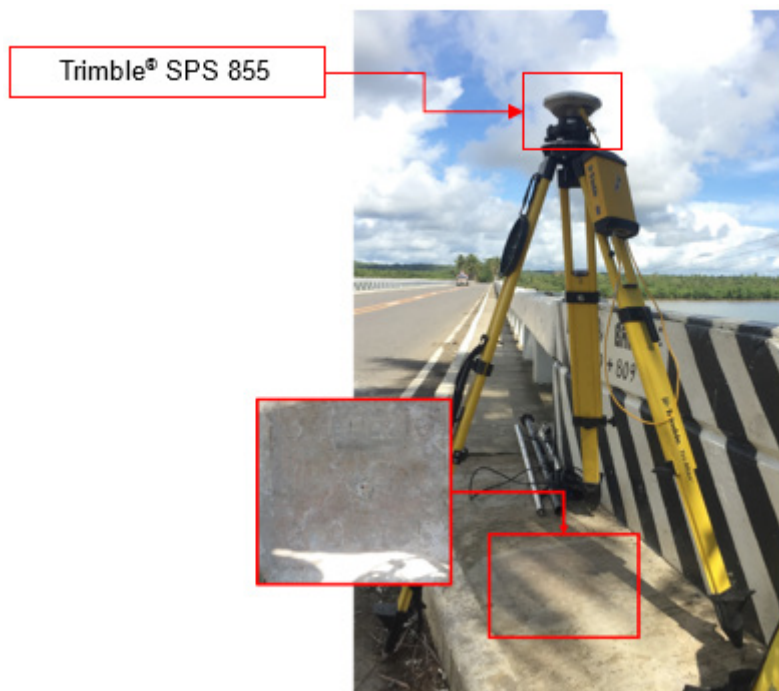


Figure 32. GNSS receiver setup, Trimble® SPS 855, at UP\_ULO-2, located at the approach of Can-Avid Bridge in Brgy. Canteros, Can-Avid, Eastern Samar





Figure 33. GNSS receiver setup, Trimble® SPS 985, at UP-SUL, located at the approach of Sulat Bridge in Brgy. Maramara, Sulat, Eastern Samar



Figure 34. GNSS receiver setup, Trimble® SPS 855, at UP-BOR, located at the approach of Can-Obing Bridge in Brgy. Can-Abong, Borongan City, Eastern Samar

### 4.3 Baseline Processing

GNSS baselines were processed simultaneously in TBC by observing that all baselines have fixed solutions with horizontal and vertical precisions within +/- 20 cm and +/- 10 cm requirement, respectively. In case where one or more baselines did not meet all of these criteria, masking is performed. Masking is done by removing/masking portions of these baseline data using the same processing software. It is repeatedly processed until all baseline requirements are met. If the reiteration yields out of the required accuracy, resurvey is initiated. Baseline processing result of control points in Ulot River Basin is summarized in Table 19 generated by TBC software.

Table 19. Baseline processing report for Ulot River static survey

Observation	Date of Observation	Solution Type	H. Prec. (Meter)	V. Prec. (Meter)	Geodetic Az.	Ellipsoid Dist. (Meter)	Height (m)
SMR-41 --- SE-172	12-6-2016	Fixed	0.003	0.019	60°19'56	23782.994	-170.787
SMR -41--- UP_ULO-2	12-6-2016	Fixed	0.004	0.027	51°26'56"	29152.677	-168.797
SE-172 --- UP_ULO-2	12-6-2016	Fixed	0.003	0.014	18°29'10"	6742.890	2.008
SMR-41--- UP-SUL	12-6-2016	Fixed	0.003	0.025	91°37'24"	23648.007	-168.014
SME-18 --- UP-SUL	12-6-2016	Fixed	0.005	0.019	340°32'04"	52735.660	-13.625
UP-SUL --- SE-172	12-6-2016	Fixed	0.003	0.018	346°36'16"	12792.116	-2.807
UP-BOR --- UP-SUL	12-6-2016	Fixed	0.003	0.014	2°25'05"	23870.045	-2.491
SMR-41 --- UP-BOR	12-6-2016	Fixed	0.003	0.018	137°16'15"	33379.379	-165.537
SME-18 --- UP-BOR	12-6-2016	Fixed	0.003	0.012	324°17'43"	31862.093	-11.163

As shown Table 19, a total of nine (9) baselines were processed with coordinate and ellipsoidal height values of SMR-41 held fixed. All of them passed the required accuracy.

#### 4.4 Network Adjustment

After the baseline processing procedure, network adjustment is performed using TBC. Looking at the adjusted grid coordinates table of the TBC generated network adjustment report, it is observed that the square root of the squares of x and y must be less than 20 cm and z less than 10 cm in equation form:

$$\sqrt{(x_e)^2 + (y_e)^2} < 20 \text{ cm and } z_e < 10 \text{ cm}$$

Where:

- $x_e$  is the Easting Error,
- $y_e$  is the Northing Error, and
- $z_e$  is the Elevation Error

for each control point. See the network adjustment report shown from Table 20 to Table 22 for the complete details.

The six (6) control points, SMR-41, SME-18, SE-172, UP\_ULO-2, UP-SUL and UP-BOR were occupied and observed simultaneously to form a GNSS loop. The coordinates and ellipsoidal height of SMR-41 were held fixed during the processing of the control points as presented in Table 20. Through this reference point, the coordinates and ellipsoidal height of the unknown control points will be computed.

Table 20. Control point constraints

Point ID	Type	East (Meter)	$\sigma$	North (Meter)	$\sigma$	Height (Meter)	$\sigma$	Elevation (Meter)	$\sigma$
SE-172	Grid							Fixed	
SME-18	Grid	Fixed		Fixed				Fixed	
SMR-41	Global	Fixed		Fixed					



Fixed = 0.000001(Meter)					
-------------------------	--	--	--	--	--

Table 21. Adjusted grid coordinates

Point ID	Easting (Meter)	East-ing Error (Meter)	Northing (Meter)	Northing Error (Meter)	Elevation (Meter)	Elevation Error (Meter)	Constraint
SE-172	763795.614	0.007	1319288.604	0.006	3.155	?	e
SMR-41	743218.063	?	1307346.858	?	171.203	0.041	LLh
SME-18	784907.431	?	1257282.043	?	17.659	?	ENe
UP_ULO-2	UP_ULO-2	0.010	1325704.856	0.009	5.912	0.053	
UP-SUL	766869.986	0.007	1306865.645	0.006	5.374	0.042	
UP-BOR	766068.889	0.006	1282998.400	0.005	5.989	0.039	

With the mentioned equation, for horizontal and for the vertical; the computation for the accuracy are as follows:

**SE-172**

$$\begin{aligned} \text{horizontal accuracy} &= \sqrt{(0.7)^2 + (0.6)^2} \\ &= \sqrt{0.49 + 0.36} \\ &= 0.85 < 20 \text{ cm} \\ \text{vertical accuracy} &= \text{Fixed} \end{aligned}$$

**SMR-41**

$$\begin{aligned} \text{horizontal accuracy} &= \text{Fixed} \\ \text{vertical accuracy} &= 0.041 < 20 \text{ cm} \end{aligned}$$

**SME-18**

$$\begin{aligned} \text{horizontal accuracy} &= \text{Fixed} \\ \text{vertical accuracy} &= \text{Fixed} \end{aligned}$$

**UP\_ULO-2**

$$\begin{aligned} \text{horizontal accuracy} &= \sqrt{(1.0)^2 + (0.9)^2} \\ &= \sqrt{1.0 + 0.81} \\ &= 1.81 < 20 \text{ cm} \\ \text{vertical accuracy} &= 5.3 < 10 \text{ cm} \end{aligned}$$

**UP-SUL**

$$\begin{aligned} \text{horizontal accuracy} &= \sqrt{(0.7)^2 + (0.6)^2} \\ &= \sqrt{0.49 + 0.36} \\ &= 0.85 < 20 \text{ cm} \\ \text{vertical accuracy} &= 4.2 < 10 \text{ cm} \end{aligned}$$

**UP-BOR**

$$\begin{aligned} \text{horizontal accuracy} &= \sqrt{(0.6)^2 + (0.5)^2} \\ &= \sqrt{0.36 + 0.25} \\ &= 0.61 < 20 \text{ cm} \\ \text{vertical accuracy} &= 3.9 < 10 \text{ cm} \end{aligned}$$

Following the given formula, the horizontal and vertical accuracy result of the six (6) occupied control points are within the required precision.

Table 22. Adjusted geodetic coordinates

Point ID	Latitude	Longitude	Height (Meter)	Height Error (Meter)	Constraint
SE-172	N11°55'25.95794"	E125°25'18.96211"	61.761	?	e
SMR-41	N11°49'03.09527"	E125°13'56.04672"	232.562	0.041	LLh
SME-18	N11°21'43.08128"	E125°36'37.41861"	78.216	?	ENe
UP_ULO-2	N11°58'54.06226"	E125°26'29.62952"	63.770	0.053	
UP-SUL	N11°48'41.00280"	E125°26'56.90219"	64.565	0.042	
UP-BOR	N11°35'44.89710"	E125°26'23.64085"	67.048	0.039	

The corresponding geodetic coordinates of the observed points are within the required accuracy as shown in Table 22. Based on the result of the computation, the equation is satisfied; hence, the required accuracy for the program was met.

The summary of reference control points used is indicated in Table 23.

Table 23. Reference and control points used and its location (Source: NAMRIA, UP-TCAGP)

Control Point	Order of Accuracy	Geographic Coordinates (WGS 58)			UTM ZONE 51 N		
		Latitude	Longitude	Ellipsoidal Height (Meter)	Northing (m)	Easting (m)	BM Ortho (m)
<a href="#">SE-172</a>	1st order, BM	11°55'25.95794"N	125°25'18.96211"E	61.761	1319288.604	763795.614	3.155
<a href="#">SMR-41</a>	2nd order, GCP	11°49'03.09527"N	125°13'56.04672"E	232.562	1307346.858	743218.063	171.203
<a href="#">SME-18</a>	2nd order, GCP	11°21'43.08128"N	125°36'37.41861"E	78.216	1257282.043	784907.431	17.659
<a href="#">UP_ULO-2</a>	Established	11°58'54.06226"N	125°26'29.62952"E	63.770	1325704.856	765878.376	5.912
<a href="#">UP-SUL</a>	Established	11°48'41.00280"N	125°26'56.90219"E	64.565	1306865.645	766869.986	5.374
<a href="#">UP-BOR</a>	Established	11°35'44.89710"N	125°26'23.64085"E	67.048	1282998.400	766068.889	5.989

#### 4.5 Bridge Cross-section and As-built Survey, and Water Level Marking

Cross-section and as-built surveys were conducted on May 14, 2016 by ABSD at the upstream side of Can-Avid Bridge in Brgy. Canteros, Municipality of Can-Avid, Eastern Samar as shown in Figure 35. A Horizon® Total Station was utilized for this survey as shown in Figure 36.



Figure 35. Upstream/downstream side of Can-Avid Bridge



Figure 36. As-built survey of Can-Avid Bridge

The cross-sectional line of Can-Avid Bridge is about 549.572 m with twenty-seven (52) cross-sectional points using the control points UP\_ULO-1 and UP\_ULO-2 as the GNSS base stations. The location map, cross-section diagram, and the bridge data form are shown in Figure 37 to Figure 39.

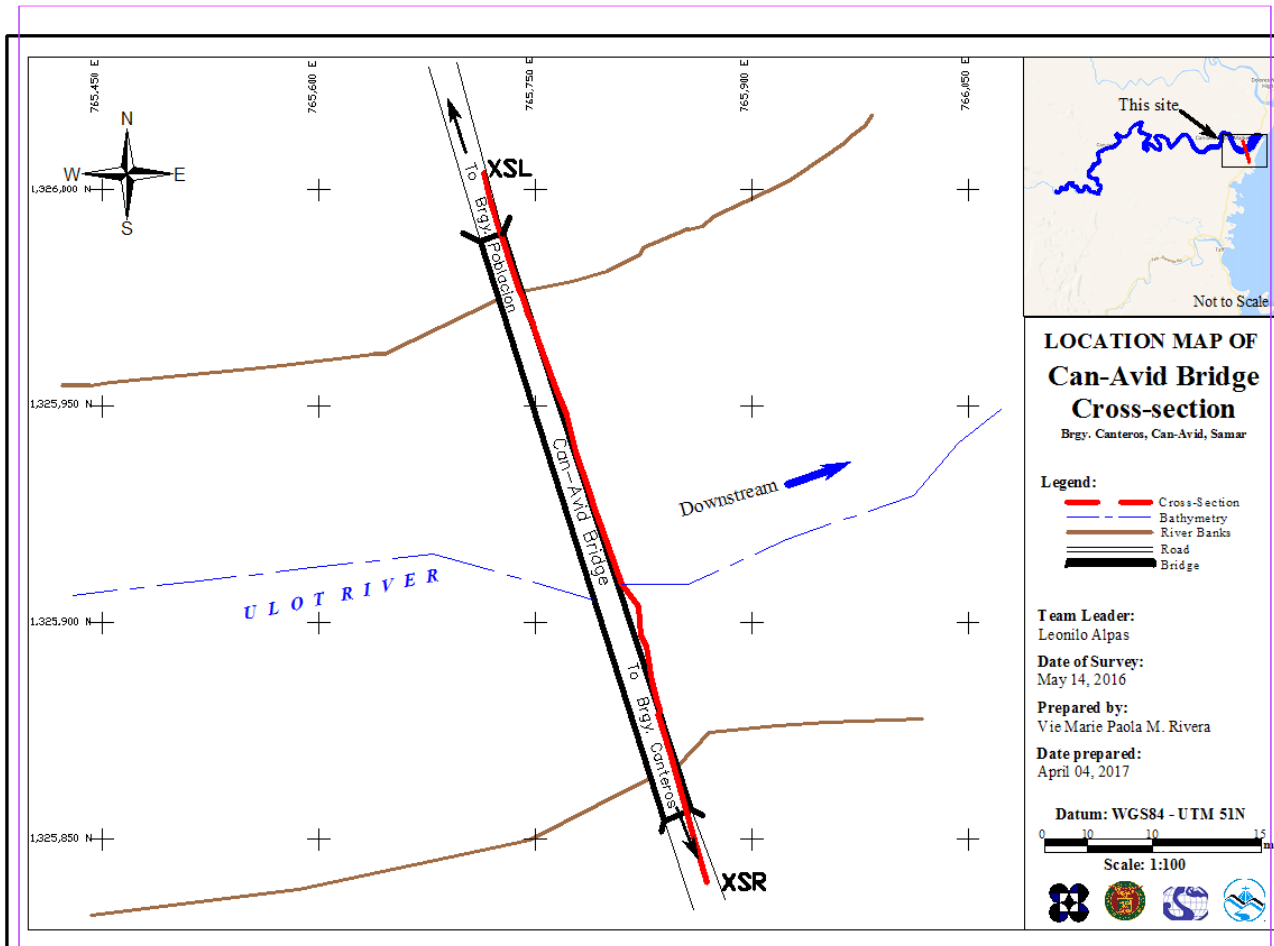


Figure 37. Can-Avid bridge location map



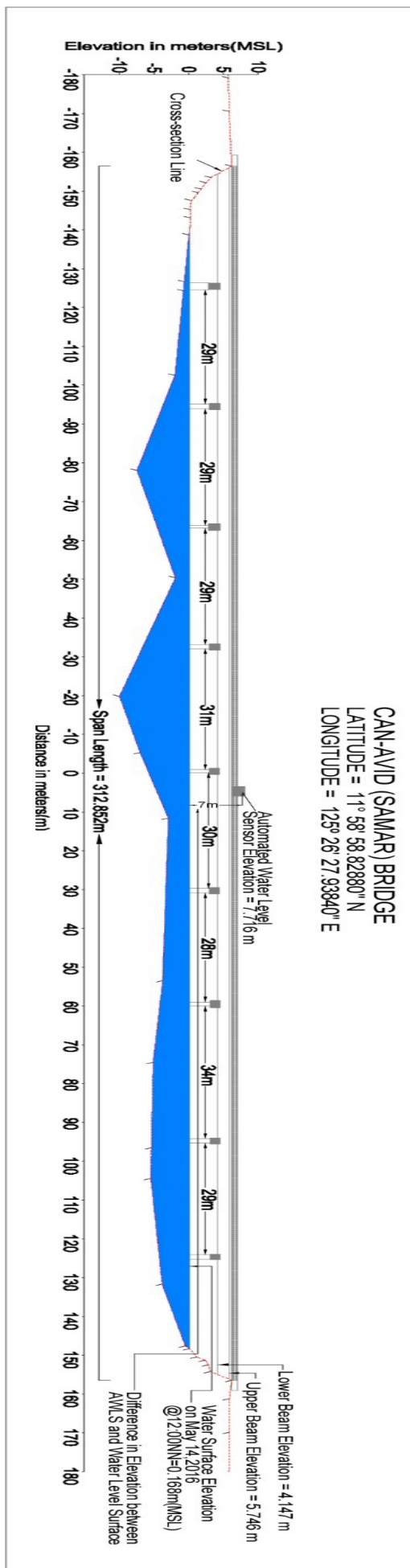
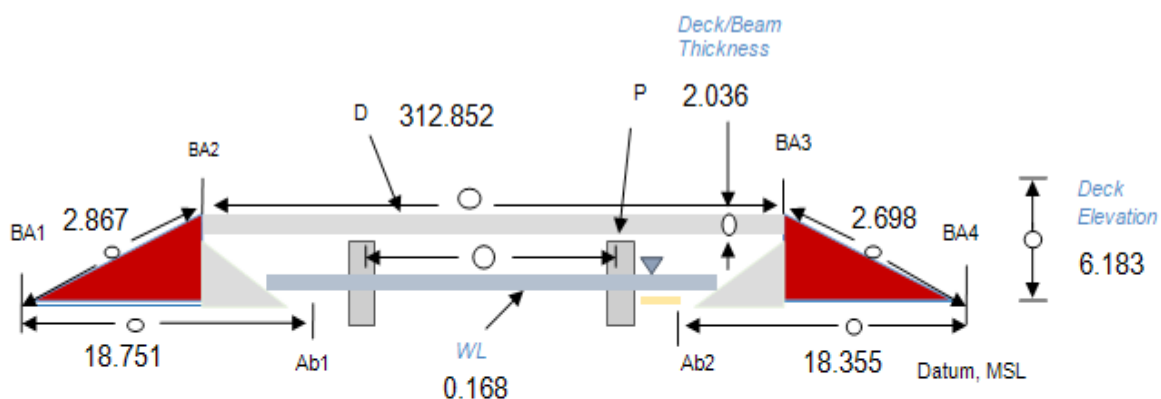


Figure 38. Can-Avid Bridge cross-section diagram

### Bridge Data Form



**Legend:**

BA = Bridge Approach

P = Pier

Ab = Abutment

D = Deck

WL = Water Level/Surface

MSL = Mean Sea Level

○ = Measurement Value

Line Segment	Measurement (m)	Remarks
1. BA1-BA2	2.867 m	
2. BA2-BA3	312.852 m	
3. BA3-BA4	2.698m	
4. BA1-Ab1	18.751 m	
5. Ab2-BA4	18.355 m	
6. Deck/beam thickness	2.036 m	
7. Deck elevation	6.183 m	

Note: Observer should be facing downstream

Figure 39. Can-Avid bridge data sheet

Water surface elevation of Ulot River was determined by a Horizon® Total Station on May 14, 2016 at 12:00 P.M. at Can-Avid Bridge area with a value of 0.168 m in MSL as shown in Figure 39. This was translated into marking on the bridge's pier as shown in Figure 40. The marking will serve as reference for flow data gathering and depth gauge deployment of the partner HEI responsible for Ulot River, Visayas State University.



Figure 40. Water-level markings on Can-Avid Bridge

#### **4.6 Validation Points Acquisition Survey**

Validation points acquisition survey was conducted by DVBC from December 10, 2016 using a survey grade GNSS Rover receiver, Trimble® SPS 882, mounted on a range pole which was attached in front of the vehicle as shown in Figure 41. It was secured with cable ties and ropes to ensure that it was horizontally and vertically balanced. The antenna height was 2.305m and measured from the ground up to the bottom of the quick release of the GNSS Rover receiver. The PPK technique utilized for the conduct of the survey was set to continuous topo mode with UP\_ULO-2 occupied as the GNSS base station in the conduct of the survey.



Figure 41. Validation points acquisition survey set-up for Ulot River

The survey started from Brgy. 12, Municipality of Dolores, Eastern Samar going southwest along the national highway and ended in Brgy. Mantang, Municipality of Taft, Eastern Samar. A total of 3,598 points were gathered with an approximate length of 19.05 km using UP\_ULO-2 as GNSS base station for the entire extent of validation points acquisition survey as illustrated in the map in Figure 42.





Figure 42. Validation points acquisition covering the Ulot River Basin area

#### 4.7 River Bathymetric Survey

Bathymetric survey was executed on May 13-18, 2016 using a Hi-Target® echo sounder as illustrated in Figure 43. The survey started downstream in Brgy. 1 Poblacion, Municipality of Can-Avid, Eastern Samar with coordinates 11° 59' 42.46566"N, 125° 27' 2.79684"E and ended upstream in Brgy. Salvacion, Municipality of Can-Avid, Eastern Samar with coordinates 11° 57' 17.06983"N, 125° 16' 42.03552"E. The control points UP\_ULO-1 was used as GNSS base station all throughout the entire survey.



Figure 43. Bathymetric survey of ABSD at Ulot River using Hi-Target® echo sounder

Gathering of random points for the checking of ABSD's bathymetric data was performed by DVBC on August 11, 2016 using a Trimble® SPS 882 GNSS PPK survey technique, see Figure 44. A map showing the DVBC bathymetric checking points is shown in Figure 45.

Linear square correlation ( $R^2$ ) and RMSE analysis were performed on the two (2) datasets. The linear square coefficient range is determined to ensure that the submitted data of the contractor is within the accuracy standard of the project which is  $\pm 20$  cm and  $\pm 10$  cm for horizontal and vertical, respectively. The  $R^2$  value must be within 0.85 to 1. An  $R^2$  approaching 1 signifies a strong correlation between the vertical (elevation values) of the two datasets. A computed  $R^2$  value of 0.990 was obtained by comparing the data of the contractor and DVBC; signifying a strong correlation between the two (2) datasets.

In addition to the Linear Square correlation, Root Mean Square (RMSE) analysis is also performed in order to assess the difference in elevation between the DVBC checking points and the contractor's. The RMSE value should only have a maximum radial distance of 5 m and the difference in elevation within the radius of 5 meters should not be beyond 0.50 m. For the bathymetric data, a computed value of 0.260 was acquired. The computed  $R^2$  and RMSE values are within the accuracy requirement of the program.



Figure 44. Gathering of random bathymetric points along Ulot River

The bathymetric survey for Ulot River gathered a total of 55,722 points covering an approximate of 29.59 km of the river traversing Brgy. Canteros, Guibuangan, Malogo, Mabuhay, Jepaco, Baruk, Camantang, Canlly, and Salvacion in the Municipality of Can-Avid, Eastern Samar. A CAD drawing was also produced to illustrate the riverbed profile of Ulot River. As shown in Figure 47, the highest and lowest elevation has a 35-m difference. The highest elevation observed was -0.974 m below MSL located in Brgy. Camantang, Can-Avid, Eastern Samar while the lowest was -13.467 m below MSL located in Brgy. Canteros, Can-Avid, Eastern Samar.





Figure 45. Bathymetric survey of Ulot River



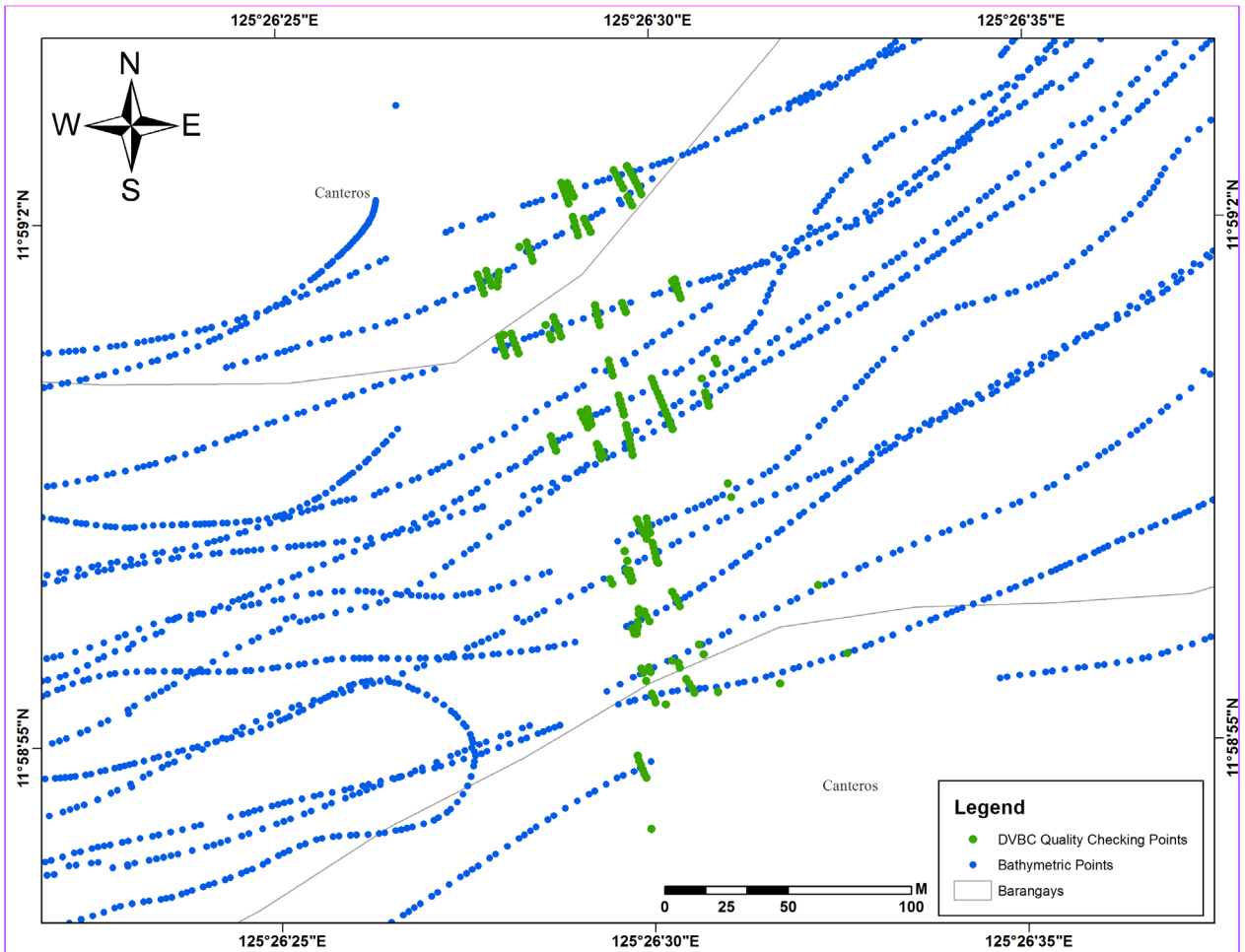


Figure 46. Quality checking points gathered along Ulot River by DVBC

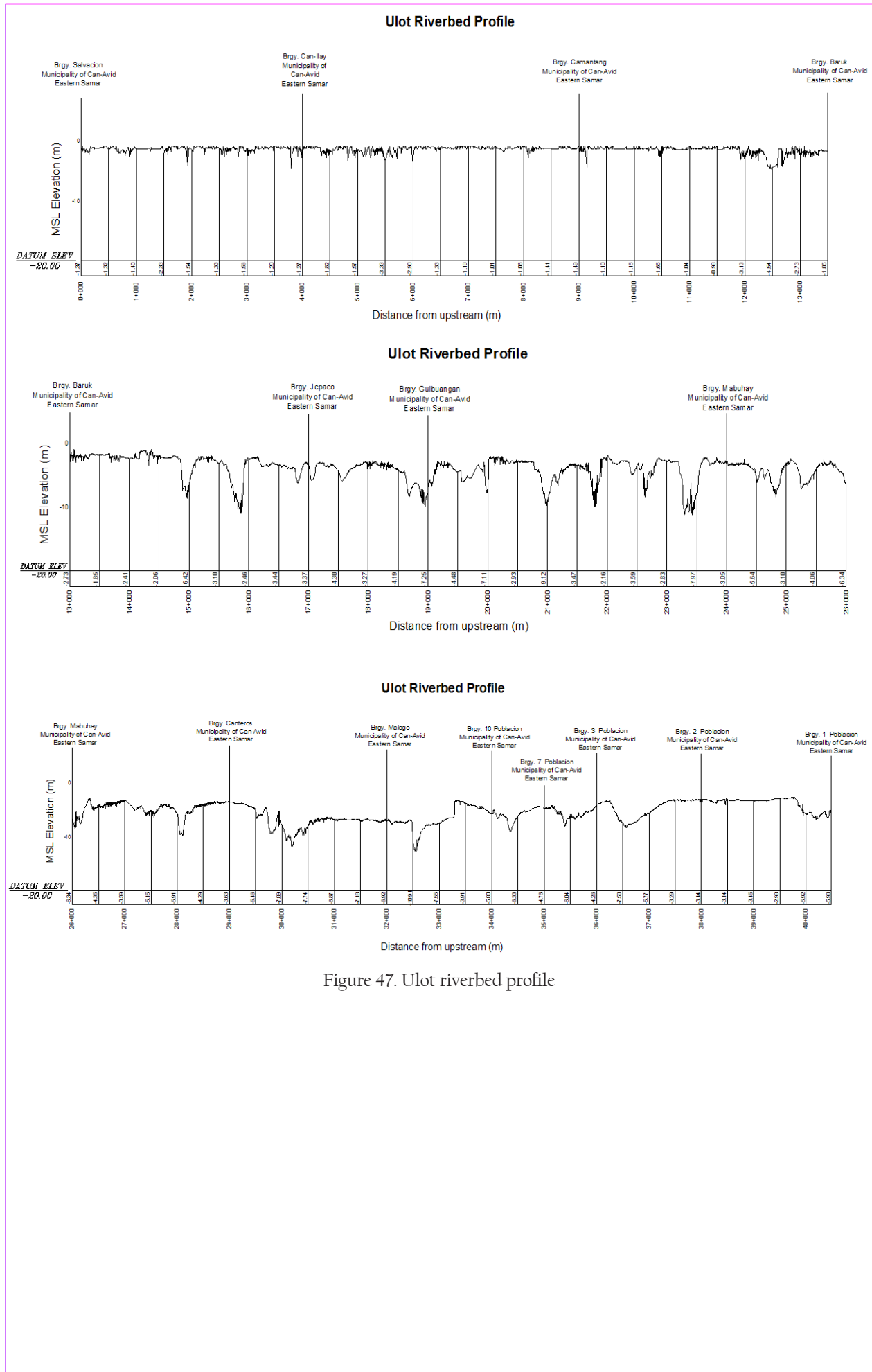


Figure 47. Ulot riverbed profile

## CHAPTER 5: FLOOD MODELING AND MAPPING

*Dr. Alfredo Mahar Lagmay, Christopher Uichanco, Sylvia Sueno, Marc Moises, Hale Ines, Miguel del Rosario, Kenneth Punay, Neil Tingin*

The methods applied in this chapter were based on the DREAM methods manual (Lagmay et al., 2014) and further enhanced and updated in Paringit et al. (2017).

### 5.1 Data Used for Hydrologic Modeling

#### 5.1.1 Hydrometry and Rating Curves

Rainfall, water level, and flow in a certain period of time, which may affect the hydrologic cycle of the Ulot River Basin, were monitored, collected, and analyzed.

#### 5.1.2 Precipitation

Precipitation data was taken from the installed rain gauge in Brgy. Cadian. The location of the rain gauges is seen in Figure 48.

Total rain from Cadian rain gauge is 253.2 mm. It peaked to 19.2 mm on 16 December 2016, 23:15. A summary of the data is seen in Table 24. The lag time between the peak rainfall and discharge is twenty three hours and thirty five minutes.

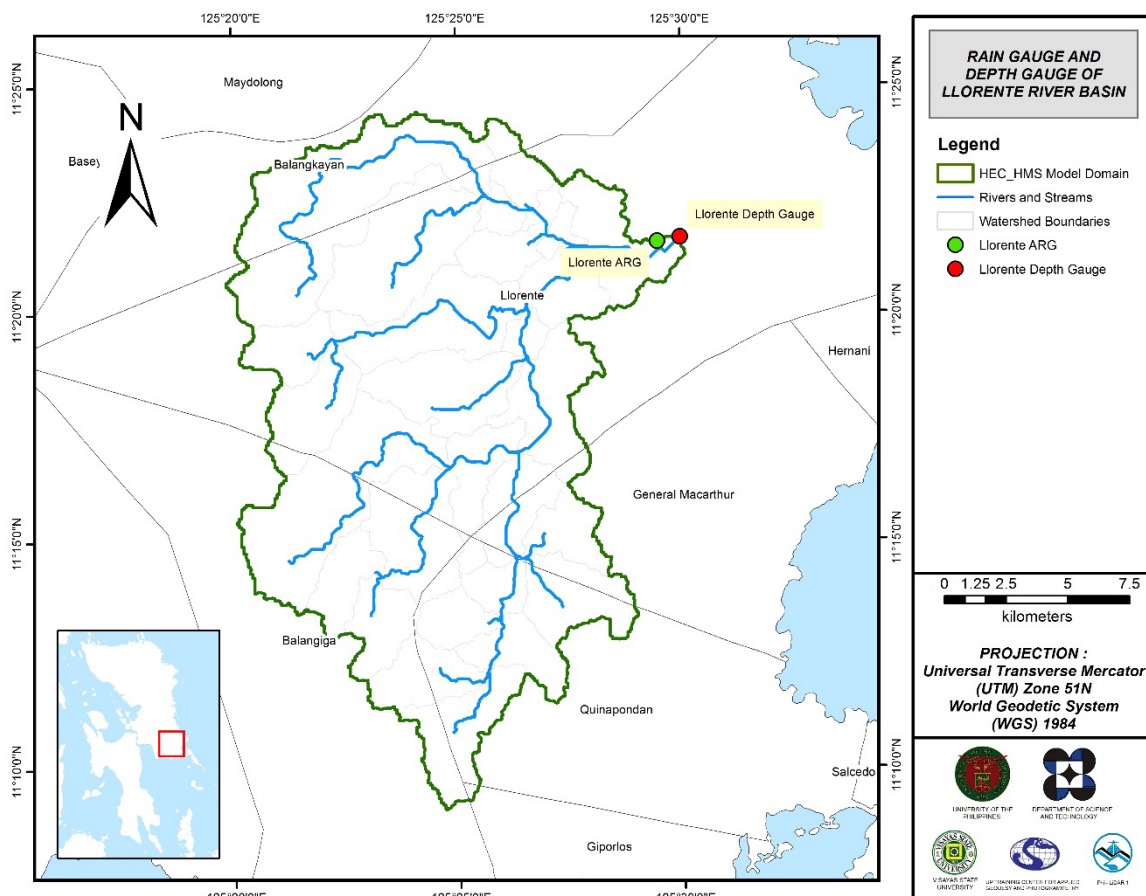


Figure 48. The location map of Ulot HEC-HMS model used for calibration

#### 5.1.3 Rating Curves and River Outflow

A rating curve was developed at Can-Avid Bridge, Can-Avid, Samar. It gives the relationship between the observed water levels and the discharge.

For Can-Avid Bridge, the rating curve is expressed as  $Q = 248.23e^{1.8681h}$  as shown in Figure 50.

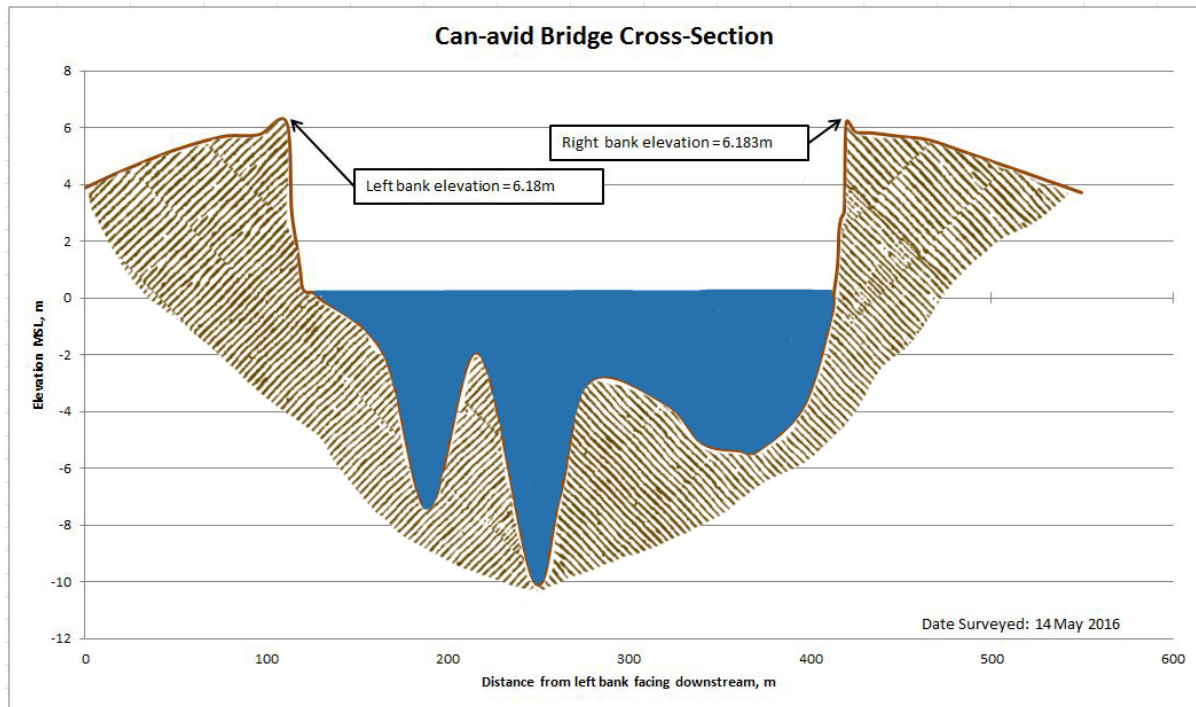


Figure 49. Cross-section plot of Can-Avid Bridge

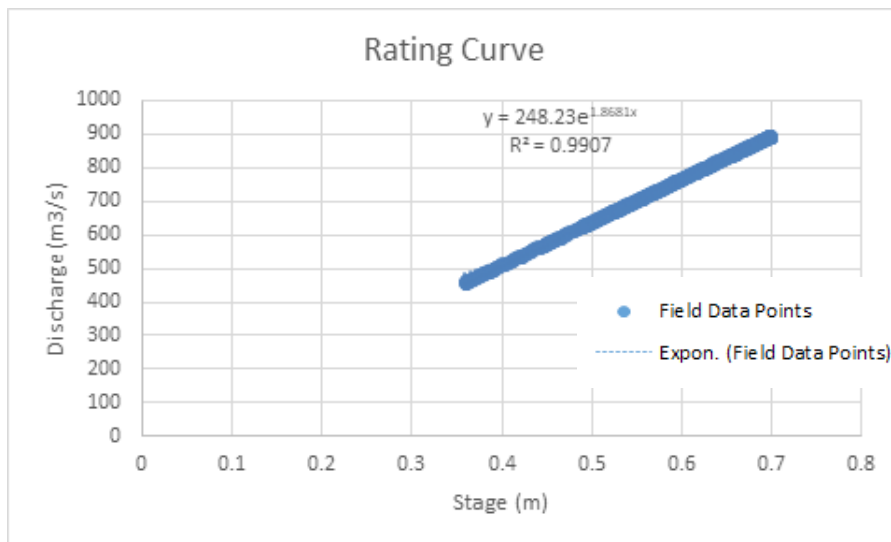


Figure 50. Rating curve at Can-Avid Bridge

This rating curve equation was used to compute the river outflow at Ulot Bridge for the calibration of the HEC-HMS model shown in Figure 4. Total rain from Cadian rain gauge is 253.2 mm. It peaked to 19.2 mm on 16 December 2016, 23:15. A summary of the data is seen in Table 1. The lag time between the peak rainfall and discharge is twenty three hours and thirty five minutes.



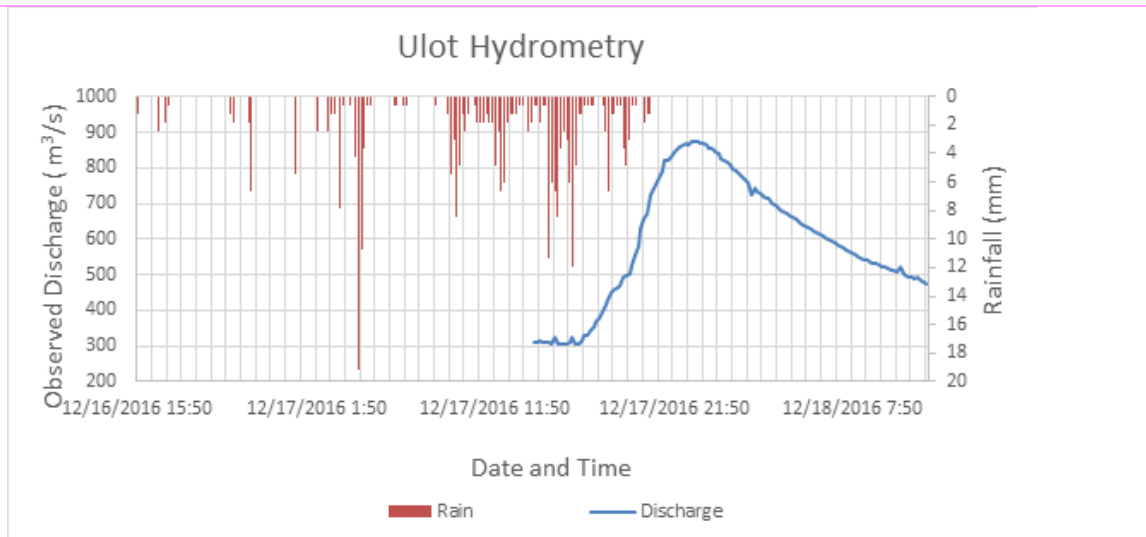


Figure 51. Rainfall and outflow data at Can-Avid Bridge used for modeling

### 5.2 RIDF Station

The Philippines Atmospheric Geophysical and Astronomical Services Administration (PAGASA) computed Rainfall Intensity Duration Frequency (RIDF) values for the Borongan Rain Gauge. The RIDF rainfall amount for 24 hours was converted to a synthetic storm by interpolating and re-arranging the value in such a way certain peak value will be attained at a certain time. This station chosen based on its proximity to the Ulot watershed. The extreme values for this watershed were computed based on a 36-year record.

Table 24. RIDF values for Borongan Rain Gauge computed by PAGASA

COMPUTED EXTREME VALUES (in mm) OF PRECIPITATION									
T (yrs)	10 mins	20 mins	30 mins	1 hr	2 hrs	3 hrs	6 hrs	12 hrs	24 hrs
2	22.5	35.3	44.5	60.6	83.7	100.8	133.7	170.7	201.4
5	31.5	49.1	61	82.3	116.1	140.8	186.5	241	283.8
10	37.4	58.2	71.9	96.6	137.6	167.2	221.4	287.6	338.4
15	40.7	63.3	104.7	104.7	149.8	182.1	241.2	313.9	369.2
20	43	66.9	110.4	110.4	158.3	192.6	255	332.3	390.8
25	44.8	69.7	114.8	114.8	164.8	200.6	265.6	346.4	407.4
50	50.4	78.2	128.3	128.3	185	225.4	298.4	390.1	458.6
100	55.9	86.7	141.6	141.6	205	205	330.9	433.4	509.4

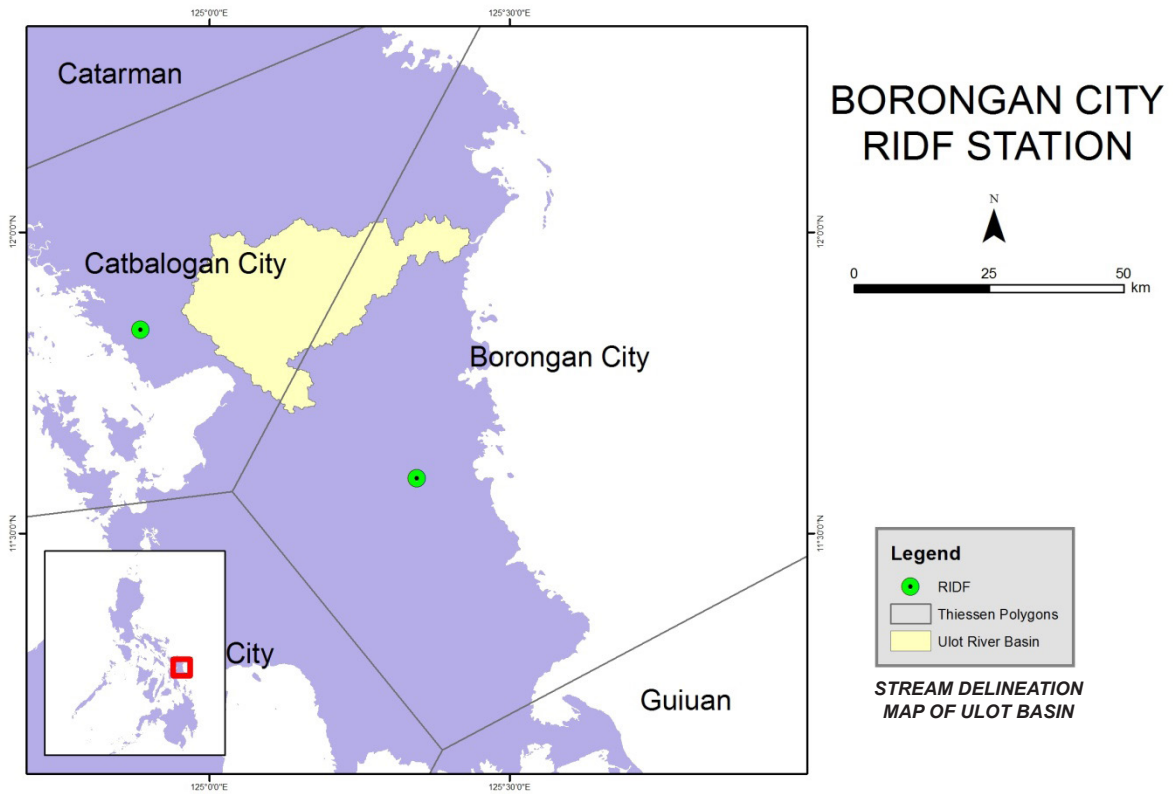


Figure 52. Location of Borongan RIDF station relative to Ulot River Basin

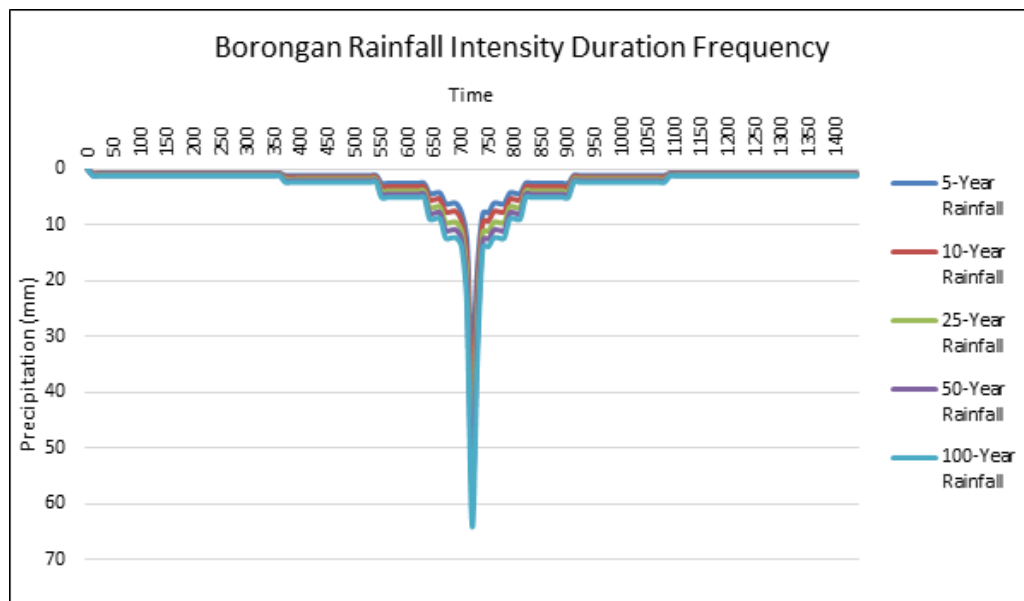


Figure 53. Synthetic storm generated for a 24-hr period rainfall for various return periods

### 5.3 HMS Model

The soil dataset was taken from and generated by the Bureau of Soils and Water Management (BSWM) under the Department of Agriculture (DA). The land cover dataset was taken from the National Mapping and Resource Information Authority (NAMRIA). The soil and land cover of the Ulot River Basin are shown in Figure 54 and Figure 55, respectively.

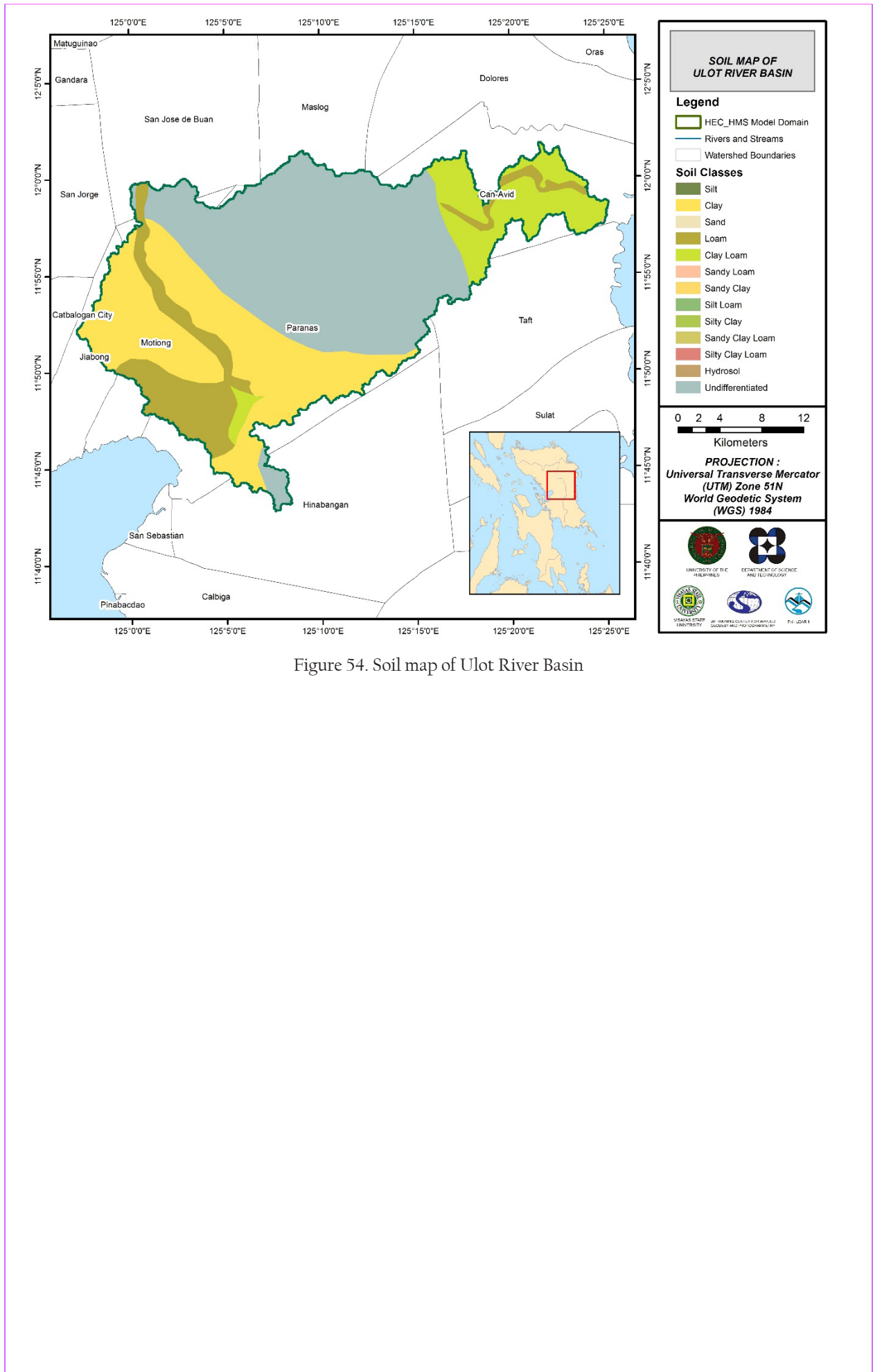


Figure 54. Soil map of Ulot River Basin

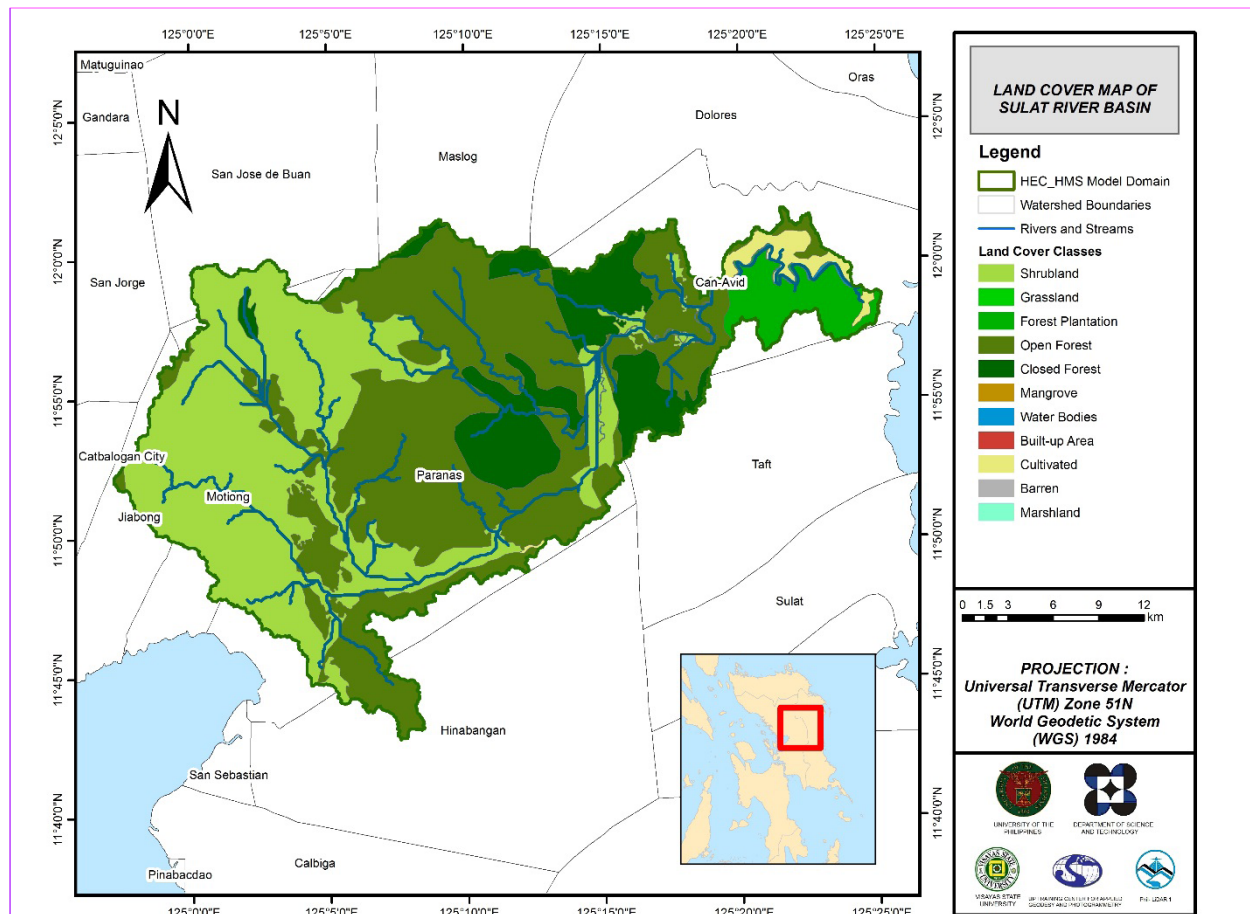


Figure 55. Land cover map of Ulot River Basin

For Ulot, the soil classes identified were clay, clay loam, loam, and undifferentiated. The land cover types identified were shrubland, grassland, forest plantation, open forest, closed forest, and cultivated area.



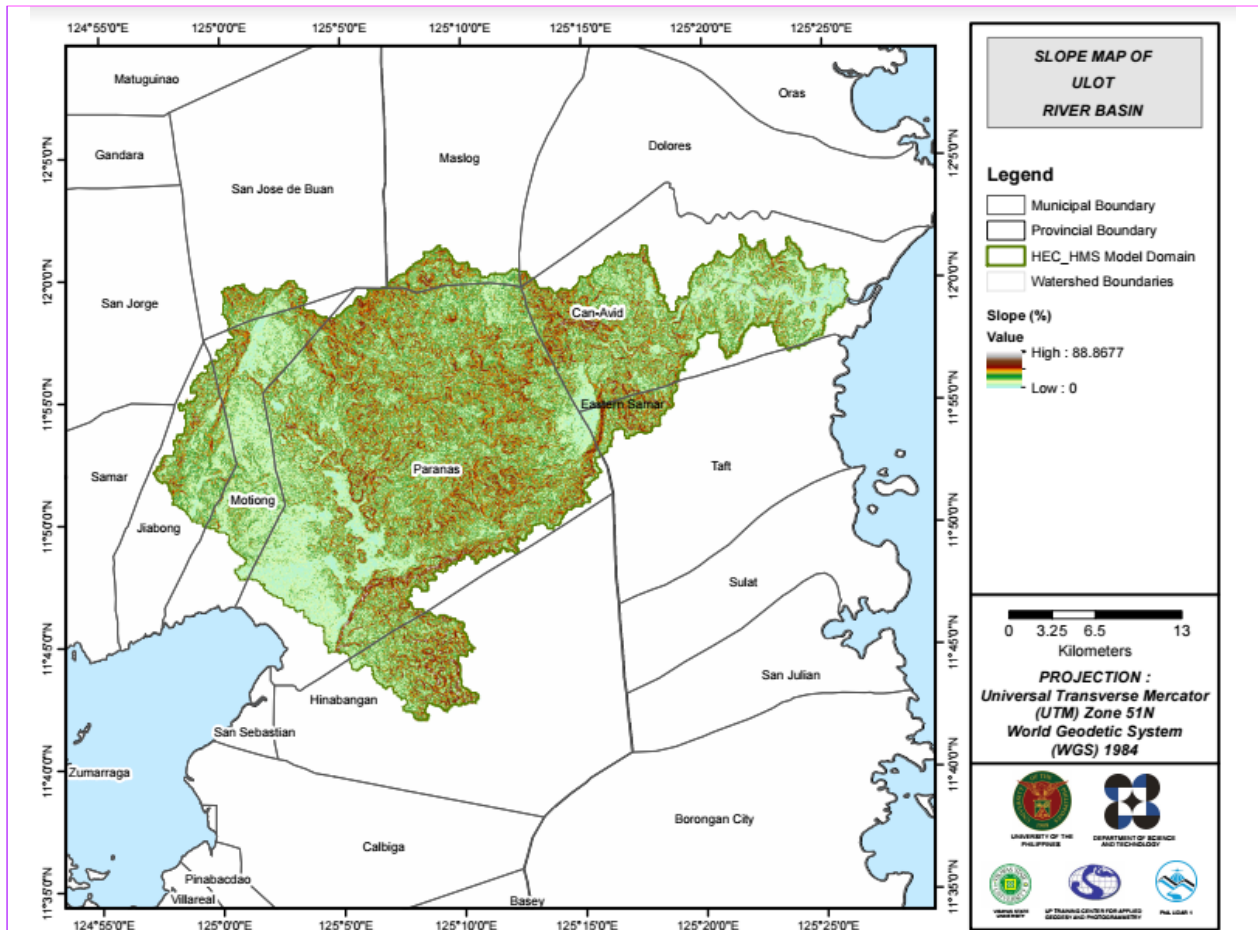


Figure 56. Slope map of the Ulot River Basin

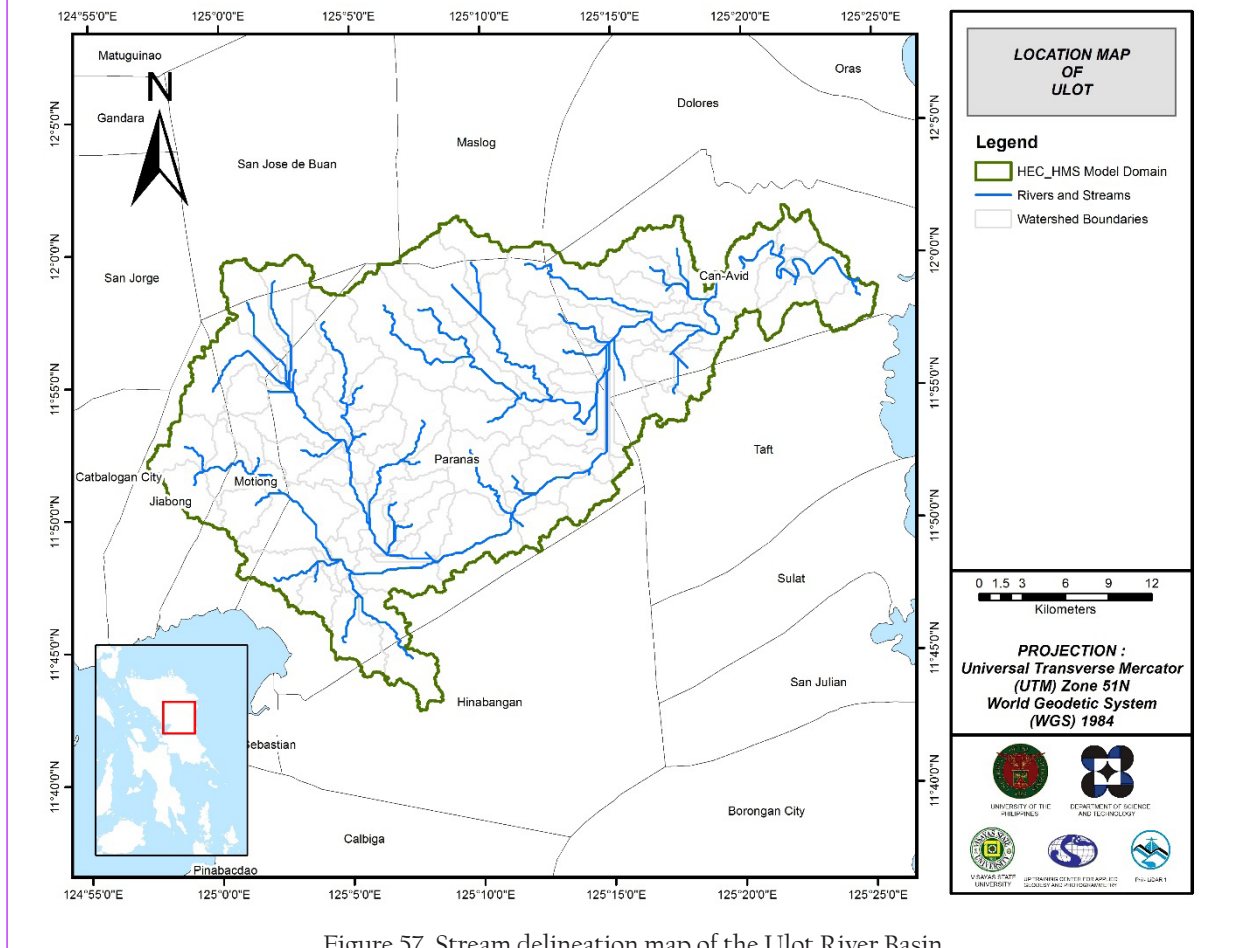


Figure 57. Stream delineation map of the Ulot River Basin



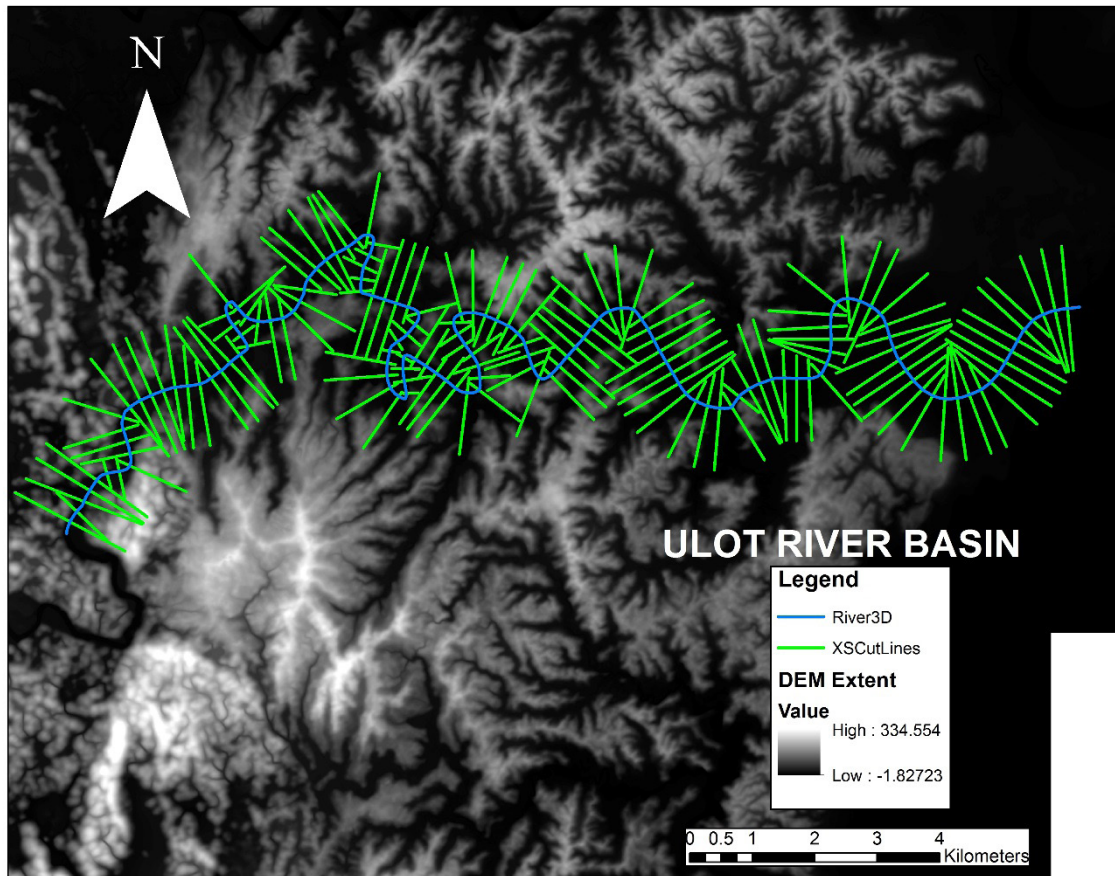


Figure 59. River cross-section of Ulot River generated through ArcMap HEC GeoRAS tool

## 5.5 FLO-2D Model

The automated modelling process allows for the creation of a model with boundaries that are almost exactly coincidental with that of the catchment area. As such, they have approximately the same land area and location. The entire area is divided into square grid elements, 10 meter by 10 meter in size. Each element is assigned a unique grid element number which serves as its identifier, then attributed with the parameters required for modelling such as x-and y-coordinate of centroid, names of adjacent grid elements, Manning coefficient of roughness, infiltration, and elevation value. The elements are arranged spatially to form the model, allowing the software to simulate the flow of water across the grid elements and in eight directions (north, south, east, west, northeast, northwest, southeast, southwest).

Based on the elevation and flow direction, it is seen that the water will generally flow from the west of the model to the east, following the main channel. As such, boundary elements in those particular regions of the model are assigned as inflow and outflow elements respectively.

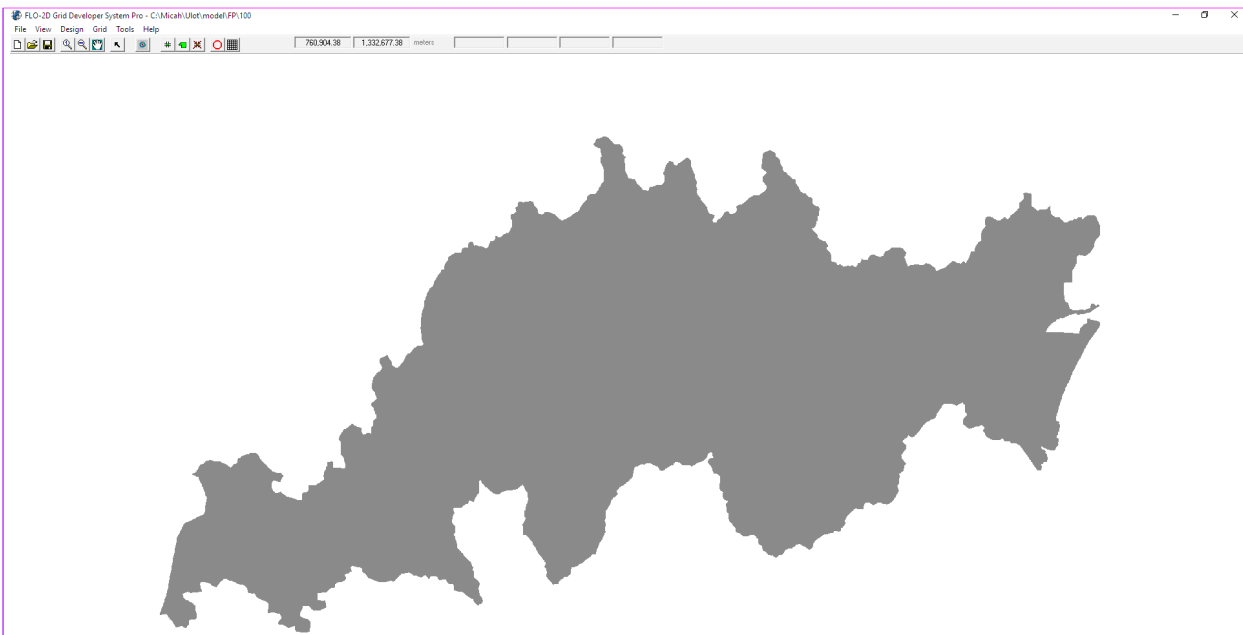


Figure 60. Screenshot of subcatchment with the computational area to be modeled in FLO-2D GDS Pro

The simulation is then run through FLO-2D GDS Pro. This particular model had a computer run time of 236.04932 hours. After the simulation, FLO-2D Mapper Pro is used to transform the simulation results into spatial data that shows flood hazard levels, as well as the extent and inundation of the flood. Assigning the appropriate flood depth and velocity values for Low, Medium, and High creates the following food hazard map. Most of the default values given by FLO-2D Mapper Pro are used, except for those in the Low hazard level. For this particular level, the minimum  $h$  (Maximum depth) is set at 0.2 m while the minimum  $vh$  (Product of maximum velocity ( $v$ ) times maximum depth ( $h$ )) is set at  $0 \text{ m}^2/\text{s}$ .

The creation of a flood hazard map from the model also automatically creates a flow depth map depicting the maximum amount of inundation for every grid element. The legend used by default in FLO-2D Mapper is not a good representation of the range of flood inundation values, so a different legend is used for the layout. In this particular model, the inundated parts cover a maximum land area of  $99\,092\,300.00 \text{ m}^2$ .

There is a total of  $313\,245\,662.01 \text{ m}^3$  of water entering the model. Of this amount,  $50\,417\,151.98 \text{ m}^3$  is due to rainfall while  $262\,828\,510.02 \text{ m}^3$  is inflow from other areas outside the model.  $17\,759\,946.00 \text{ m}^3$  of this water is lost to infiltration and interception, while  $290\,114\,874.39 \text{ m}^3$  is stored by the floodplain. The rest, amounting up to  $5\,370\,686.02 \text{ m}^3$ , is outflow.

## 5.6 Results of HMS Calibration

After calibrating the Ulot HEC-HMS river basin model, its accuracy was measured against the observed values. Figure 61 shows the comparison between the two discharge data.



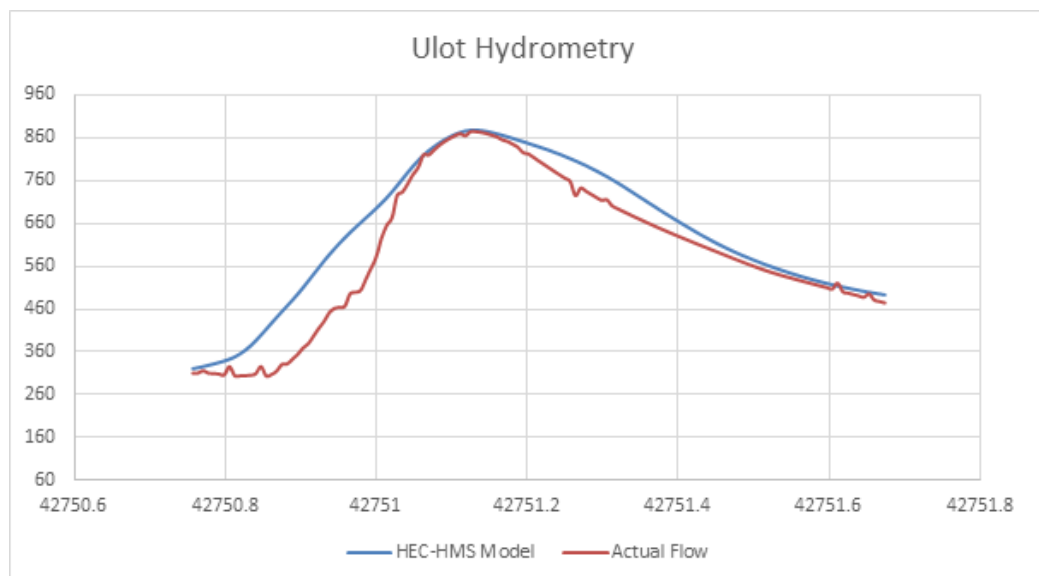


Figure 61. Outflow hydrograph of Ulot Bridge generated in HEC-HMS model compared with observed outflow

Table 25. Range of calibrated values for Ulot

Hydrologic Element	Calculation Type	Method	Parameter	Range of Calibrated Values
Basin	Loss	SCS Curve number	Initial Abstraction (mm)	39 – 348
			Curve Number	48 - 89
	Transform	Clark Unit Hydrograph	Time of Concentration (hr)	0.2 - 18
			Storage Coefficient (hr)	0.4 - 15
Reach	Routing	Muskingum-Cunge	Recession Constant	0.68
			Ratio to Peak	0.43
			Manning’s Coefficient	0.04

Initial abstraction defines the amount of precipitation that must fall before surface runoff. The magnitude of the outflow hydrograph increases as initial abstraction decreases. The range of values from 39 to 348mm means that there is a high amount of infiltration or rainfall interception by vegetation.

Curve number is the estimate of the precipitation excess of soil cover, land use, and antecedent moisture. The magnitude of the outflow hydrograph increases as curve number increases. The range of 48 to 89 for curve number is advisable for Philippine watersheds depending on the soil and land cover of the area (M. Horritt, personal communication, 2012).

Time of concentration and storage coefficient are the travel time and index of temporary storage of runoff in a watershed. The range of calibrated values from 0.2 hours to 18 hours determines the reaction time of the model with respect to the rainfall. The peak magnitude of the hydrograph also decreases when these parameters are increased.

Recession constant is the rate at which baseflow recedes between storm events and ratio to peak is the ratio of the baseflow discharge to the peak discharge. Recession constant of 0.68 indicates that the basin is unlikely to quickly go back to its original discharge and instead, will be higher. Ratio to peak of 0.43 indicates a steeper receding limb of the outflow hydrograph.

Manning’s roughness coefficient of 0.04 corresponds to the common roughness Ulot watershed, which is determined to be cultivated with mature field crops (Brunner, 2010).

Table 26. Summary of the efficiency test of Ulot HMS Model

RMSE	40.1
r <sup>2</sup>	0.9741
NSE	0.87
PBIAS	-7.69
RSR	0.37

The Root Mean Square Error (RMSE) method aggregates the individual differences of these two measurements. It computed as 40.1 (m<sup>3</sup>/s).

The Pearson correlation coefficient (r<sup>2</sup>) assesses the strength of the linear relationship between the observations and the model. This value being close to 1 corresponds to an almost perfect match of the observed discharge and the resulting discharge from the HEC HMS model. Here, it measured 0.9741.

The Nash-Sutcliffe (E) method was also used to assess the predictive power of the model. Here the optimal value is 1. The model attained an efficiency coefficient of 0.87.

A positive Percent Bias (PBIAS) indicates a model’s propensity towards under-prediction. Negative values indicate bias towards over-prediction. Again, the optimal value is 0. In the model, the PBIAS is -7.69.

The Observation Standard Deviation Ratio, RSR, is an error index. A perfect model attains a value of 0 when the error in the units of the valuable a quantified. The model has an RSR value of 0.37.

## 5.7 Calculated Outflow Hydrographs and Discharge Values for Different Rainfall Return Periods

### 5.7.1 Hydrograph Using the Rainfall Runoff Model

The summary graph (Figure 62) shows the Ulot outflow using the Borongan Rainfall Intensity-Duration-Frequency curves (RIDF) in 5 different return periods (5-year, 10-year, 25-year, 50-year, and 100-year rainfall time series) based on the Philippine Atmospheric Geophysical and Astronomical Services Administration (PAG-ASA) data. The simulation results reveal significant increase in outflow magnitude as the rainfall intensity increases for a range of durations and return periods.

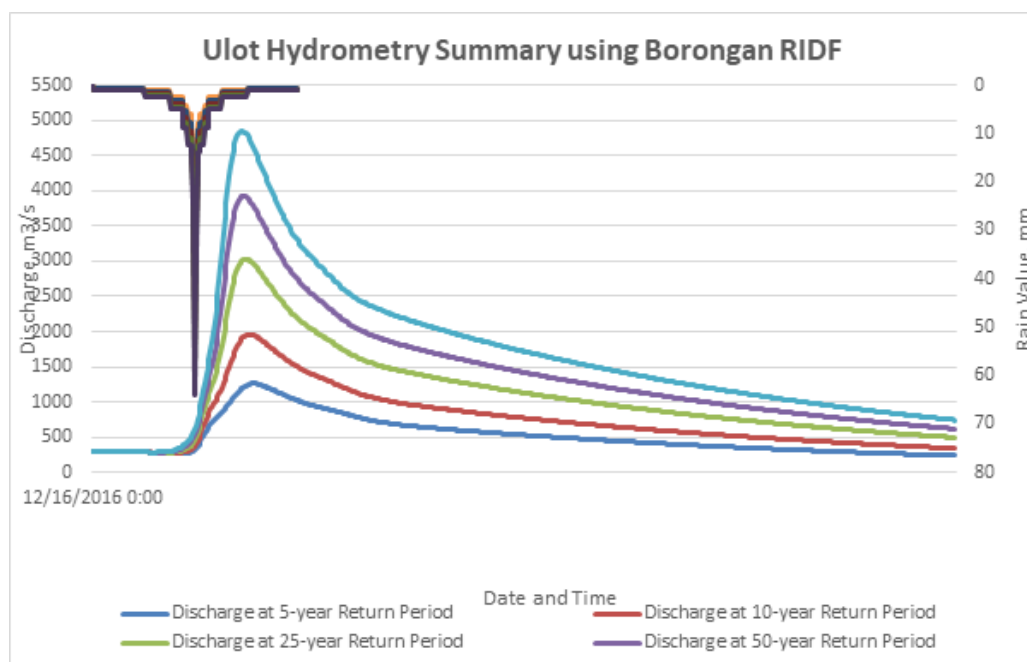


Figure 62. Outflow hydrograph at Ulot Station generated using Borongan RIDF simulated in HEC-HMS

A summary of the total precipitation, peak rainfall, peak outflow and time to peak of Ulot discharge using the Ulot Rainfall Intensity-Duration-Frequency curves (RIDF) in five different return periods is shown in Table 27.

Table 27. Peak values of the Ulot HEC-HMS model outflow using the Borongan RIDF

RIDF Period	Total Precipitation (mm)	Peak rainfall (mm)	Peak outflow (m <sup>3</sup> /s)	Time to Peak
5-Year	278.6	33.2	1261	6 hours, 50 minutes
10-Year	344.7	40.6	1958.3	6 hours, 20 minutes
25-Year	428.2	50.1	3031	6 hours
50-Year	490.2	57.1	3918.7	5 hours, 40 minutes
100-Year	551.7	64	4847.2	5 hours, 30 minutes

### 5.7.2 Discharge Data Using Dr. Horritts’s Recommended Hydrologic Method

The river discharge values for the river entering the floodplain are shown in and the peak values are summarized in Table 28.

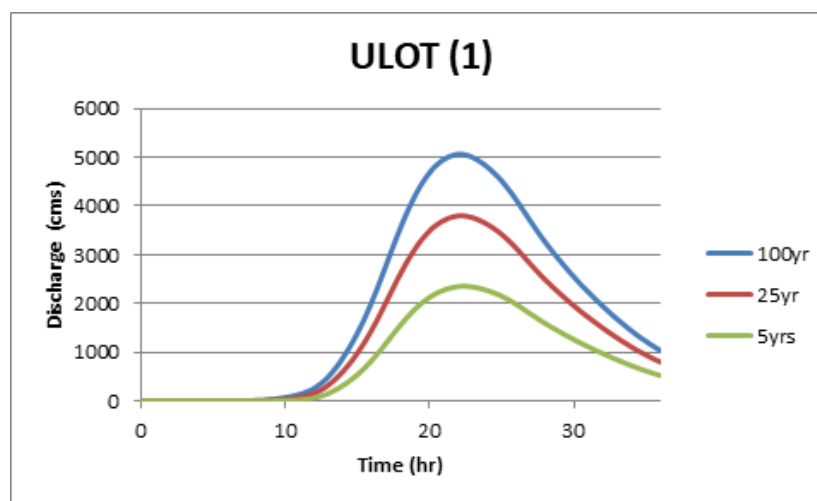


Figure 63. Ulot River (1) generated discharge using 5-, 25-, and 100-year Catbalogan rainfall intensity-duration-frequency (RIDF) in HEC-HMS

Table 28. Summary of Ulot River (1) discharge generated in HEC-HMS

RIDF Period	Peak discharge (cms)	Time-to-peak
100-Year	5065.7	22 hours, 10 minutes
25-Year	3804.6	22 hours, 10 minutes
5-Year	2357.8	22 hours, 20 minutes

Table 29. Validation of river discharge estimates

Discharge Point	Q <sub>MED(SCS)</sub> , cms	Q <sub>BANKFUL</sub> , cms	Q <sub>MED(SPEC)</sub> , cms	VALIDATION			
				Bankful Discharge	Discharge	Specific Discharge	Discharge
Ulot (1)	2074.864	1944.273	732.805	Pass		Fail	

The HEC-HMS river discharge estimates were able to satisfy the conditions for validation using the bankful method but not for the specific discharge methods and will need further recalculation. The passing values are based on theory but are supported using other discharge computation methods so they were good to use for flood modeling. These values will need further investigation for the purpose of validation. It is therefore recommended to obtain actual values of the river discharges for higher-accuracy modeling.

## 5.8 River Analysis Model Simulation

The HEC-RAS flood model produced a simulated water level at every cross-section for every time step for every flood simulation created. The resulting model will be used in determining the flooded areas within the model. The simulated model will be an integral part in determining real-time flood inundation extent of the river after it has been automated and uploaded on the DREAM website. For this publication, only a sample output map river was to be shown, since only the VSU-FMC base flow was calibrated. The sample generated map of Ulot River using the calibrated HMS base flow is shown in Figure 64.



Figure 64. Sample output Ulot RAS Model

## 5.9 Flood Hazard and Flow Depth Map

The resulting hazard and flow depth maps have a 10m resolution. Figure 65 to Figure 70 shows the 5-, 25-, and 100-year rain return scenarios of the Ulot Floodplain.

The floodplain, with an area of 99.09 sq km, covers two municipalities namely Can-Avid and Taft. Table shows the percentage of area affected by flooding per municipality.

Table 30. Municipalities affected in Ulot Floodplain

City / Municipality	Total Area	Area Flooded	% Flooded
Can-Avid	285.22	97.92	34.33%
Taft	150.05	0.25	0.17%



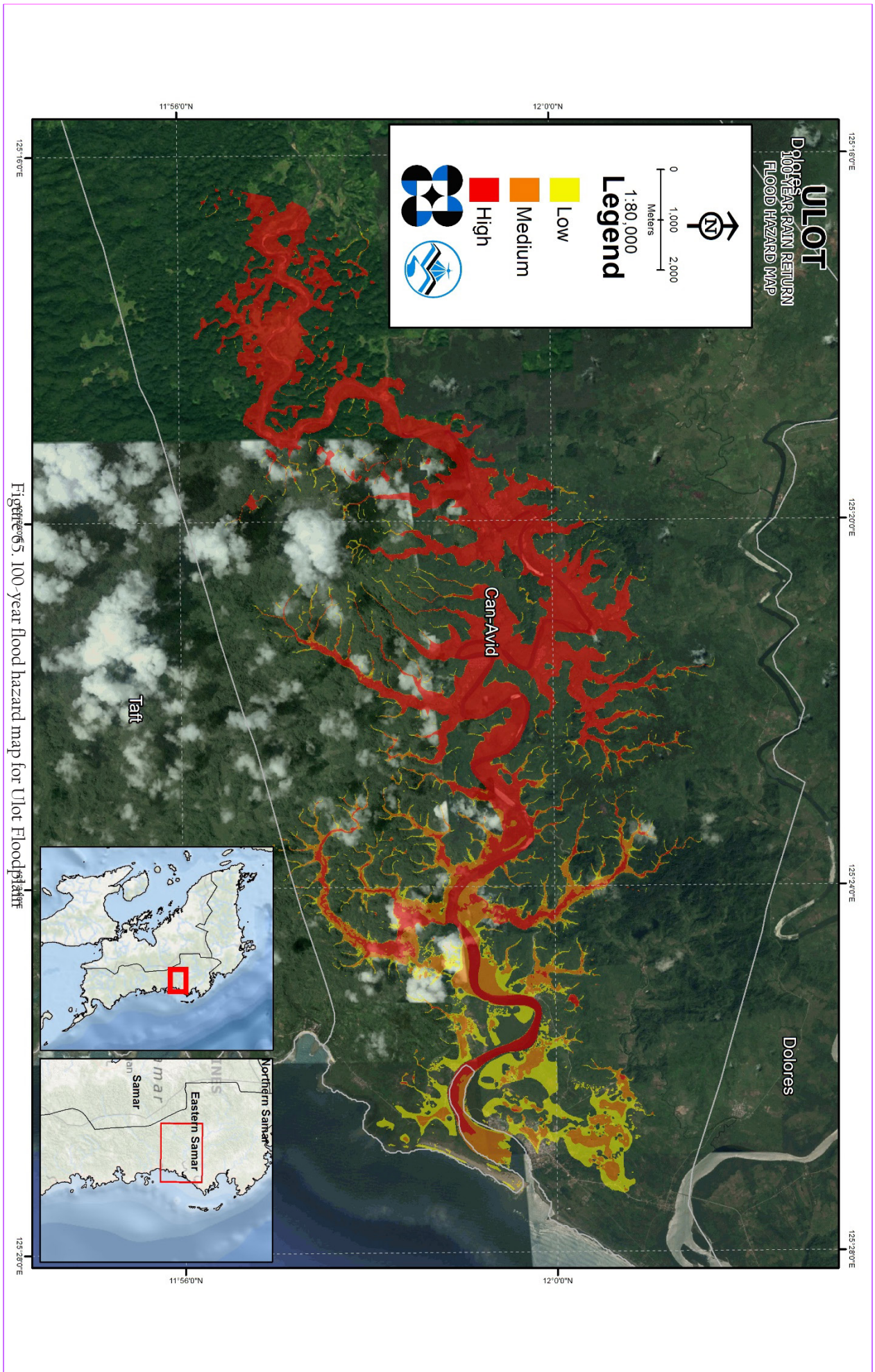


Figure 65. 100-year flood hazard map for Ulot Floodplains



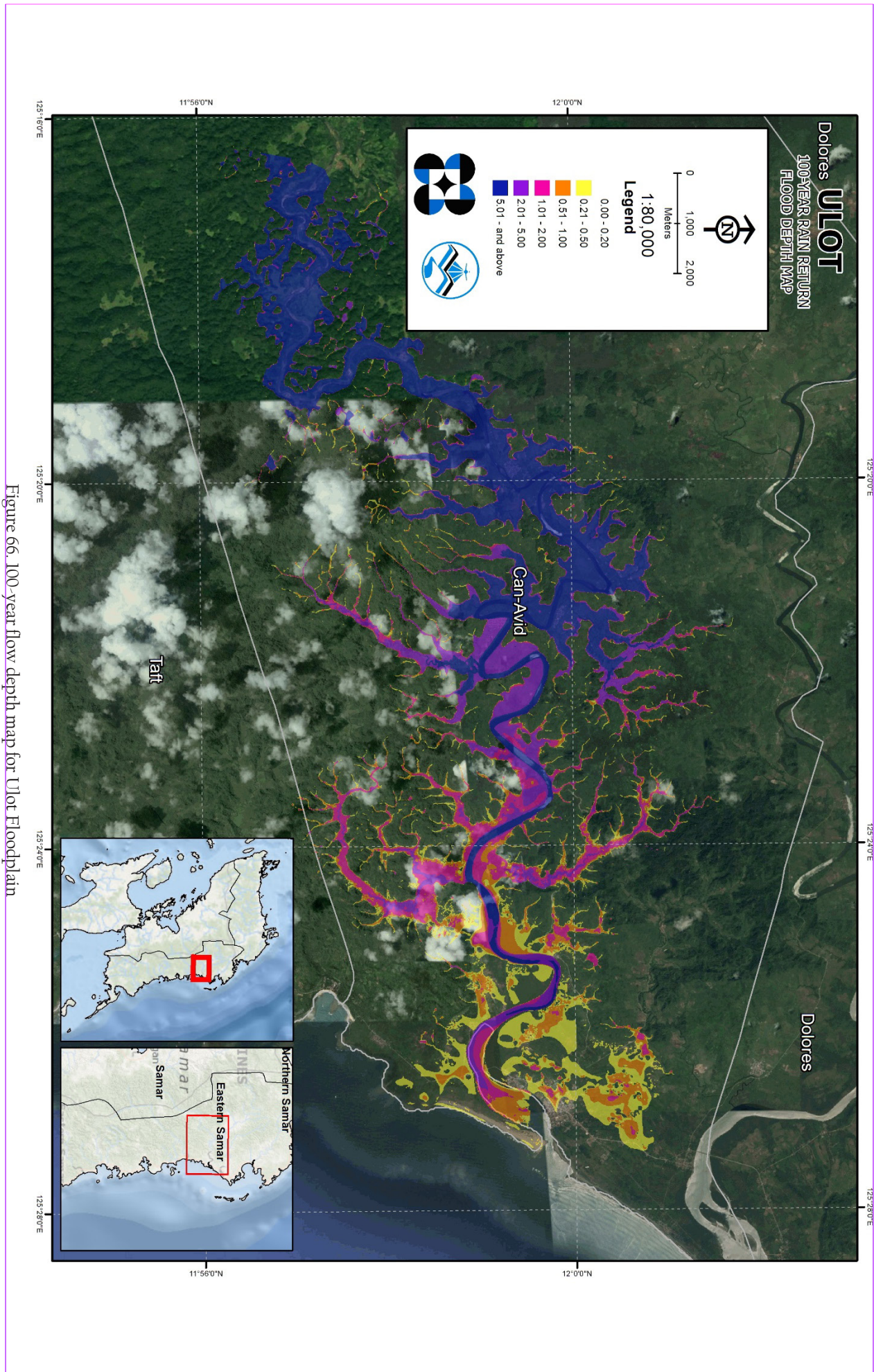


Figure 66. 100-year flow depth map for Ulot Floodplain



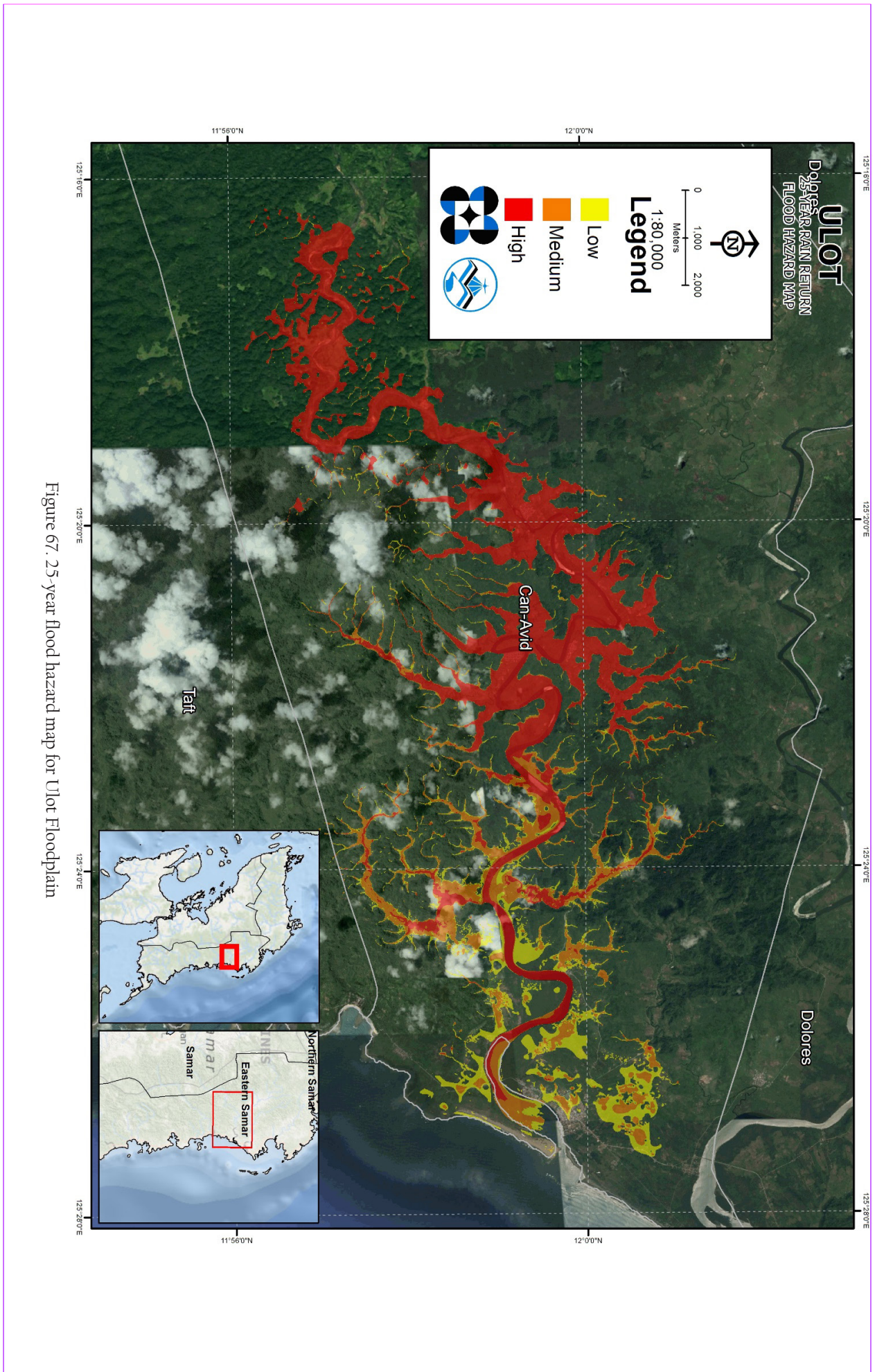


Figure 67. 25-year flood hazard map for Ulot Floodplain



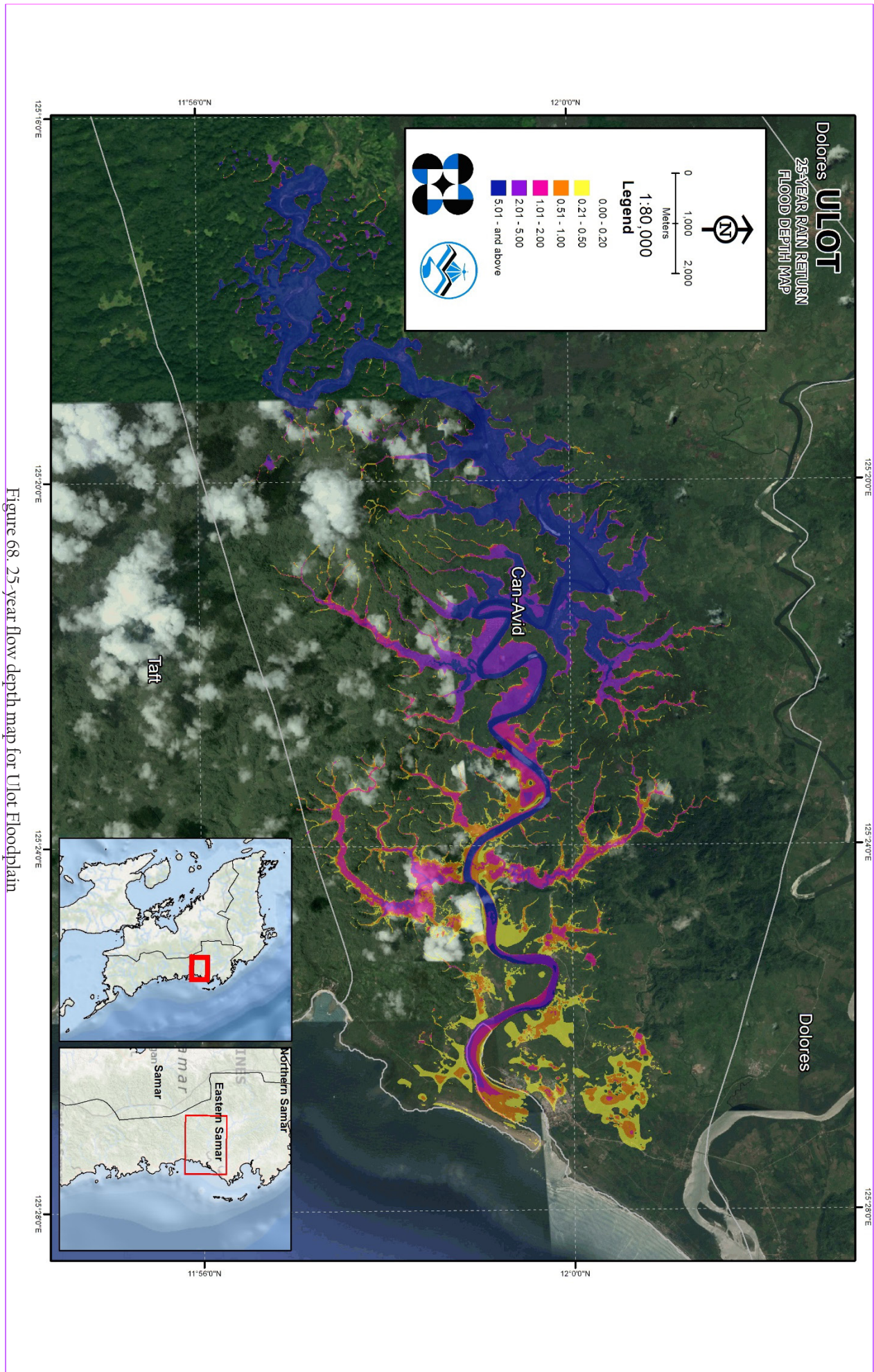


Figure 68. 25-year flow depth map for Ulot Floodplain



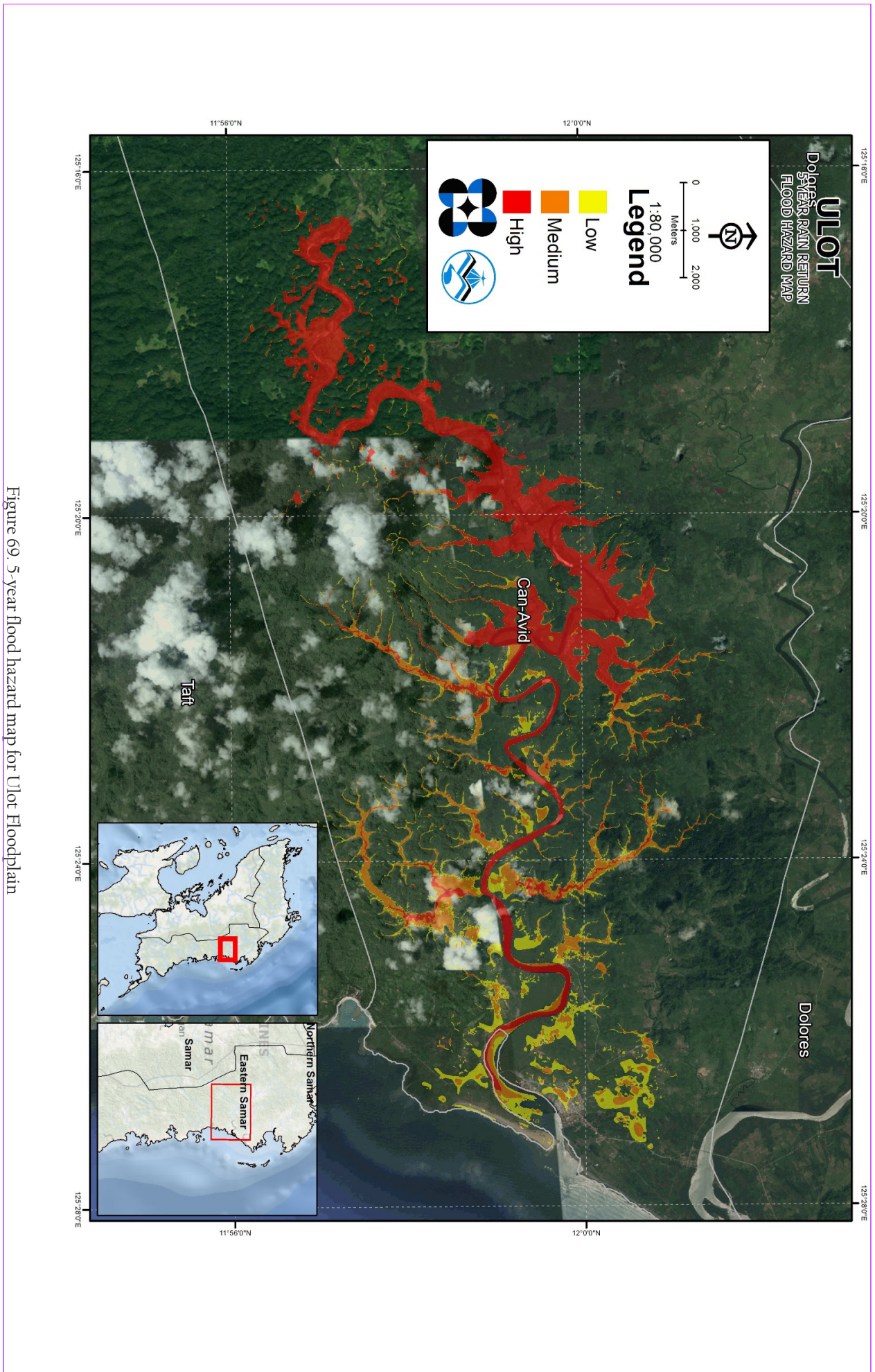


Figure 69. 5-year flood hazard map for Ulot Floodplain



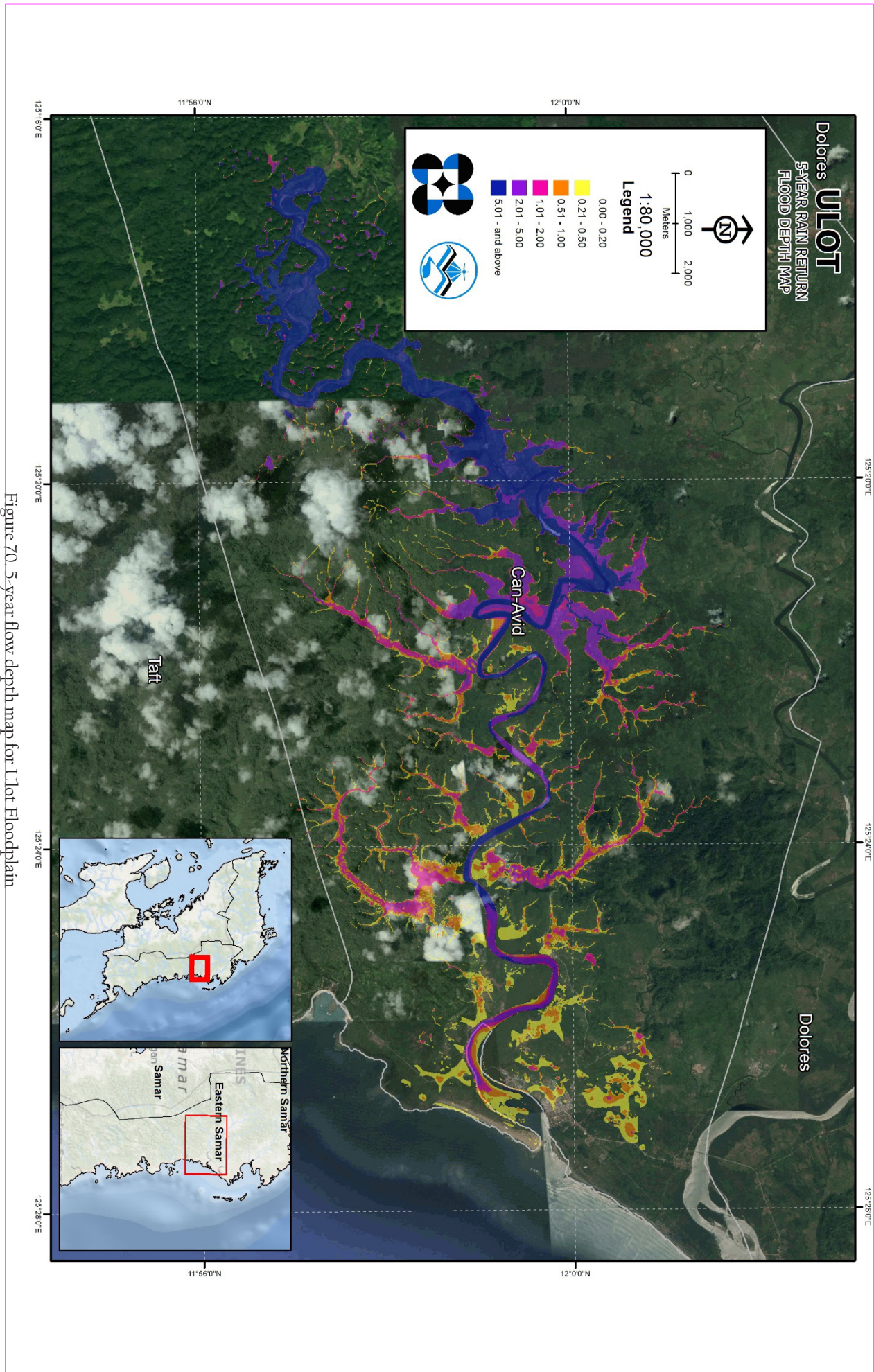


Figure 70. 5-year flow depth map for ULOT Floodplain

## 5.10 Inventory of Areas Exposed to Flooding

Affected barangays in Ulot River Basin, grouped by municipality, are listed below. For the said basin, 2 municipalities consisting of 28 barangays are expected to experience flooding when subjected to 5-yr rainfall return period.

For the 5-year return period, 25.21% of the municipality of Can-avid with an area of 285.22 sq km will experience flood levels of less 0.20 meters. 1.86% of the area will experience flood levels of 0.21 to 0.50 meters while 1.36%, 1.31%, 1.56% and 3.01% of the area will experience flood depths of 0.51 to 1 meter, 1.01 to 2 meters, 2.01 to 5 meters and more than 5 meters, respectively. Listed in Table 31 to Table 33 are the affected areas in square kilometers by flood depth per barangay.

Table 31. Affected areas in Can-avid, Eastern Samar during a 5-year rainfall return period

ULOT BASIN		Affected Barangays in Can-avid							
		Balagon	Brgy 1	Brgy 10	Brgy 2	Brgy 3	Brgy 4	Brgy 5	Brgy 6
Area	0.03-0.20	0.001	0.033	1.56	0.15	0.44	0.65	0.22	0.28
	0.21-0.50	0	0	0.29	0.019	0.053	0.37	0.14	0.052
	0.51-1.00	0	0	0.11	0.0089	0.031	0.13	0.044	0.026
Affected	1.01-2.00	0	0	0.013	0.0001	0.00099	0.007	0.00033	0.0027
	2.01-5.00	0	0	0.043	0	0	0	0	0
	> 5.00	0	0	0.0032	0	0	0	0	0

Table 32. Affected areas in Can-avid, Eastern Samar during a 5-year rainfall return period

ULOT BASIN		Affected Barangays in Can-avid							
		Brgy 7	Brgy 8	Brgy 9	Baruk	Caghalong	Camantang	Can-Ilay	Cansan-gaya
Area	0.03-0.20	0.58	0.52	0.22	19.8	1.89	6.96	3.3	3.98
	0.21-0.50	0.16	0.089	0.13	0.65	0.039	0.12	0.038	0.39
	0.51-1.00	0.029	0.031	0.048	0.68	0.032	0.11	0.037	0.33
Affected (sq km.)	1.01-2.00	0.013	0.018	0.0023	1.19	0.043	0.14	0.079	0.39
	2.01-5.00	0.0068	0	0	2.69	0.17	0.25	0.19	0.037
	> 5.00	0	0	0	2.47	0.74	2.34	1.55	0

Table 33. Affected areas in Can-avid, Eastern Samar during a 5-year rainfall return period

<b>ULOT BASIN</b>		<b>Affected Barangays in Can-avid</b>									
<b>Canteros</b>		<b>Carolina</b>	<b>Guibuangan</b>	<b>Jepaco</b>	<b>Mabuhay</b>	<b>Malogo</b>	<b>Obong</b>	<b>Salvation</b>	<b>Solong</b>		
<b>Area</b>	0.03-0.20	5.12	0.17	9.19	2.57	6.16	3.43	1.58	2.95	0.15	
	0.21-0.50	0.94	0.028	0.68	0.14	0.36	0.54	0.047	0.039	0.0036	
	0.51-1.00	0.51	0.0007	0.6	0.23	0.42	0.4	0.056	0.035	0.0015	
	1.01-2.00	0.33	0	0.36	0.38	0.28	0.36	0.047	0.067	0.0006	
	2.01-5.00	0.43	0	0.32	0.12	0.023	0.086	0.0009	0.11	0	
<b>Affected (sq km.)</b>	> 5.00	0.16	0	0.27	0.099	0.041	0	0	0.92	0	



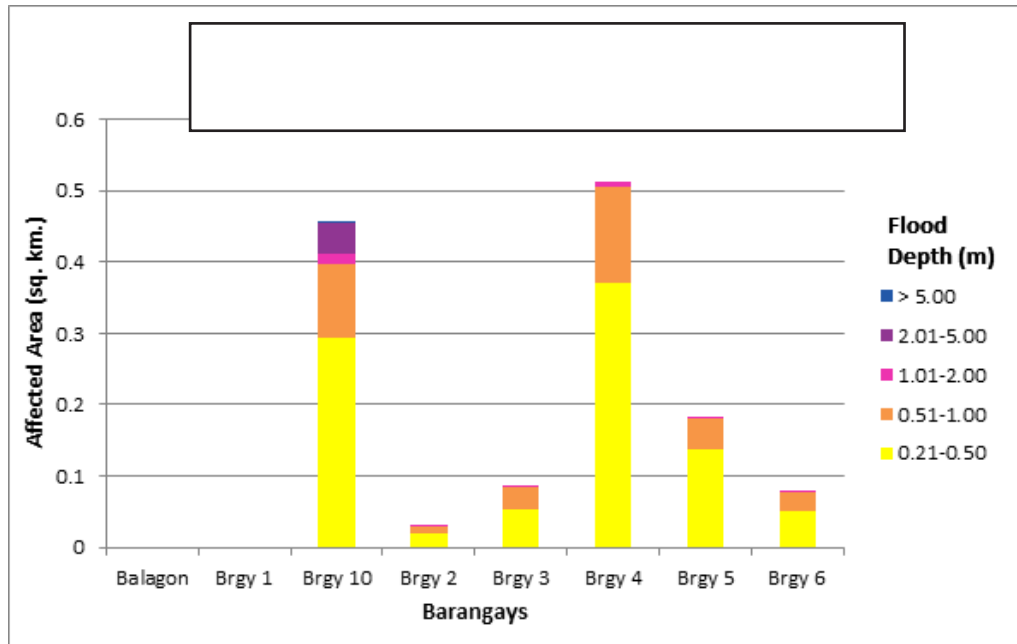


Figure 71. Affected areas in Can-avid, Eastern Samar during a 5-year rainfall return period

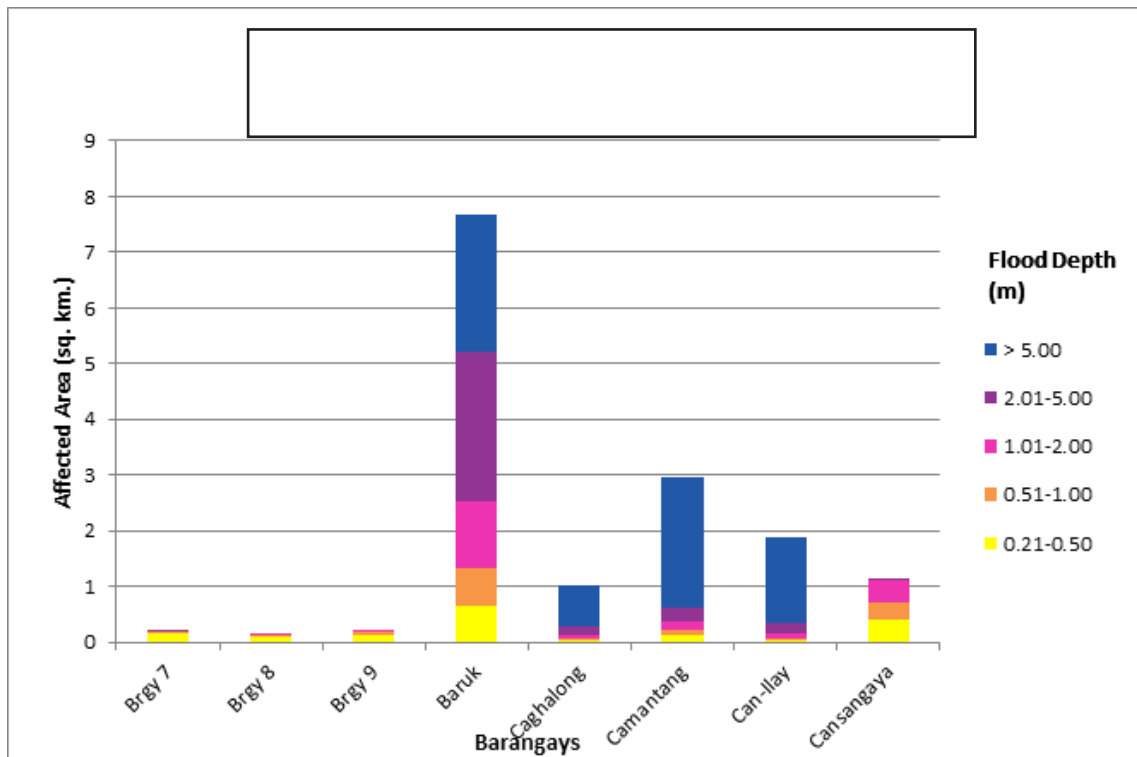


Figure 72. Affected areas in Can-avid, Eastern Samar during a 5-year rainfall return period

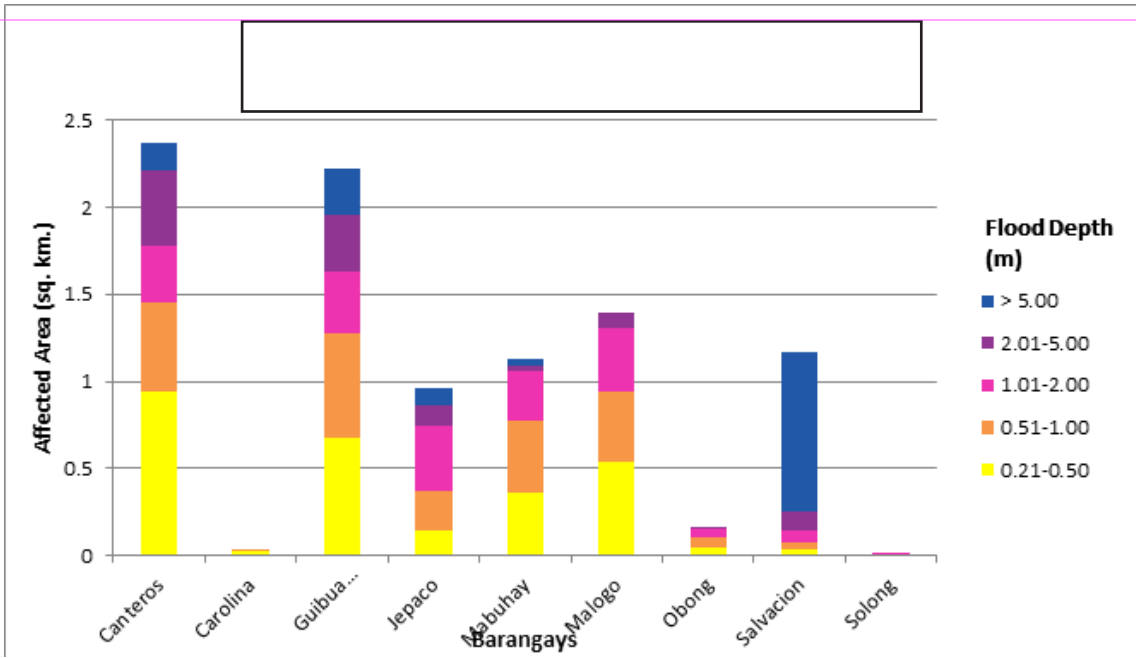


Figure 73. Affected areas in Can-avid, Eastern Samar during a 5-year rainfall return period

For the municipality of Taft, with an area of 230.266 sq km, 0.102% will experience flood levels of less 0.20 meters. 0.002% of the area will experience flood levels of 0.21 to 0.50 meters while 0.002%, 0.0006%, and 0.12% of the area will experience flood depths of 0.51 to 1 meter, 1.01 to 2 meters, and above 2 meters, respectively. Listed in Table 34 are the affected areas in square kilometers by flood depth per barangay.

Table 34. Affected areas in Taft, Eastern Samar during a 5-year rainfall return period

ULOT BASIN		Affected Barangays in Taft		
		Batiawan	Beto	Pangabutan
Area	0.03-0.20	0.0038	0.0023	0.23
	0.21-0.50	0.0001	0	0.0052
Affected (sq km.)	0.51-1.00	0	0	0.0037
	1.01-2.00	0	0	0.0015
	2.01-5.00	0	0	0.00046
	> 5.00	0	0	0

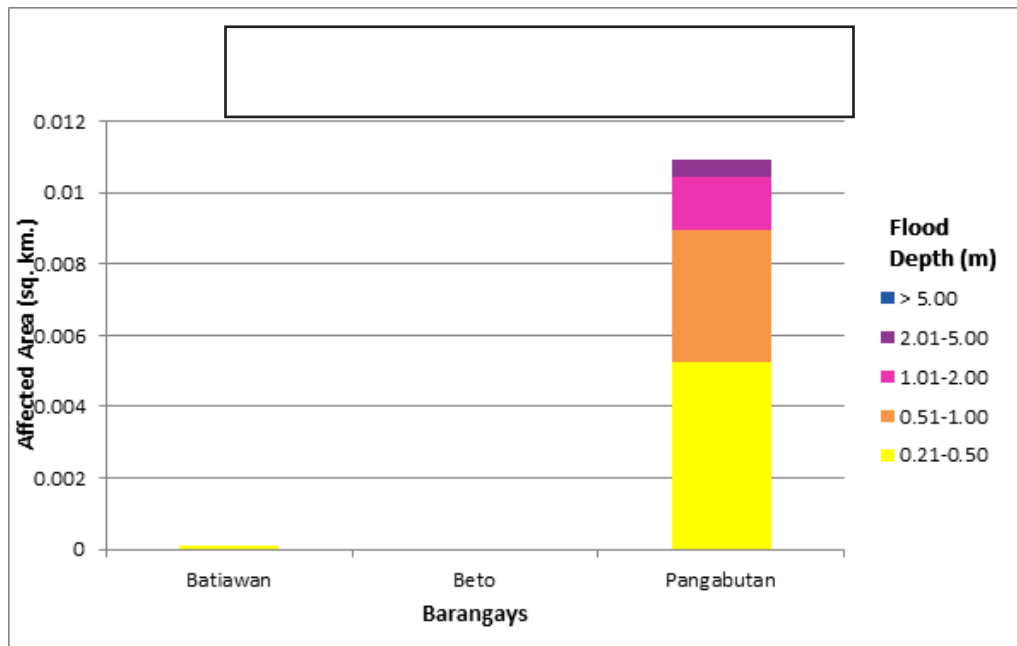


Figure 74. Affected areas in Taft, Eastern Samar during a 5-year rainfall return period

For the 25-year return period, 23.00% of the municipality of Ulot with an area of 285.22 sq km will experience flood levels of less 0.20 meters. 2.01% of the area will experience flood levels of 0.21 to 0.50 meters while 1.40%, 1.49%, 1.80% and 4.64% of the area will experience flood depths of 0.51 to 1 meter, 1.01 to 2 meters, 2.01 to 5 meters and more than 5 meters, respectively. Listed in Table 35 to Table 37 are the affected areas in square kilometers by flood depth per barangay.

Table 35. Affected areas in Can-avid, Eastern Samar during a 25-year rainfall return period

ULOT BASIN		Affected Barangays in Can-avid									
		Balagon	Brgy 1	Brgy 10	Brgy 2	Brgy 3	Brgy 4	Brgy 5	Brgy 6		
Area	0.03-0.20	0.001	0.033	1.37	0.14	0.4	0.46	0.16	0.25		
	0.21-0.50	0	0	0.4	0.022	0.086	0.45	0.16	0.067		
	0.51-1.00	0	0	0.18	0.015	0.033	0.23	0.078	0.034		
	1.01-2.00	0	0	0.014	0.00084	0.009	0.015	0.0027	0.0055		
	2.01-5.00	0	0	0.036	0	0	0	0	0		
Affected (sq km.)	> 5.00	0	0	0.02	0	0	0	0	0		

Table 36. Affected areas in Can-avid, Eastern Samar during a 25-year rainfall return period

ULOT BASIN		Affected Barangays in Can-avid									
		Brgy 7	Brgy 8	Brgy 9	Baruk	Caghalong	Camantang	Can-Ilay	Cansangaya		
Area	0.03-0.20	0.48	0.46	0.14	18.47	1.72	6.54	2.92	3.78		
	0.21-0.50	0.24	0.13	0.15	0.48	0.04	0.14	0.032	0.43		
	0.51-1.00	0.046	0.037	0.096	0.43	0.035	0.1	0.038	0.3		
	1.01-2.00	0.017	0.026	0.0051	0.74	0.043	0.13	0.061	0.5		
	2.01-5.00	0.0052	0	0	2.16	0.095	0.25	0.21	0.12		
Affected (sq km.)	> 5.00	0.0025	0	0	5.19	0.97	2.77	1.93	0		



Table 37. Affected areas in Can-avid, Eastern Samar during a 25-year rainfall return period

<b>ULOT BASIN</b>		<b>Affected Barangays in Can-avid</b>									
	<b>Canteros</b>	<b>Carolina</b>	<b>Guibuangan</b>	<b>Jepaco</b>	<b>Mabuhay</b>	<b>Malogo</b>	<b>Obong</b>	<b>Salvacion</b>	<b>Solong</b>		
<b>Area</b>	0.03-0.20	4.44	0.11	7.96	2.23	5.92	3.2	1.56	2.69	0.15	
	0.21-0.50	1.2	0.084	0.52	0.063	0.33	0.58	0.055	0.045	0.0083	
	0.51-1.00	0.64	0.0019	0.71	0.059	0.4	0.43	0.052	0.036	0.0015	
	1.01-2.00	0.44	0	1	0.18	0.48	0.45	0.064	0.054	0.0009	
	2.01-5.00	0.5	0	0.62	0.73	0.099	0.16	0.004	0.14	0	
<b>Affected (sq km.)</b>	> 5.00	0.28	0	0.6	0.27	0.051	0	0.0001	1.15	0	

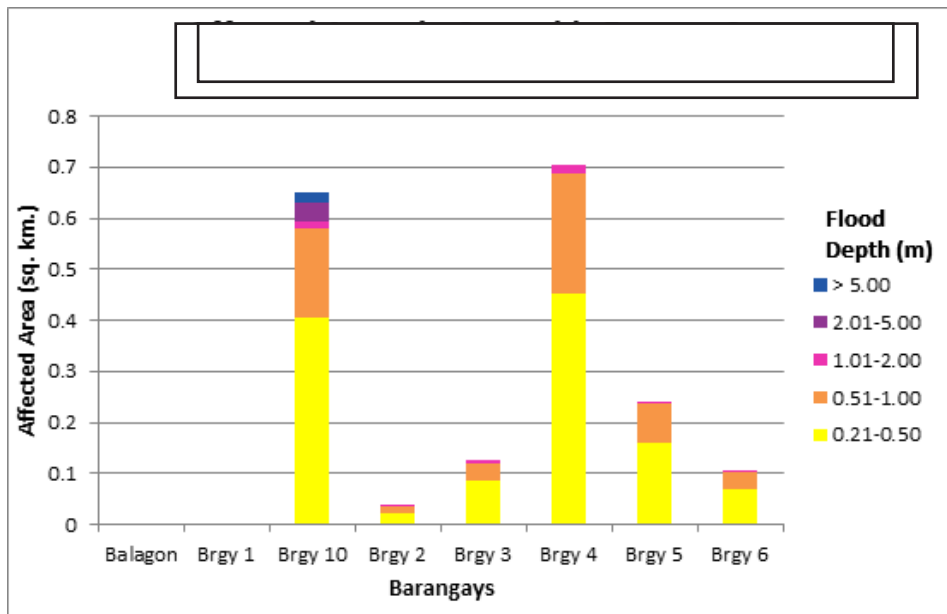


Figure 75. Affected areas in Can-avid, Eastern Samar during a 25-year rainfall return period

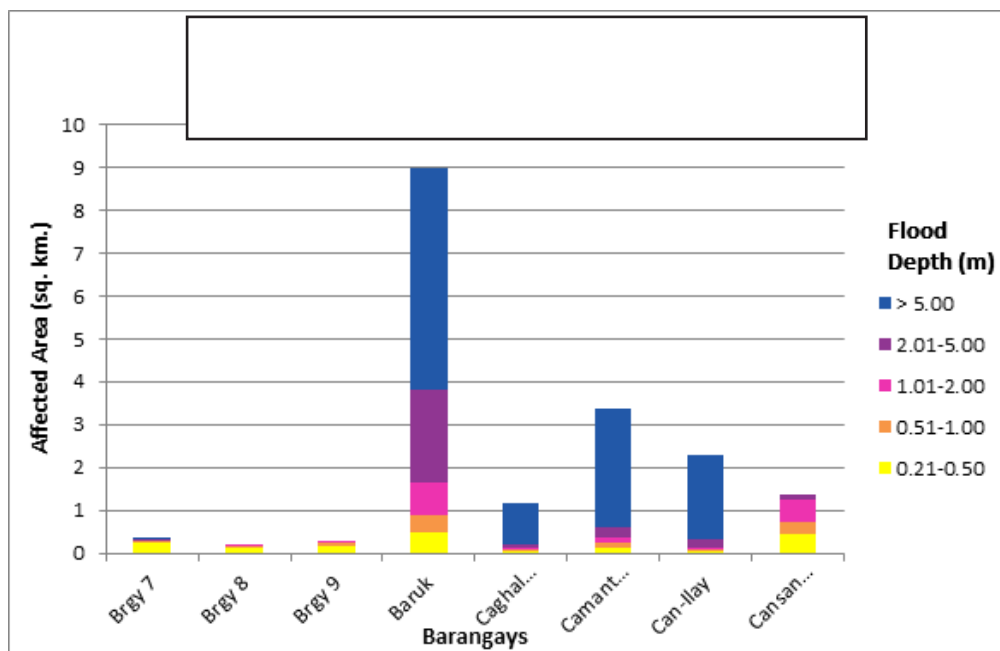


Figure 76. Affected areas in Can-avid, Eastern Samar during a 25-year rainfall return period

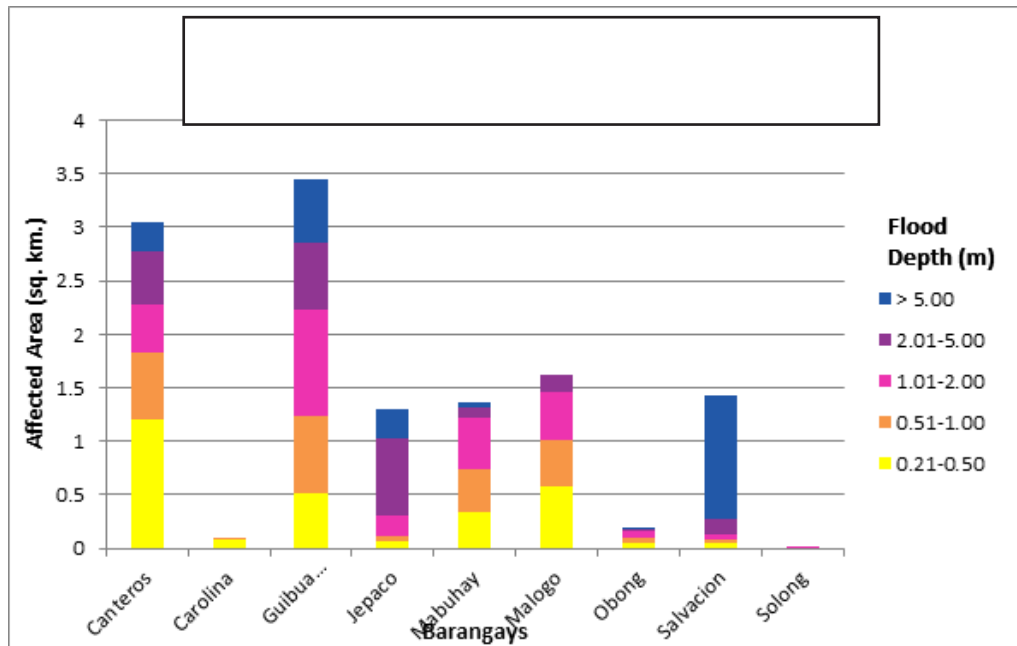


Figure 77. Affected areas in Can-avid, Eastern Samar during a 25-year rainfall return period

For the municipality of Taft, with an area of 230.266 sq km, 0.10% will experience flood levels of less 0.20 meters. 0.0025% of the area will experience flood levels of 0.21 to 0.50 meters while 0.002%, 0.0007%, and 0.0002% of the area will experience flood depths of 0.51 to 1 meter, 1.01 to 2 meters, and above 2 meters, respectively. Listed in Table are the affected areas in square kilometers by flood depth per barangay.

Table 38. Affected areas in Taft, Eastern Samar during a 25-year rainfall return period

TAFT BASIN		Affected Barangays in Taft		
		Batiawan	Beto	Pangabutan
Area	0.03-0.20	0.0038	0.0023	0.23
	0.21-0.50	0.0001	0	0.0059
Affected (sq km.)	0.51-1.00	0	0	0.0046
	1.01-2.00	0	0	0.0017
	2.01-5.00	0	0	0.00056
	> 5.00	0	0	0

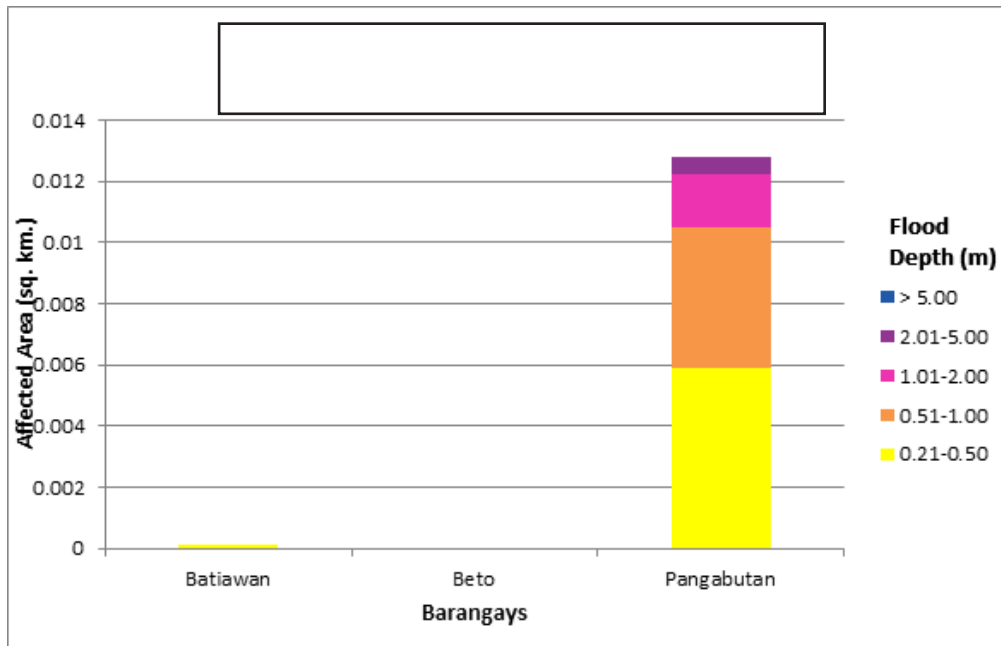


Figure 78. Affected areas in Taft, Eastern Samar during a 25-year rainfall return period

For the 100-year return period, 21.607% of the municipality of Ulot with an area of 285.22 sq km will experience flood levels of less 0.20 meters. 2.13% of the area will experience flood levels of 0.21 to 0.50 meters while 1.47%, 1.68%, 1.97% and 5.47% of the area will experience flood depths of 0.51 to 1 meter, 1.01 to 2 meters, 2.01 to 5 meters and more than 5 meters, respectively. Listed in Table 39 to Table 41 are the affected areas in square kilometers by flood depth per barangay.



Table 39. Affected areas in Can-avid, Eastern Samar during a 100-year rainfall return period

ULOT BASIN										
Affected Barangays in Can-avid										
Area	Balagon	Brgy 1	Brgy 10	Brgy 2	Brgy 3	Brgy 4	Brgy 5	Brgy 6		
0.03-0.20	0.001	0.033	1.22	0.14	0.32	0.35	0.11	0.19		
0.21-0.50	0	0	0.51	0.024	0.16	0.46	0.17	0.12		
0.51-1.00	0	0	0.22	0.019	0.034	0.33	0.11	0.042		
1.01-2.00	0	0	0.021	0.002	0.017	0.029	0.0092	0.0093		
2.01-5.00	0	0	0.03	0	0	0	0	0		
> 5.00	0	0	0.03	0	0	0	0	0		
Affected (sq km.)										

Table 40. Affected areas in Can-avid, Eastern Samar during a 100-year rainfall return period

ULOT BASIN										
Affected Barangays in Can-avid										
Area	Brgy 7	Brgy 8	Brgy 9	Baruk	Caghalong	Camantang	Can-llay	Cansangaya		
0.03-0.20	0.34	0.39	0.1	18.06	1.63	6.23	2.49	3.63		
0.21-0.50	0.35	0.19	0.15	0.51	0.043	0.15	0.031	0.47		
0.51-1.00	0.069	0.05	0.13	0.4	0.036	0.1	0.033	0.29		
1.01-2.00	0.019	0.031	0.0072	0.69	0.04	0.13	0.059	0.55		
2.01-5.00	0.0041	0	0	1.84	0.11	0.28	0.2	0.2		
> 5.00	0.0039	0	0	5.99	1.05	3.03	2.38	0		
Affected (sq km.)										

Table 41. Affected areas in Can-avid, Eastern Samar during a 100-year rainfall return period

ULOT BASIN	Affected Barangays in Can-avid									
	Canteros	Carolina	Guibuangan	Jepaco	Mabuhay	Malogo	Obong	Salvacion	Solong	
Area	0.03-0.20	3.81	0.087	7.69	2.2	5.75	3	1.54	2.19	0.14
	0.21-0.50	1.27	0.11	0.39	0.063	0.29	0.53	0.058	0.037	0.012
	0.51-1.00	0.77	0.0038	0.46	0.05	0.38	0.57	0.049	0.038	0.0016
	1.01-2.00	0.74	0	1.09	0.14	0.57	0.51	0.076	0.053	0.0011
	2.01-5.00	0.5	0	1.16	0.7	0.25	0.21	0.0095	0.14	0
Affected (sq km.)	> 5.00	0.4	0	0.62	0.38	0.054	0	0.0003	1.67	0

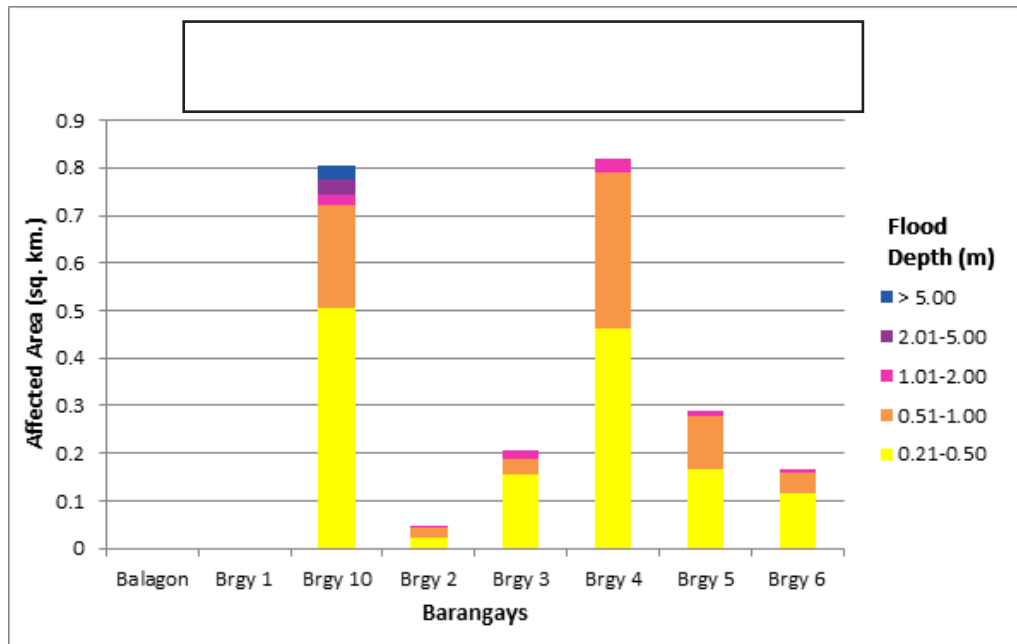


Figure 79. Affected areas in Can-avid, Eastern Samar during a 100-year rainfall return period

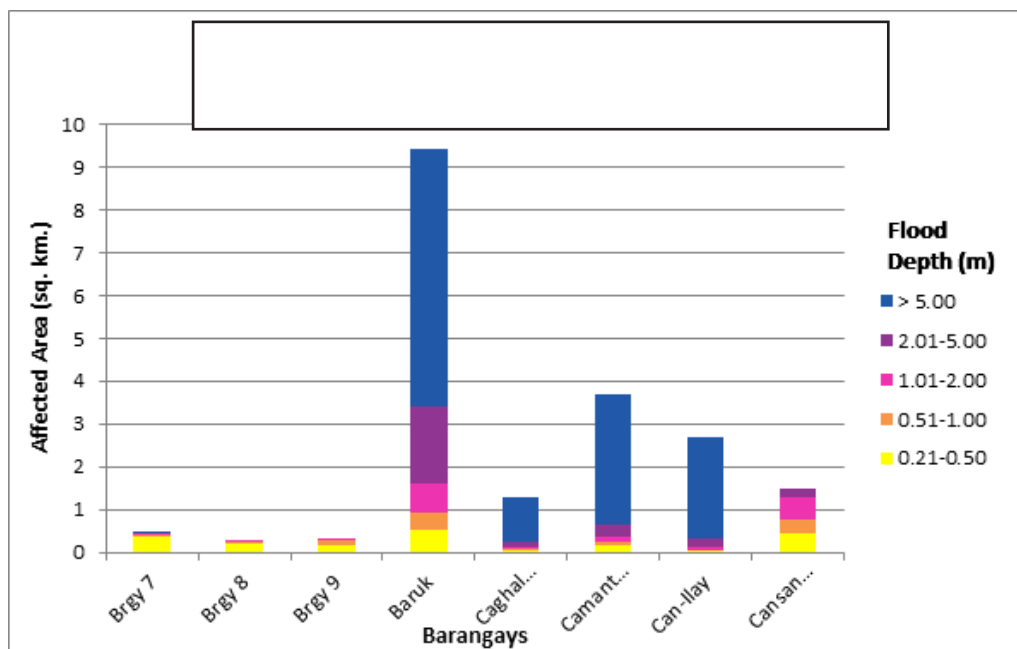


Figure 80. Affected areas in Can-avid, Eastern Samar during a 100-year rainfall return period

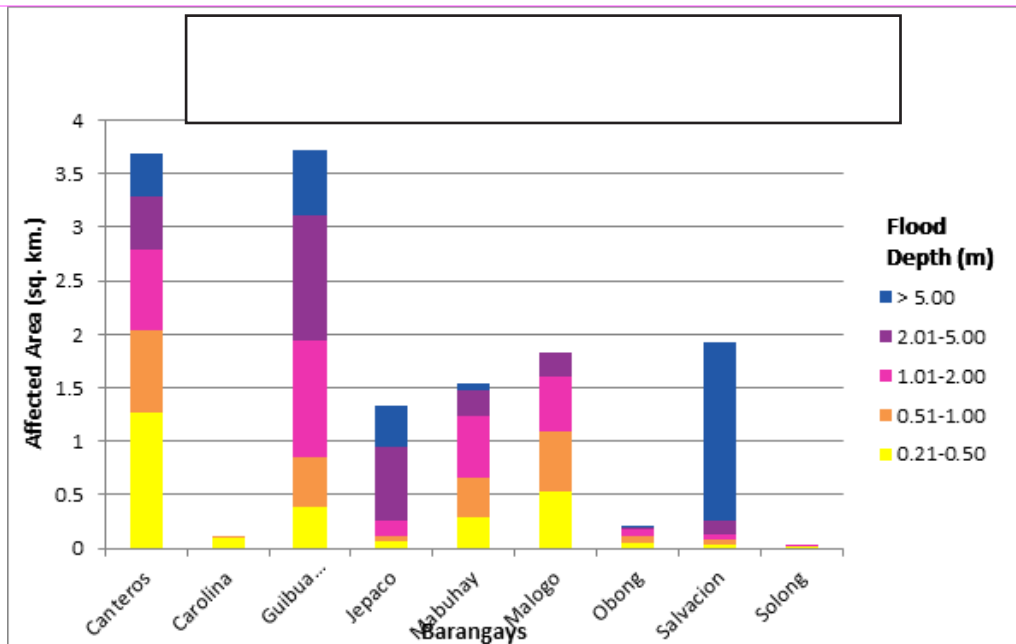


Figure 81. Affected areas in Can-avid, Eastern Samar during a 100-year rainfall return period

For the municipality of Taft, with an area of 230.266 sq km, 0.10% will experience flood levels of less 0.20 meters. 0.002% of the area will experience flood levels of 0.21 to 0.50 meters while 0.0016%, 0.0006%, and 0.0002% of the area will experience flood depths of 0.51 to 1 meter, 1.01 to 2 meters, and above 2 meters, respectively. Listed in Table are the affected areas in square kilometers by flood depth per barangay.

Table 42. Affected areas in Taft, Eastern Samar during a 100-year rainfall return period

ULOT BASIN		Affected Barangays in Santa Fe		
		Batiawan	Beto	Pangabutan
Area	0.03-0.20	0.0038	0.0023	0.23
	0.21-0.50	0.0001	0	0.0052
Affected (sq km.)	0.51-1.00	0	0	0.0037
	1.01-2.00	0	0	0.0015
	2.01-5.00	0	0	0.00046
	> 5.00	0	0	0



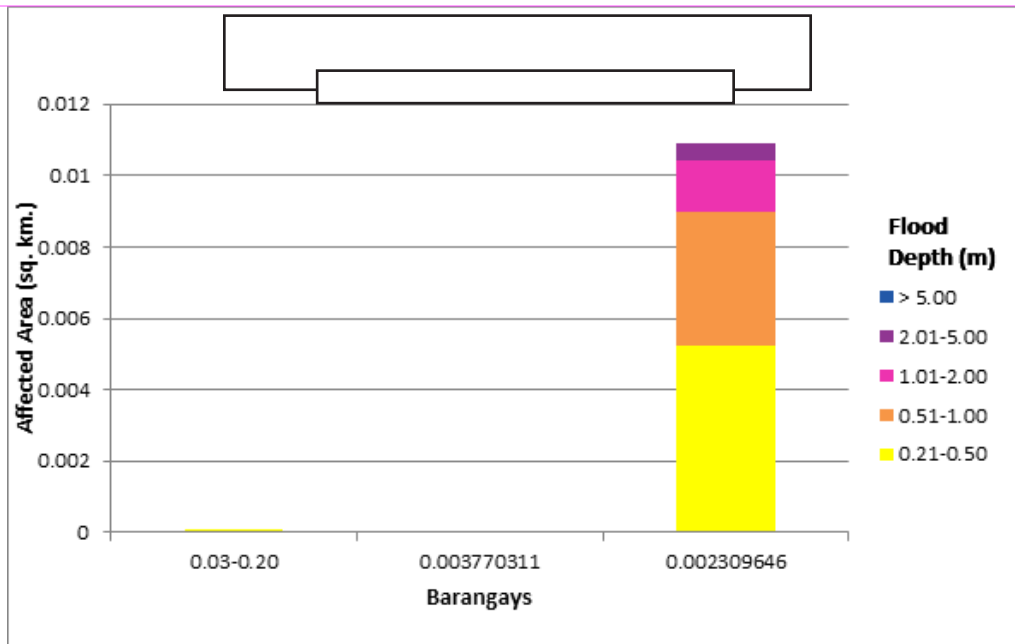


Figure 82. Affected areas in Taft, Eastern Samar during a 100-year rainfall return period

Among the barangays in the municipality of Can-avid, Guibuangan is projected to have the highest percentage of area that will experience flood levels at 4%. Meanwhile, Camantang posted the second highest percentage of area that may be affected by flood depths at 3.48%.

Among the barangays in the municipality of Taft, Pangabutan is projected to have the highest percentage of area that will experience flood levels at 0.105%. Meanwhile, Batiawan posted the second highest percentage of area that may be affected by flood depths at 0.0017%.

### 5.11 Flood Validation

In order to check and validate the extent of flooding in different river systems, there is a need to perform validation survey work. Field personnel gathered secondary data regarding flood occurrence in the area within the major river system in the Philippines.

From the flood depth maps produced by Phil-LiDAR 1 Program, multiple points representing the different flood depths for different scenarios were identified for validation.

The validation personnel then went the specified points identified in a river basin and gathered data regarding the actual flood level in each location. Data gathering was done through a local DRRM office to obtain maps or situation reports about the past flooding events or by interviewing some residents with knowledge of or have experienced flooding in a particular area.

After which, the actual data from the field was compared to the simulated data to assess the accuracy of the flood depth maps produced and to improve on what is needed.

The flood validation consists of 408 points randomly selected all over the Ulot Floodplain. It has an RMSE value of 1.40.

The validation data were obtained on February 23, 2017.

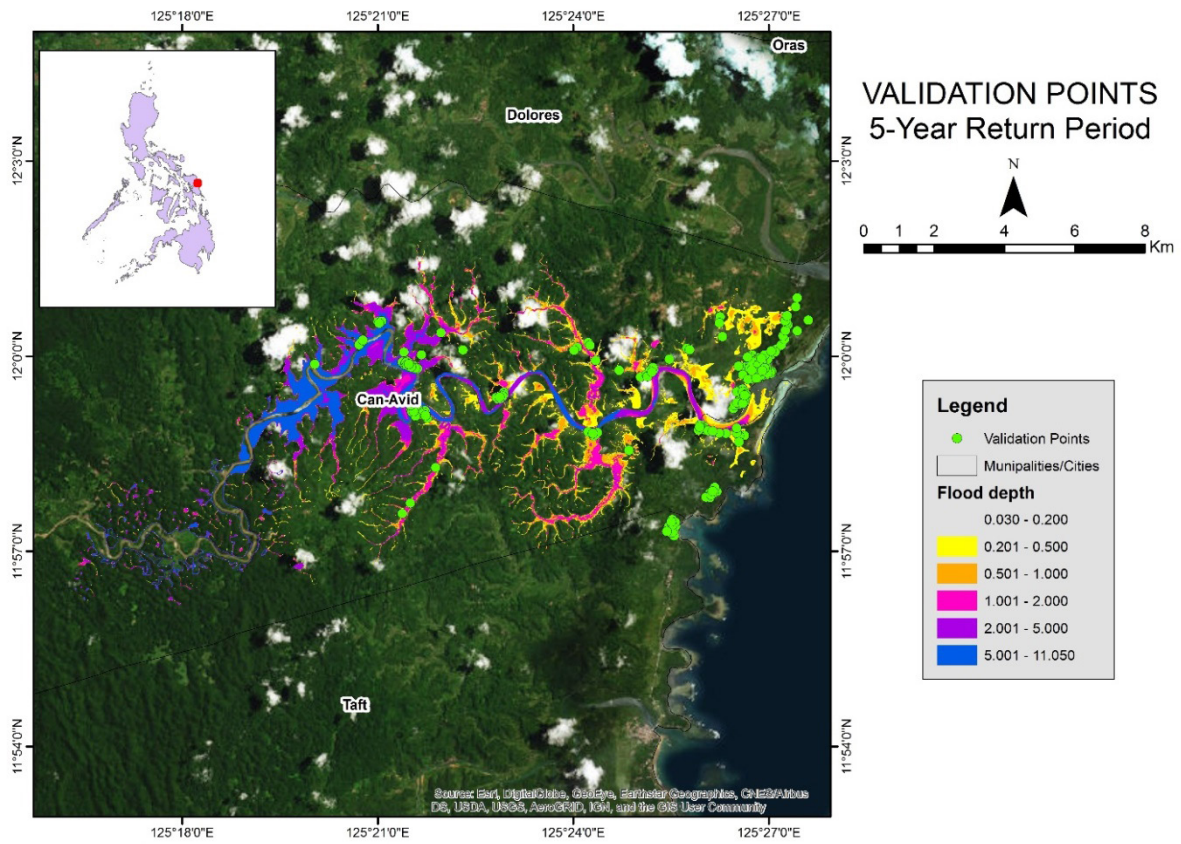


Figure 83. Validation points for 100-year Flood Depth Map of Ulot Floodplain

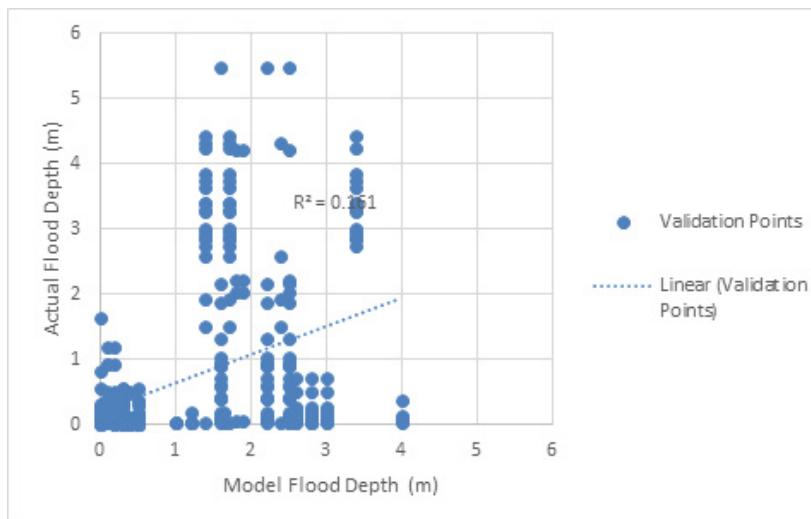


Figure 84. Flood map depth vs actual flood depth

Table 43. Actual flood depth vs simulated flood depth in Ulot

ULOT BASIN		Modeled Flood Depth (m)						Total
		0-0.20	0.21-0.50	0.51-1.00	1.01-2.00	2.01-5.00	> 5.00	
Actual Flood Depth (m)	0-0.20	93	80	4	24	47	0	248
	0.21-0.50	15	8	0	3	13	0	39
	0.51-1.00	7	3	0	7	20	0	37
	1.01-2.00	3	0	0	7	8	0	18
	2.01-5.00	0	0	0	41	22	0	63
	> 5.00	0	0	0	1	2	0	3
	Total	118	91	4	83	112	0	408

The overall accuracy generated by the flood model is estimated at 31.86% with 130 points correctly matching the actual flood depths. In addition, there were 153 points estimated one level above and below the correct flood depths while there were 35 points and 87 points estimated two levels above and below, and three or more levels above and below the correct flood. A total of 4 points were overestimated while a total of 72 points were underestimated in the modelled flood depths of Ulot.

Table 44. Summary of accuracy assessment in Ulot

	No. of Points	%
Correct	130	31.86
Overestimated	206	50.49
Underestimated	72	17.65
Total	408	100.00

## REFERENCES

Ang M.O., Paringit E.C., et al. 2014. *DREAM Data Processing Component Manual*. Quezon City, Philippines: UP Training Center for Applied Geodesy and Photogrammetry.

Balicanta L.P., Paringit E.C., et al. 2014. *DREAM Data Validation Component Manual*. Quezon City, Philippines: UP Training Center for Applied Geodesy and Photogrammetry.

Brunner, G. H. 2010a. *HEC-RAS River Analysis System Hydraulic Reference Manual*. Davis, CA: U.S. Army Corps of Engineers, Institute for Water Resources, Hydrologic Engineering Center.

Lagmay A.F., Paringit E.C., et al. 2014. *DREAM Flood Modeling Component Manual*. Quezon City, Philippines: UP Training Center for Applied Geodesy and Photogrammetry.

Paringit E.C., Balicanta L.P., Ang, M.O., Sarmiento, C. 2017. *Flood Mapping of Rivers in the Philippines Using Airborne Lidar: Methods*. Quezon City, Philippines: UP Training Center for Applied Geodesy and Photogrammetry.

Sarmiento C., Paringit E.C., et al. 2014. *DREAM Data Acquisition Component Manual*. Quezon City, Philippines: UP Training Center for Applied Geodesy and Photogrammetry.

UP TCAGP 2016, *Acceptance and Evaluation of Synthetic Aperture Radar Digital Surface Model (SAR DSM) and Ground Control Points (GCP)*. Quezon City, Philippines: UP Training Center for Applied Geodesy and Photogrammetry.



## ANNEXES

### ANNEX 1. OPTECH Technical Specification of the Aquarius Sensor

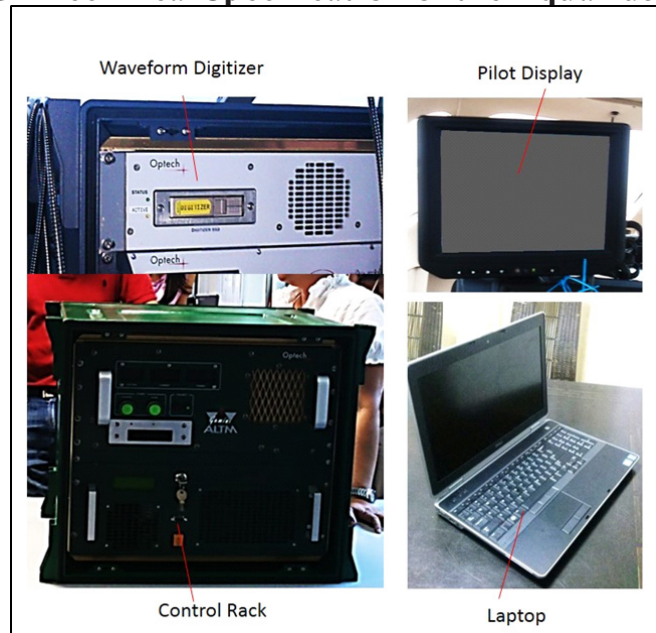



Figure A-1.1. Aquarius Sensor

Table A-1.1. Parameters and Specifications of Aquarius Sensor

Parameter	Specification
Operational altitude	300-600 m AGL
Laser pulse repetition rate	33, 50. 70 kHz
Scan rate	0-70 Hz
Scan half-angle	0 to $\pm 25^\circ$
Laser footprint on water surface	30-60 cm
Depth range	0 to > 10 m (for $k < 0.1/m$ )
Topographic mode	
Operational altitude	300-2500
Range Capture	Up to 4 range measurements, including 1st, 2nd, 3rd, and last returns
Intensity capture	12-bit dynamic measurement range
Position and orientation system	POS AVTM 510 (OEM) includes embedded 72-channel GNSS receiver (GPS and GLONASS)
Data Storage	Ruggedized removable SSD hard disk (SATA III)
Power	28 V, 900 W, 35 A
Image capture	5 MP interline camera (standard); 60 MP full frame (optional)
Full waveform capture	12-bit Optech IWD-2 Intelligent Waveform Digitizer (optional)
Dimensions and weight	Sensor: 250 x 430 x 320 mm; 30 kg; Control rack: 591 x 485 x 578 mm; 53 kg
Operating temperature	0-35°C
Relative humidity	0-95% no-condensing

## Annex 2. NAMRIA Certificates of Reference Points Used in the LiDAR Survey

### 1. SME-3139



Republic of the Philippines  
Department of Environment and Natural Resources  
**NATIONAL MAPPING AND RESOURCE INFORMATION AUTHORITY**

June 24, 2014

### CERTIFICATION

To whom it may concern:

This is to certify that according to the records on file in this office, the requested survey information is as follows -


<b>Province: EASTERN SAMAR</b>		
<b>Station Name: SME-3139</b>		
<b>Island: VISAYAS</b>	<b>Order: 4th</b>	<b>Barangay: SANTO NIÑO</b>
<b>Municipality: SULAT</b>		
<b>PRS92 Coordinates</b>		
Latitude: <b>11° 50' 2.95701"</b>	Longitude: <b>125° 26' 3.02189"</b>	Ellipsoidal Hgt: <b>0.35600 m.</b>
<b>WGS84 Coordinates</b>		
Latitude: <b>11° 49' 58.57713"</b>	Longitude: <b>125° 26' 8.12160"</b>	Ellipsoidal Hgt: <b>62.18500 m.</b>
<b>PTM Coordinates</b>		
Northing: <b>1308628.152 m.</b>	Easting: <b>547309.911 m.</b>	Zone: <b>5</b>
<b>UTM Coordinates</b>		
Northing: <b>1,309,289.26</b>	Easting: <b>765,219.59</b>	Zone: <b>51</b>


Location Description

SME-3139


From Tacloban City, travel about 70 Km. NE towards the junction of Buena Vista, Quinapondan. Then travel about 170 Km. NW pass Gen. Mc Arthur, Hernani, Llorente, Balangkayan, Maydolong, Borongan and San Julian pass Sulat proper towards Brgy. Sto. Niño until reaching a bridge near the Km. post 900 S-4. Station is located at the right side of the road about 1 m S of the bridge, about 100 m S of Km. post 900 S-4, about 500 m S of the brgy. basketball court. Mark is the head of a 4 in. copper nail centered on a 0.20 m x 0.20 m x 1.00 m concrete monument with inscriptions, "SME-3139, 2008, NAMRIA".

Requesting Party: **Engr. Cruz**  
 Purpose: **Reference**  
 OR Number: **8796376 A**  
 T.N.: **2014-1442**

*For*   
**RUEL DM. BELEN, MNSA**  
 Director, Mapping And Geodesy Branch



9 9 0 6 2 4 2 0 1 4 1 1 7 1 8



CIP/4701/12/09/814

NAMRIA OFFICES:  
 Main : Lawton Avenue, Fort Bonifacio, 1634 Taguig City, Philippines Tel. No.: (632) 810-4831 to 41  
 Branch : 421 Barraca St. San Nicolas, 1010 Manila, Philippines, Tel. No. (632) 241-3494 to 98  
[www.namria.gov.ph](http://www.namria.gov.ph)  
 ISO 9001: 2008 CERTIFIED FOR MAPPING AND GEOSPATIAL INFORMATION MANAGEMENT

Figure A-2.1. SME-3139

### Annex 3. Baseline Processing Reports of Reference Points Used in the LiDAR Survey

1. SE-16

SME-3139 - SE-16 (6:11:03 AM-11:04:02 AM) (S2)

Baseline observation:	SME-3139 — SE-16 (B2)
Processed:	6/30/2014 5:42:19 PM
Solution type:	Fixed
Frequency used:	Dual Frequency (L1, L2)
Horizontal precision:	0.001 m
Vertical precision:	0.002 m
RMS:	0.000 m
Maximum PDOP:	3.434
Ephemeris used:	Broadcast
Antenna model:	Trimble Relative
Processing start time:	6/9/2014 6:11:10 AM (Local: UTC+8hr)
Processing stop time:	6/9/2014 11:04:02 AM (Local: UTC+8hr)
Processing duration:	04:52:52
Processing interval:	1 second

Vector Components (Mark to Mark)

From: SME-3139					
Grid		Local		Global	
Easting	765219.591 m	Latitude	N11°50'02.95701"	Latitude	N11°49'58.57713"
Northing	1309289.260 m	Longitude	E125°26'03.02189"	Longitude	E125°26'08.12160"
Elevation	2.987 m	Height	0.356 m	Height	62.185 m

To: SE-16					
Grid		Local		Global	
Easting	765219.942 m	Latitude	N11°50'03.05106"	Latitude	N11°49'58.67117"
Northing	1309292.154 m	Longitude	E125°26'03.03429"	Longitude	E125°26'08.13400"
Elevation	3.103 m	Height	0.472 m	Height	62.301 m

Vector					
ΔEasting	0.350 m	NS Fwd Azimuth	7°23'58"	ΔX	-0.028 m
ΔNorthing	2.894 m	Ellipsoid Dist.	2.914 m	ΔY	-0.608 m
ΔElevation	0.116 m	ΔHeight	0.116 m	ΔZ	2.852 m

Standard Errors

Vector errors:					
σ ΔEasting	0.000 m	σ NS fwd Azimuth	0°00'35"	σ ΔX	0.001 m
σ ΔNorthing	0.000 m	σ Ellipsoid Dist.	0.000 m	σ ΔY	0.001 m
σ ΔElevation	0.001 m	σ ΔHeight	0.001 m	σ ΔZ	0.000 m

Figure A-3.1. SE-16

### Annex 4. The LiDAR Survey Team Composition

Table A-4.1. The LiDAR Survey Team Composition

Data Acquisition Component Sub-Team	Designation	Name	Agency/ Affiliation
PHIL-LIDAR 1	Program Leader	ENRICO C. PARINGIT, D.ENG	UP-TCAGP
Data Acquisition Component Leader	Data Component Project Leader - I	ENGR. CZAR JAKIRI SARMIENTO	UP-TCAGP
	Data Component Project Leader – I	ENGR. LOUIE P. BALICANTA	UP-TCAGP
Survey Supervisor	Chief Science Research Specialist (CSRS)	ENGR. CHRISTOPHER CRUZ	UP-TCAGP
	Supervising Science Research Specialist (Supervising SRS)	LOVELY GRACIA ACUÑA	UP-TCAGP
		LOVELYN ASUNCION	UP-TCAGP
FIELD TEAM			
LiDAR Operation	Research Associate (RA)	PAULINE JOANNE ARCEO	UP-TCAGP
	RA	MARY CATHERINE ELIZABETH BALIGUAS	UP-TCAGP
Ground Survey, Data Download and Transfer	RA	JERIEL PAUL ALAMBAN	UP-TCAGP
LiDAR Operation	Airborne Security	SSG. RAYMUND DOMINE	PHILIPPINE AIR FORCE (PAF)
	Pilot	CAPT. NEIL ACHILLES AGAWIN	ASIAN AEROSPACE CORPORATION (AAC)
		CAPT. JACKSON JAVIER	AAC



# Annex 5. Data Transfer Sheet for Ulot Floodplain

**DATA TRANSFER SHEET**  
6/19/2014 (Samar - Leyte) *Final*

DATE	FLIGHT NO.	MISSION NAME	SENSOR	RAW LAS		LOGS	POS	RAW IMAGES	MISSION LOG FILE	RANGE	DIGITIZER	BASE STATION(S)		OPERATOR LOGS (OPLOG)	FLIGHT PLAN		SERVER LOCATION
				Output LAS	KMIL (swath)							BASE STATION(S)	Base Info (.tif)		Actual	KMIL	
30-May-14	1570A	3BLK33V5S150A	Aquarius	NA	424/602	1.48	289	88.5	748	14	164	10.5	1KB	1KB	4	NA	X:\Airborne_Raw1\520A
31-May-14	1572A	3BLK33SS151A	Aquarius	NA	288	469KB	112	9.78/21	164/69	4.87	59.1	4.53	1KB	1KB	5	NA	X:\Airborne_Raw1\522A
1-Jun-14	1526A	3BLK33SR152A	Aquarius	NA	456/784	1.68	277	119	403	15.5	204	8.36	1KB	1KB	6	NA	X:\Airborne_Raw1\526A
2-Jun-14	1530A	3BLK33RSQ153A	Aquarius	NA	353/605	1.48	254	30.9/80.2	555/246	15.6	165	7.88	1KB	1KB	3	NA	X:\Airborne_Raw1\530A
3-Jun-14	1534A	3BLK33Q154A	Aquarius	NA	1175	1.49	250	56.9/35.1	399/154	14.5	114/95.5	6.6	1KB	1KB	7	NA	X:\Airborne_Raw1\534A
7-Jun-14	1550A	3BLK33P158A	Aquarius	NA	657	1.03	189	52.9	na	10.8	149	7	1KB	1KB	3	NA	X:\Airborne_Raw1\550A
8-Jun-14	1554A	3BLK33PSM159A	Aquarius	NA	533/1012	1.78	257	99.8	695	14.5	27.2/59/32.2	16.4	1KB	1KB	3	NA	X:\Airborne_Raw1\554A
8-Jun-14	1556A	3BLK33MS159B	Aquarius	NA	982	1.52	281	97.2	477	15.9	216	16.4	1KB	1KB	5	NA	X:\Airborne_Raw1\556A
9-Jun-14	1558A	3BLK33J160A	Aquarius	NA	853	1.27	277	95.7	452	14.2	95.6/80.5	16.1	1KB	1KB	4	NA	X:\Airborne_Raw1\558A
9-Jun-14	1560A	3BLK33J	Aquarius	NA	1583	1.67	223	72.2	357	12.1	123	16.1	1KB	1KB	5	NA	X:\Airborne_Raw1\560A

Received by

Name: JOLA PRIETO  
 Position: Surveyor  
 Signature: [Signature]  
 Date: 6/19/14

Received from

Name: [Signature]  
 Position: Surveyor  
 Signature: [Signature]

14-43

Figure A-5.1. Data Transfer Sheet

## Annex 6. Flight Logs for the Flight Missions

### 1. Flight Log for 3BLK33J160A Mission

Flight Log No.: 1528

**DREAM Data Acquisition Flight Log**

1 LiDAR Operator: P. Arcebo	2 ALTM Model: Aova	3 Mission Name: 3BLK33J160A	4 Type: VFR	5 Aircraft Type: Cessna T206H	6 Aircraft Identification: 9132
7 Pilot: J. JAVIER	8 Co-Pilot: N. ARANIN	9 Route:	12 Airport of Arrival (Airport, City/Province):	17 Landing:	18 Total Flight Time:
10 Date: 07 JUN 14	12 Airport of Departure (Airport, City/Province):	15 Total Engine Time: 37:23	16 Take off:		
13 Engine On: 1030	14 Engine Off: 1353				
19 Weather:					
20 Remarks:					

21 Problems and Solutions:

Acquisition Flight Approved by

*[Signature]*

Signature over Printed Name  
(End User Representative)

Acquisition Flight Certified by

*[Signature]*

Signature over Printed Name  
(PAF Representative)

Pilot-in-Command


*[Signature]*

Signature over Printed Name

Lidar Operator

*[Signature]*

Signature over Printed Name



**DREAM**

Disaster Risk and Exposure Assessment for Mitigation

Figure A-6.1. Flight Log for Mission 3BLK33J160A



2. Flight Log for 3BLK33J160A Mission

PHIL-LIDAR 1 Data Acquisition Flight Log

Flight Log No.: 1560A

1 LIDAR Operator: C. BALLOUS		2 ALTM Model: A9VA		3 Mission Name: 3BLK33J5		4 Type: VFR		5 Aircraft Type: Cessna 170GH		6 Aircraft Identification: 9122	
7 Pilot: J. JAVIER		8 Co-Pilot: M. A. AGUIAR		9 Route:		10 Date: 09 June 14		11 Airport of Departure (Airport, City/Province):		12 Airport of Arrival (Airport, City/Province):	
13 Engine On:		14 Engine Off:		15 Total Engine Time: 4:53		16 Take off:		17 Landing:		18 Total Flight Time:	
19 Weather						20 Flight Classification					
20.a Billable						20.b Non Billable					
<input checked="" type="radio"/> Acquisition Flight <input type="radio"/> Ferry Flight <input type="radio"/> System Test Flight <input type="radio"/> Calibration Flight						<input type="radio"/> Aircraft Test Flight <input type="radio"/> AAC Admin Flight <input type="radio"/> Others: _____					
						<input type="radio"/> LIDAR System Maintenance <input type="radio"/> Aircraft Maintenance <input type="radio"/> Phil-LIDAR Admin Activities					
21 Remarks						Mission completed over BLK33J					
22 Problems and Solutions											
<input type="radio"/> Weather Problem <input type="radio"/> System Problem <input type="radio"/> Aircraft Problem <input type="radio"/> Pilot Problem <input type="radio"/> Others: _____											


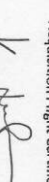


Acquisition Flight Approved by	Acquisition Flight Certified by	Pilot-in-Command	LIDAR Operator
			
Signature over Printed Name (End User Representative)	Signature over Printed Name (PAF Representative)	Signature over Printed Name	Signature over Printed Name
		Aircraft Mechanic/ LIDAR Technician	
		Signature over Printed Name	

Figure A-6.2. Flight Log for Mission 3BLK33J160A

## Annex 7. Flight Status Reports

Table A-7.1. Flight Status Reports  
TACLOBAN

FLIGHT NO	AREA	MISSION	OPERATOR	DATE FLOWN	REMARKS
1558A	BLK33J	3BLK33J160A	PJ ARCEO	9 JUN 14	Completed 12 lines over BLK33J
1560A	BLK33J	3BLK33JS160B	MCE BALIGUAS	9 JUN 14	Mission completed over BLK33J

Flight No. : 1558A  
 Area: BLOCK 33J  
 Total Area: 115.55 sq km.  
 Mission Name: 3BLK33J60A  
 Altitude: 500m  
 PRF: 50 kHz                      SCF: 45 Hz  
 Lidar FOV: 22 deg                Sidelap:30%



Figure A-7.1. Swath for Flight No. 1558A



Flight No. : 1560A  
Area: BLOCK 33J  
Total Area: 105.37 sq km.  
Mission Name: 3BLK33JS60A  
Altitude: 500m  
PRF: 50 kHz            SCF: 45 Hz  
Lidar FOV: 22 deg        Sidelap: 25%



Figure A-7.1. Swath for Flight No. 1560A

## Annex 8. Mission Summary Reports

Table A-8.1. Mission Summary Report for Mission Blk33J

Flight Area	Samar-Leyte
Mission Name	Blk33J
Inclusive Flights	1560A, 1558A
Range data size	26.3 GB
POS	500 MB
Image	167.9 GB
Transfer date	June 19, 2014
<i>Solution Status</i>	
Number of Satellites (>6)	Yes
PDOP (<3)	Yes
Baseline Length (<30km)	No
Processing Mode (<=1)	No
<i>Smoothed Performance Metrics (in cm)</i>	
RMSE for North Position (<4.0 cm)	2.1
RMSE for East Position (<4.0 cm)	2.2
RMSE for Down Position (<8.0 cm)	3.1
Boresight correction stdev (<0.001deg)	0.000327
IMU attitude correction stdev (<0.001deg)	0.000898
GPS position stdev (<0.01m)	0.0098
Minimum % overlap (>25)	36.01%
Ave point cloud density per sq.m. (>2.0)	2.71
Elevation difference between strips (<0.20 m)	Yes
Number of 1km x 1km blocks	291
Maximum Height	248.48 m
Minimum Height	49.30 m
<i>Classification (# of points)</i>	
Ground	110,486,647
Low vegetation	51,277,620
Medium vegetation	61,095,498
High vegetation	151,119,077
Building	2,518,830
Orthophoto	Yes
Processed by	Engr. Jommer Medina, Engr. Edgardo Gubatanga Jr., Engr. Gladys Mae Apat

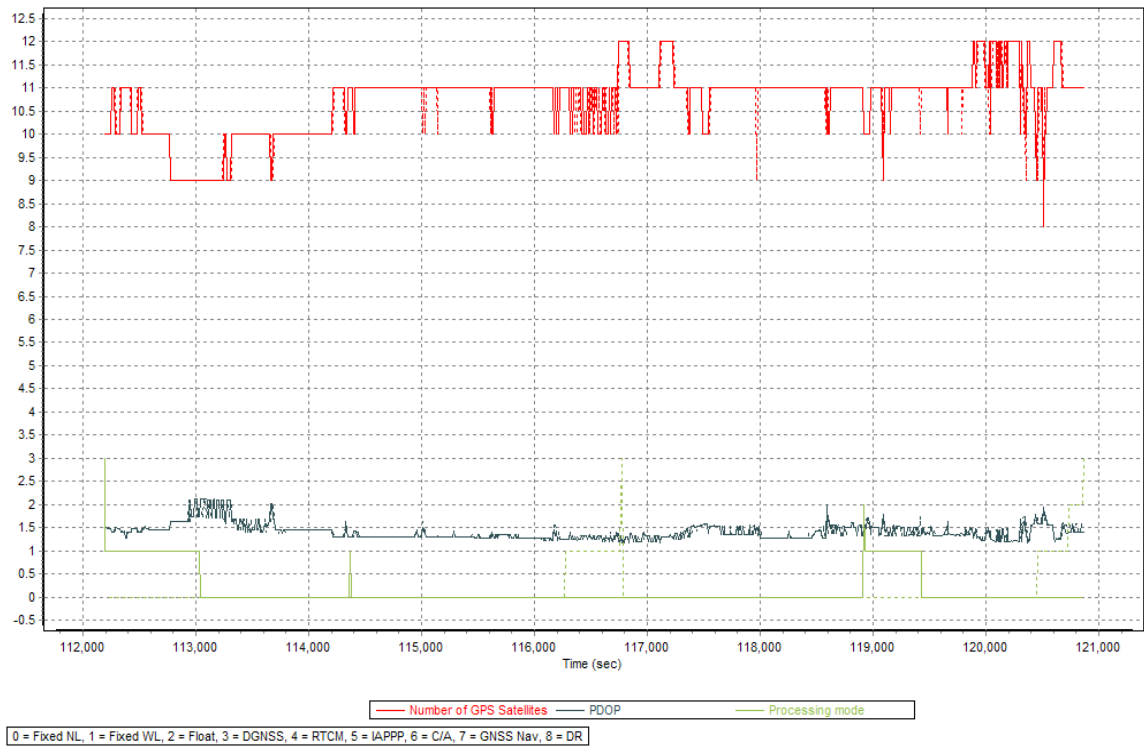


Figure A-8.1. Solution Status

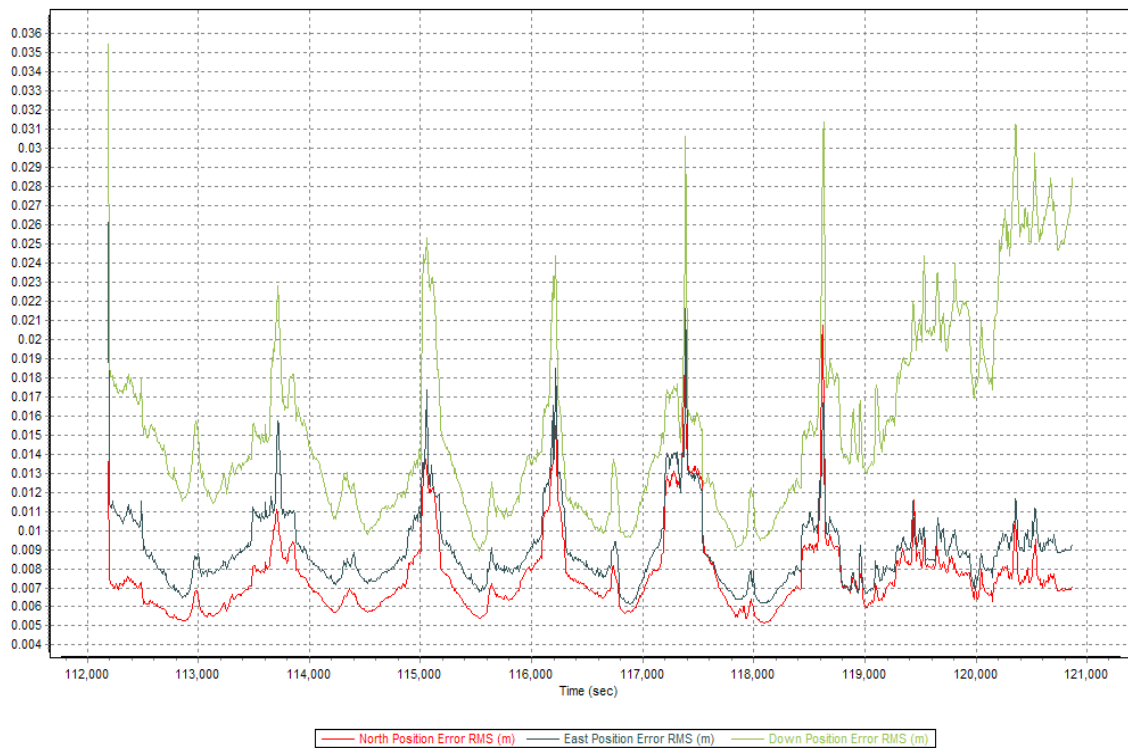


Figure A-8.2. Smoothed Performance Metrics Parameters

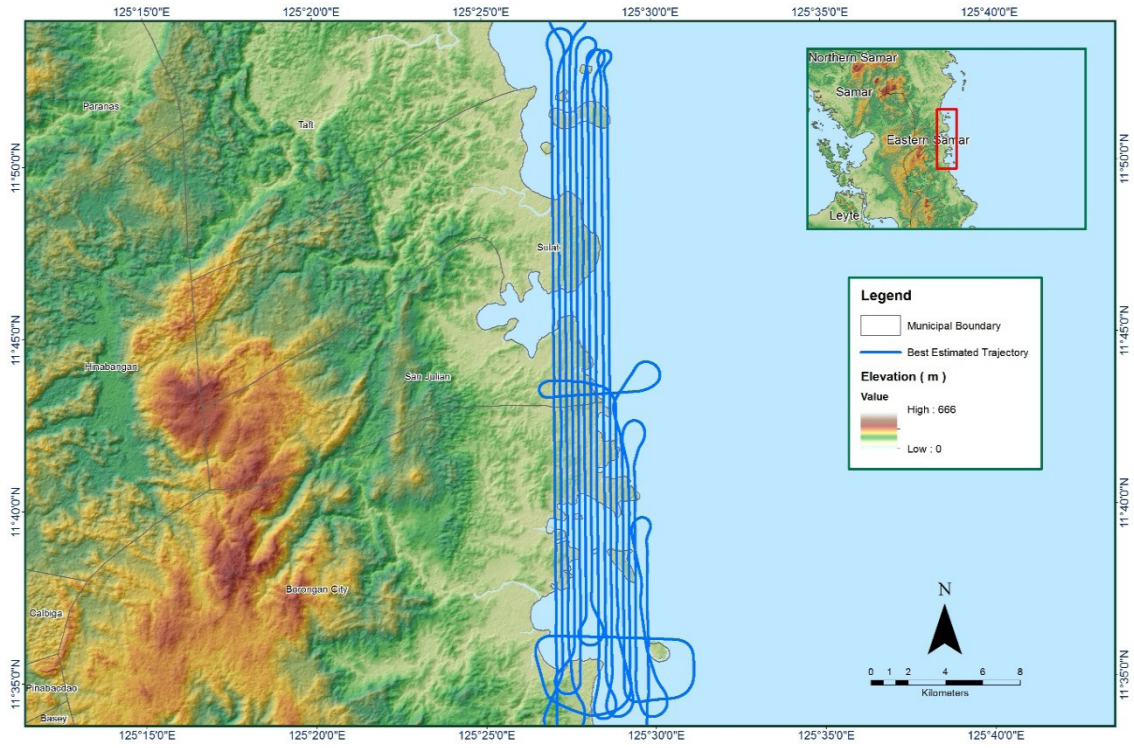


Figure A-8.3. Best Estimated Trajectory

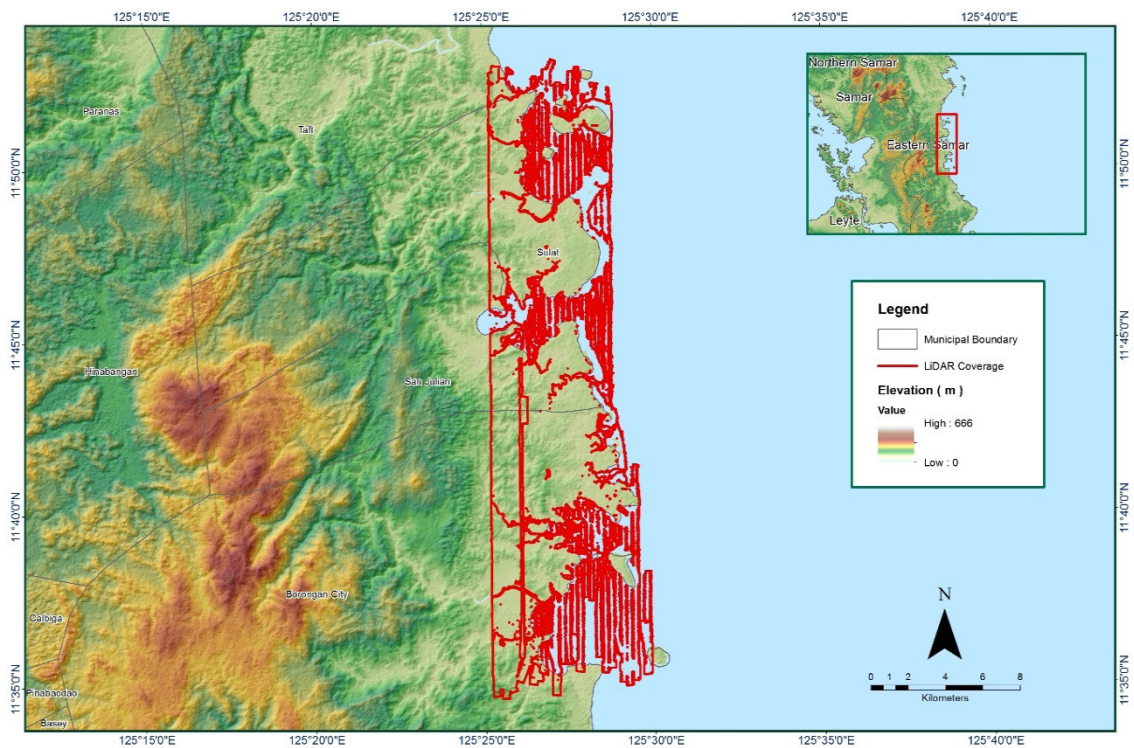


Figure A-8.4. Coverage of LiDAR data



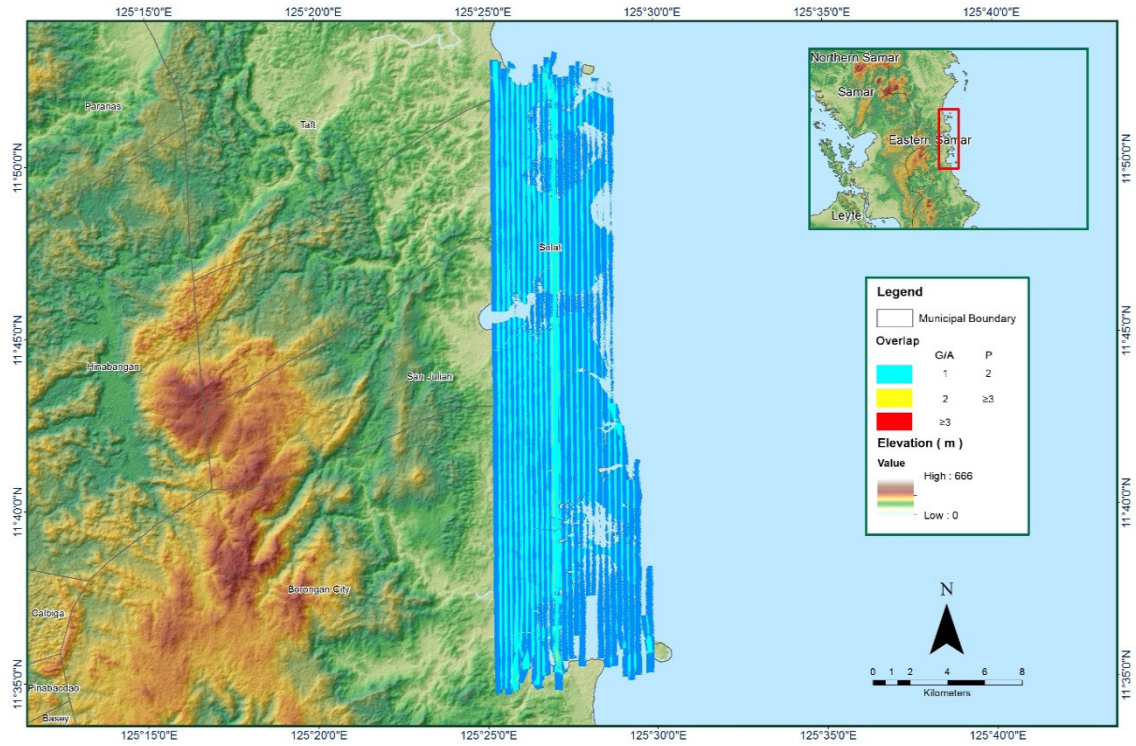


Figure A-8.5. Image of data overlap

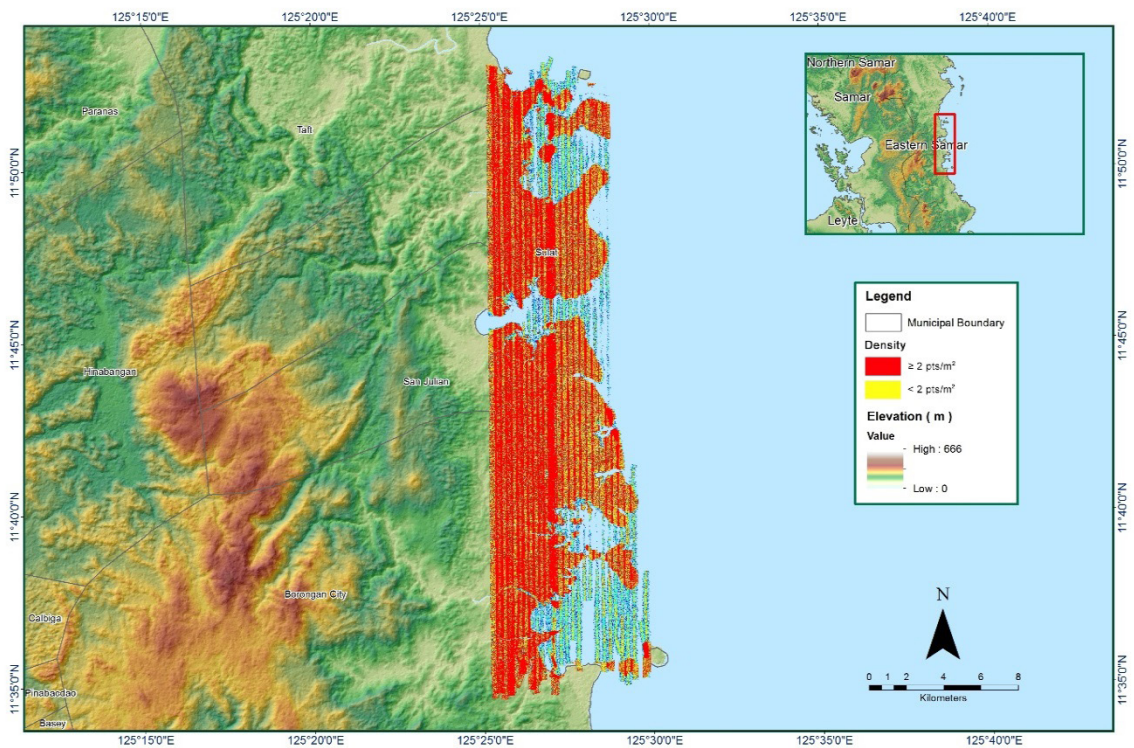


Figure A-8.6. Density map of merged LiDAR data

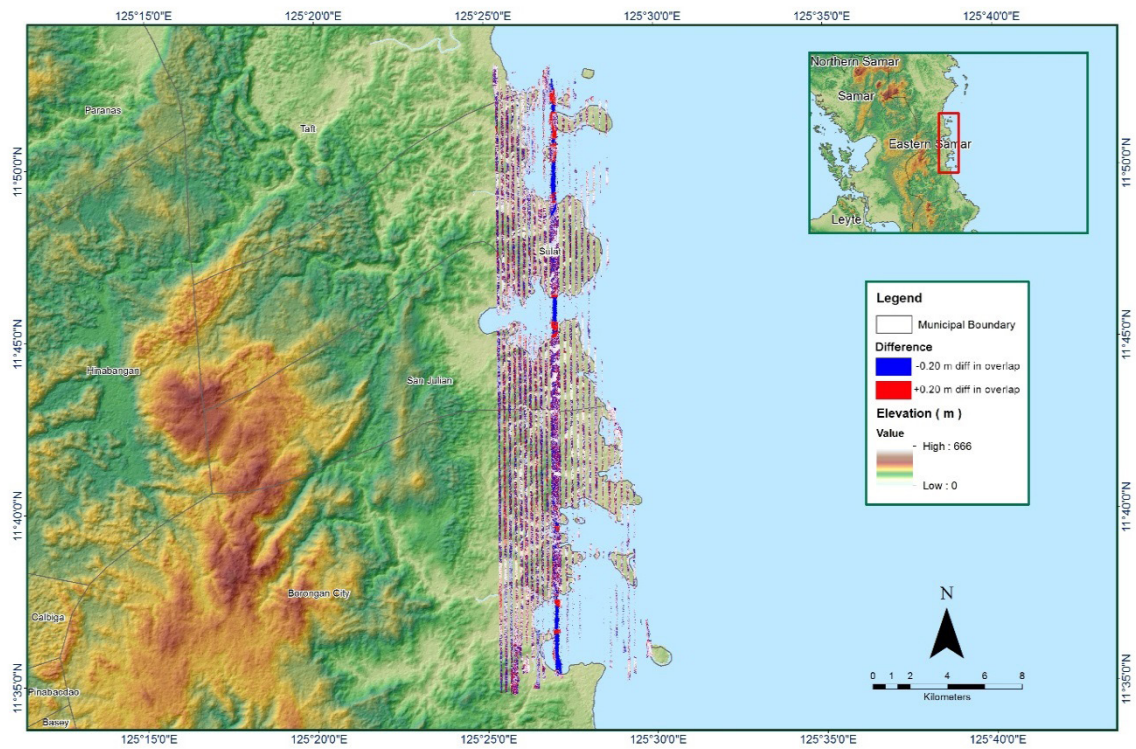


Figure A-8.7. Elevation difference between flight lines

**Annex 9. Ulot Model Basin Parameters**

Table A-9.1. Ulot Model Basin Parameters

Basin Number	SCS Curve Number Loss			Clark Unit Hydrograph Transform			Recession Baseflow			
	Initial Abstraction (mm)	Curve Number	Impervious (%)	Time of Concentration (HR)	Storage Coefficient (HR)	Initial Type	Initial Discharge (M3/S)	Recession Constant	Threshold Type	Ratio to Peak
W1840	139.1013	69.802	0	2.61495	7.64313	Discharge	4.7317	0.68	Ratio to Peak	0.43
W1830	154.8906	67.488	0	3.20437	5.971415	Discharge	3.4153	0.68	Ratio to Peak	0.43
W1820	231.4873	58.14	0	2.50354	3.504265	Discharge	0.36007	0.68	Ratio to Peak	0.43
W1810	346.8228	48.107	0	1.469195	10.2828	Discharge	1.711	0.68	Ratio to Peak	0.43
W1800	348.3101	48	0	4.31093	12.5666	Discharge	3.2455	0.68	Ratio to Peak	0.43
W1790	116.943	73.329	0	5.26851	6.01388	Discharge	3.1268	0.68	Ratio to Peak	0.43
W1780	308.6519	51.021	0	2.521285	5.049535	Discharge	0.53864	0.68	Ratio to Peak	0.43
W1770	183.5633	63.656	0	2.116985	9.42495	Discharge	6.2849	0.68	Ratio to Peak	0.43
W1760	251.2152	56.138	0	3.95135	4.6056	Discharge	0.95122	0.68	Ratio to Peak	0.43
W1750	116.5633	73.392	0	1.93089	3.78898	Discharge	0.30756	0.68	Ratio to Peak	0.43
W1740	117.7468	73.19514	0	1.588535	2.89636	Discharge	0.5419	0.68	Ratio to Peak	0.43
W1730	99.68354	76.334	0	1.214265	3.14944	Discharge	1.6258	0.68	Ratio to Peak	0.43
W1720	122.943	72.339	0	1.32041	2.207325	Discharge	0.28187	0.68	Ratio to Peak	0.43
W1710	154.6341	67.52429	0	0.925405	5.147955	Discharge	1.3399	0.68	Ratio to Peak	0.43
W1700	92.291	77.697	0	2.15826	3.665385	Discharge	1.6955	0.68	Ratio to Peak	0.43
W1690	97.892	76.659	0	1.53673	4.292575	Discharge	5.2653	0.68	Ratio to Peak	0.43
W1680	90.127	78.106	0	1.799655	2.92467	Discharge	1.7763	0.68	Ratio to Peak	0.43
W1670	103.9304	75.571	0	1.22616	0.47595	Discharge	0.005268	0.68	Ratio to Peak	0.43
W1660	93.013	77.562	0	0.199537	4.538245	Discharge	1.719	0.68	Ratio to Peak	0.43
W1650	87.886	78.534	0	1.90268	1.457585	Discharge	0.65267	0.68	Ratio to Peak	0.43
W1640	228.6618	58.439	0	0.611078	6.97775	Discharge	2.1655	0.68	Ratio to Peak	0.43
W1630	190.9304	62.742	0	2.92539	8.983295	Discharge	3.7922	0.68	Ratio to Peak	0.43
W1620	190.962	62.738	0	3.76623	6.23295	Discharge	1.8196	0.68	Ratio to Peak	0.43
W1610	192.7025	62.525	0	2.61313	8.34556	Discharge	1.2252	0.68	Ratio to Peak	0.43

Basin Num-ber	SCS Curve Number Loss			Clark Unit Hydrograph Trans-form			Recession Baseflow					
	Initial Abstraction (mm)	Curve Number	Impervious (%)	Time of Concentration (HR)	Storage Coefficient (HR)	Initial Type	Initial Discharge (M3/S)	Recession Constant	Threshold Type	Ratio to Peak		
W1600	238.6456	57.397	0	3.49882	6.857385	Discharge	1.6994	0.68	Ratio to Peak	0.43		
W1590	118.918	73	0	2.87495	3.32348	Discharge	1.1213	0.68	Ratio to Peak	0.43		
W1580	144.981	68.922	0	1.39334	5.36123	Discharge	2.7157	0.68	Ratio to Peak	0.43		
W1570	147.2595	68.586	0	2.2477	3.41981	Discharge	1.9373	0.68	Ratio to Peak	0.43		
W1560	211.0063	60.376	0	1.43377	5.03025	Discharge	2.2385	0.68	Ratio to Peak	0.43		
W1550	173.9494	64.892	0	2.108925	4.399925	Discharge	1.5851	0.68	Ratio to Peak	0.43		
W1540	119.6203	72.884	0	1.844635	5.04849	Discharge	2.6384	0.68	Ratio to Peak	0.43		
W1530	90.658	78.005	0	2.116595	4.28374	Discharge	1.7598	0.68	Ratio to Peak	0.43		
W1520	118.918	73	0	1.79595	4.0014	Discharge	1.4456	0.68	Ratio to Peak	0.43		
W1510	98.538	76.542	0	1.677585	2.54353	Discharge	0.94224	0.68	Ratio to Peak	0.43		
W1500	115.1013	73.638	0	1.06639	3.75307	Discharge	2.9605	0.68	Ratio to Peak	0.43		
W1490	129.5253	71.283	0	1.573455	6.42428	Discharge	2.3519	0.68	Ratio to Peak	0.43		
W1480	93.943	77.388	0	2.69334	1.393935	Discharge	0.25629	0.68	Ratio to Peak	0.43		
W1470	88.848	78.35	0	0.584383	0.995315	Discharge	0.18003	0.68	Ratio to Peak	0.43		
W1460	154.6962	67.515	0	0.417281	3.9938	Discharge	1.6991	0.68	Ratio to Peak	0.43		
W1450	207.2532	60.805	0	1.6744	7.1041	Discharge	3.4798	0.68	Ratio to Peak	0.43		
W1440	147.5316	68.547	0	2.978365	4.16784	Discharge	1.8451	0.68	Ratio to Peak	0.43		
W1430	239.8291	57.276	0	1.74733	8.563205	Discharge	2.1947	0.68	Ratio to Peak	0.43		
W1420	236.4937	57.619	0	3.59008	7.27871	Discharge	3.7752	0.68	Ratio to Peak	0.43		
W1410	250.6392	56.194	0	3.051555	7.96214	Discharge	1.58	0.68	Ratio to Peak	0.43		
W1400	263.0063	55.005	0	3.338075	3.547205	Discharge	0.69248	0.68	Ratio to Peak	0.43		
W1390	125.3782	71.945	0	1.4872	7.947985	Discharge	4.4229	0.68	Ratio to Peak	0.43		
W1380	118.8987	73.003	0	3.33216	3.82831	Discharge	1.9237	0.68	Ratio to Peak	0.43		
W1370	108.2215	74.817	0	1.605045	2.37215	Discharge	0.31834	0.68	Ratio to Peak	0.43		
W1360	114.8797	73.676	0	0.9945	3.162455	Discharge	0.14838	0.68	Ratio to Peak	0.43		



Basin Number	SCS Curve Number Loss			Clark Unit Hydrograph Transform		Recession Baseflow				
	Initial Abstraction (mm)	Curve Number	Impervious (%)	Time of Concentration (HR)	Storage Coefficient (HR)	Initial Type	Initial Discharge (M <sup>3</sup> /S)	Recession Constant	Threshold Type	Ratio to Peak
W1350	304.3418	51.372	0	1.325805	6.11914	Discharge	2.1812	0.68	Ratio to Peak	0.43
W1340	282.6646	53.215	0	2.56542	8.509055	Discharge	2.2927	0.68	Ratio to Peak	0.43
W1330	95.361	77.125	0	3.567395	2.060075	Discharge	1.8258	0.68	Ratio to Peak	0.43
W1320	255.1456	55.755	0	0.863655	6.66938	Discharge	1.637	0.68	Ratio to Peak	0.43
W1310	227.3165	58.582	0	2.796105	5.70095	Discharge	2.4037941	0.68	Ratio to Peak	0.43
W1300	286.1582	52.91	0	2.390115	10.279	Discharge	7.0724	0.68	Ratio to Peak	0.43
W1290	225.462	58.781	0	4.309435	5.42811	Discharge	2.8313	0.68	Ratio to Peak	0.43
W1280	149.8228	68.213	0	2.275715	2.202005	Discharge	0.15076	0.68	Ratio to Peak	0.43
W1270	257.5127	55.527	0	0.923195	3.984775	Discharge	1.5186	0.68	Ratio to Peak	0.43
W1260	110.8338	74.36496	0	1.67063	6.438625	Discharge	5.5874	0.68	Ratio to Peak	0.43
W1250	249.1139	56.344	0	2.699385	11.48455	Discharge	1.8709	0.68	Ratio to Peak	0.43
W1240	275.1646	53.884	0	4.814745	12.596	Discharge	2.5244	0.68	Ratio to Peak	0.43
W1230	301.3608	51.618	0	5.28099	3.033445	Discharge	0.14576	0.68	Ratio to Peak	0.43
W1220	234.3038	57.846	0	1.271725	9.04324	Discharge	0.52995	0.68	Ratio to Peak	0.43
W1210	264.2292	54.89	0	3.791385	8.261295	Discharge	3.356	0.68	Ratio to Peak	0.43
W1200	300.2848	51.708	0	3.463525	9.28682	Discharge	0.82637	0.68	Ratio to Peak	0.43
W1190	106.5253	75.114	0	3.893435	3.04741	Discharge	0.79029	0.68	Ratio to Peak	0.43
W1180	39.739	58.687	0	1.27764	7.598385	Discharge	2.987	0.68	Ratio to Peak	0.43
W1170	39.739	72.98	0	3.185585	5.32437	Discharge	1.1047	0.68	Ratio to Peak	0.43
W1160	39.739	48.725	0	2.23223	11.121	Discharge	4.9963	0.68	Ratio to Peak	0.43
W1150	39.739	55.928	0	4.66232	5.417375	Discharge	1.7544	0.68	Ratio to Peak	0.43
W1140	39.739	59.246	0	5.1714	12.3348	Discharge	5.9268	0.68	Ratio to Peak	0.43
W1130	39.739	57.247	0	3.380715	8.063695	Discharge	4.1452	0.68	Ratio to Peak	0.43
W1120	39.739	63.556	0	3.33723	7.96005	Discharge	4.1559	0.68	Ratio to Peak	0.43
W1110	39.739	76.029	0	1.66738	3.97708	Discharge	1.7968	0.68	Ratio to Peak	0.43

Basin Num-ber	SCS Curve Number Loss			Clark Unit Hydrograph Trans-form			Recession Baseflow				
	Initial Abstraction (mm)	Curve Number	Impervious (%)	Time of Concentration (HR)	Storage Coefficient (HR)	Initial Type	Initial Discharge (M3/S)	Recession Constant	Threshold Type	Ratio to Peak	
W1100	39.739	76.014	0	1.30819	3.120275	Discharge	0.79478	0.68	Ratio to Peak	0.43	
W1090	39.739	63.255	0	1.817205	4.334565	Discharge	1.4347	0.68	Ratio to Peak	0.43	
W1080	39.739	59.347	0	2.452385	5.84953	Discharge	4.4564	0.68	Ratio to Peak	0.43	
W1070	39.739	78.594	0	0.71825	1.713135	Discharge	0.45	0.945	Ratio to Peak	0.43	
W1060	39.739	50.136	0	5.69426	13.58215	Discharge	0.45	0.945	Ratio to Peak	0.43	
W1050	39.739	83.52	0	2.04698	4.88262	Discharge	0.45	0.945	Ratio to Peak	0.43	
W1040	39.739	89	0	0.166348	0.396777	Discharge	0.45	0.945	Ratio to Peak	0.43	
W1030	39.739	85.352	0	1.770405	4.222845	Discharge	0.45	0.945	Ratio to Peak	0.43	
W1020	39.739	83.121	0	1.29454	3.087785	Discharge	0.45	0.945	Ratio to Peak	0.43	
W1010	39.739	64.188	0	2.139085	5.102165	Discharge	0.45	0.945	Ratio to Peak	0.43	
W1000	39.739	83.305	0	1.713855	4.08804	Discharge	0.45	0.945	Ratio to Peak	0.43	
W990	235.0506	57.768	0	18.361	14.59865	Discharge	0.45	0.945	Ratio to Peak	0.43	
W980	222.7532	59.073	0	6.120465	5.675965	Discharge	0.45	0.945	Ratio to Peak	0.43	
W970	58.847	84.529	0	2.379585	2.209985	Discharge	0.45	0.945	Ratio to Peak	0.43	
W960	68.905	82.352	0	0.92651	8.992035	Discharge	0.45	0.945	Ratio to Peak	0.43	
W950	92.196	77.715	0	3.76987	4.712855	Discharge	0.45	0.945	Ratio to Peak	0.43	
W940	63.747	83.454	0	1.97587	3.29118	Discharge	0.45	0.945	Ratio to Peak	0.43	
W930	81.133	79.851	0	1.37982	6.237225	Discharge	0.45	0.945	Ratio to Peak	0.43	

**Annex 10. Ulot Model Reach Parameters**

Table A-10.1. Ulot Model Reach Parameters

Reach Number	Muskingum Cunge Channel Routing						
	Time Step Method	Length (m)	Slope	Manning's n	Shape	Width	Side Slope
R20	Automatic Fixed Interval	4130.3	1.84E-05	0.04	Trapezoid	82.804	1
R30	Automatic Fixed Interval	2497	1.84E-05	0.04	Trapezoid	92.41	1
R50	Automatic Fixed Interval	7809.7	5.94E-05	0.04	Trapezoid	7.844	1
R60	Automatic Fixed Interval	197.99	1.84E-05	0.04	Trapezoid	9.61	1
R110	Automatic Fixed Interval	1733.7	1.84E-05	0.04	Trapezoid	60.686	1
R130	Automatic Fixed Interval	9402.9	0.001582	0.04	Trapezoid	15.464	1
R140	Automatic Fixed Interval	1672.5	0.006548	0.04	Trapezoid	9.44	1
R180	Automatic Fixed Interval	4481.4	1.84E-05	0.04	Trapezoid	33.958	1
R190	Automatic Fixed Interval	4229.3	0.002471	0.04	Trapezoid	7.874	1
R200	Automatic Fixed Interval	3329.5	0.000897	0.04	Trapezoid	41.012	1
R220	Automatic Fixed Interval	438.41	0.017319	0.04	Trapezoid	30.018	1
R230	Automatic Fixed Interval	70.711	1.84E-05	0.04	Trapezoid	31.742	1
R240	Automatic Fixed Interval	268.7	0.046163	0.04	Trapezoid	21.988	1
R250	Automatic Fixed Interval	2836.1	0.006505	0.04	Trapezoid	7.918	1
R290	Automatic Fixed Interval	570.83	0.018326	0.04	Trapezoid	22.866	1
R340	Automatic Fixed Interval	197.99	0.003153	0.04	Trapezoid	6.994	1
R380	Automatic Fixed Interval	353.55	1.84E-05	0.04	Trapezoid	41.046	1
R400	Automatic Fixed Interval	3563.4	0.0083	0.04	Trapezoid	13.148	1
R420	Automatic Fixed Interval	5183.1	0.003146	0.04	Trapezoid	12.582	1
R430	Automatic Fixed Interval	10502	0.00918	0.04	Trapezoid	17.002	1
R440	Automatic Fixed Interval	3135.6	0.008989	0.04	Trapezoid	8.498	1
R480	Automatic Fixed Interval	6852	1.84E-05	0.04	Trapezoid	12.184	1
R500	Automatic Fixed Interval	2997.6	0.004477	0.04	Trapezoid	11.34	1
R520	Automatic Fixed Interval	5427	0.008111	0.04	Trapezoid	9.134	1
R530	Automatic Fixed Interval	1207.4	0.026027	0.04	Trapezoid	12.526	1
R540	Automatic Fixed Interval	1030.8	1.84E-05	0.04	Trapezoid	7.032	1
R580	Automatic Fixed Interval	9500.5	0.00177	0.04	Trapezoid	12.27	1
R600	Automatic Fixed Interval	4749	0.006266	0.04	Trapezoid	29.268	1
R640	Automatic Fixed Interval	2385	0.001392	0.04	Trapezoid	16.628	1
R660	Automatic Fixed Interval	3088.1	1.84E-05	0.04	Trapezoid	8.668	1
R670	Automatic Fixed Interval	4441.7	0.002344	0.04	Trapezoid	10.382	1
R700	Automatic Fixed Interval	2340.8	0.00385	0.04	Trapezoid	8.252	1
R720	Automatic Fixed Interval	42.426	1.84E-05	0.04	Trapezoid	20.79	1
R740	Automatic Fixed Interval	3697.5	0.001448	0.04	Trapezoid	6.104	1
R750	Automatic Fixed Interval	6685.6	0.006438	0.04	Trapezoid	4.462	1
R780	Automatic Fixed Interval	2192.2	1.84E-05	0.04	Trapezoid	29.89	1
R790	Automatic Fixed Interval	1163.7	1.84E-05	0.04	Trapezoid	3.508	1
R800	Automatic Fixed Interval	3226	0.003061	0.04	Trapezoid	14.454	1
R820	Automatic Fixed Interval	6839.2	0.00488	0.04	Trapezoid	44.072	1
R830	Automatic Fixed Interval	571.13	0.010741	0.04	Trapezoid	8.95	1
R840	Automatic Fixed Interval	7173.8	0.001004	0.04	Trapezoid	5.918	1
R850	Automatic Fixed Interval	1936.5	0.001953	0.04	Trapezoid	10.116	1

Reach Number	Muskingum Cunge Channel Routing						
	Time Step Method	Length (m)	Slope	Manning's n	Shape	Width	Side Slope
R860	Automatic Fixed Interval	1595.8	0.002607	0.04	Trapezoid	5.6	1
R870	Automatic Fixed Interval	6272.8	0.002586	0.04	Trapezoid	4.564	1
R900	Automatic Fixed Interval	1982.4	0.004155	0.04	Trapezoid	6.286	1



**Annex 11. Ulot Field Validation Points**

Table A-11.1. Ulot Field Validation Points

Pt. No.	Validation Coordinates		Model Var (m)	Validation Points (m)	Error	Event/Date	Rain Return/ Scenario
	Latitude	Longitude					
1	11.99782862	125.3569166	2.4	4.33	-1.93	Yolanda/November 8, 2013	2 year
2	11.99782862	125.3569166	1.7	4.33	-2.63	Ruby/December 6, 2014	5 year
3	11.99782862	125.3569166	1.4	4.33	-2.93	Low Pressure 2/January 9-10, 2017	2 year
4	11.99815828	125.357053	2.4	1.93	0.47	Yolanda/November 8, 2013	2 year
5	11.99815828	125.357053	1.7	1.93	-0.23	Ruby/December 6, 2014	5 year
6	11.99815828	125.357053	1.4	1.93	-0.53	Low Pressure 2/January 9-10, 2017	2 year
7	11.98912896	125.3813247	2.4	0.03	2.37	Yolanda/November 8, 2013	2 year
8	11.98912896	125.3813247	1.7	0.03	1.67	Ruby/December 6, 2014	5 year
9	11.98912896	125.3813247	1.4	0.03	1.37	Low Pressure 2/January 9-10, 2017	2 year
10	11.99868919	125.3574503	2.4	2.59	-0.19	Yolanda/November 8, 2013	2 year
11	11.99868919	125.3574503	1.7	2.59	-0.89	Ruby/December 6, 2014	5 year
12	11.99868919	125.3574503	1.4	2.59	-1.19	Low Pressure 2/January 9-10, 2017	2 year
13	11.99849239	125.3562836	2.4	1.52	0.88	Yolanda/November 8, 2013	2 year
14	11.99849239	125.3562836	1.7	1.52	0.18	Ruby/December 6, 2014	5 year
15	11.99849239	125.3562836	1.4	1.52	-0.12	Low Pressure 2/January 9-10, 2017	2 year
16	12.00030128	125.3611643	2.5	2.22	0.28	Yolanda/November 8, 2013	2 year
17	12.00030128	125.3611643	1.9	2.22	-0.32	Ruby/December 6, 2014	5 year
18	12.00030128	125.3611643	1.8	2.22	-0.42	Low Pressure 2/January 9-10, 2017	2 year
19	12.00104023	125.3566547	2.5	2.02	0.48	Yolanda/November 8, 2013	2 year
20	12.00104023	125.3566547	1.9	2.02	-0.12	Ruby/December 6, 2014	5 year
21	12.00104023	125.3566547	1.8	2.02	-0.22	Low Pressure 2/January 9-10, 2017	2 year
22	12.00596049	125.3661735	2.5	4.22	-1.72	Yolanda/November 8, 2013	2 year
23	12.00596049	125.3661735	1.9	4.22	-2.32	Ruby/December 6, 2014	5 year
24	12.00596049	125.3661735	1.8	4.22	-2.42	Low Pressure 2/January 9-10, 2017	2 year
25	12.00155371	125.3717402	2.5	0.07	2.43	Yolanda/November 8, 2013	2 year
26	12.00155371	125.3717402	1.9	0.07	1.83	Ruby/December 6, 2014	5 year
27	12.00155371	125.3717402	1.8	0.07	1.73	Low Pressure 2/January 9-10, 2017	2 year
28	11.98410728	125.3626445	2.5	0.20	2.30	Yolanda/November 8, 2013	2 year
29	11.98410728	125.3626445	2.2	0.20	2.00	Ruby/December 6, 2014	5 year
30	11.98410728	125.3626445	1.6	0.20	1.40	Low Pressure 2/January 9-10, 2017	2 year
31	11.98474741	125.3622098	2.5	0.03	2.47	Yolanda/November 8, 2013	2 year
32	11.98474741	125.3622098	2.2	0.03	2.17	Ruby/December 6, 2014	5 year
33	11.98474741	125.3622098	1.6	0.03	1.57	Low Pressure 2/January 9-10, 2017	2 year
34	11.98516231	125.3611637	2.5	0.13	2.37	Yolanda/November 8, 2013	2 year

35	11.98516231	125.3611637	2.2	0.13	2.07	Ruby/December 6, 2014	5 year
36	11.98516231	125.3611637	1.6	0.13	1.47	Low Pressure 2/January 9-10, 2017	2 year
37	11.9855265	125.3618792	2.5	0.43	2.07	Yolanda/November 8, 2013	2 year
38	11.9855265	125.3618792	2.2	0.43	1.77	Ruby/December 6, 2014	5 year
39	11.9855265	125.3618792	1.6	0.43	1.17	Low Pressure 2/January 9-10, 2017	2 year
40	11.98603746	125.362099	2.5	2.16	0.34	Yolanda/November 8, 2013	2 year
41	11.98603746	125.362099	2.2	2.16	0.04	Ruby/December 6, 2014	5 year
42	11.98603746	125.362099	1.6	2.16	-0.56	Low Pressure 2/January 9-10, 2017	2 year
43	11.98462101	125.3596631	2.5	0.07	2.43	Yolanda/November 8, 2013	2 year
44	11.98462101	125.3596631	2.2	0.07	2.13	Ruby/December 6, 2014	5 year
45	11.98462101	125.3596631	1.6	0.07	1.53	Low Pressure 2/January 9-10, 2017	2 year
46	11.98505921	125.3593306	2.5	0.06	2.44	Yolanda/November 8, 2013	2 year
47	11.98505921	125.3593306	2.2	0.06	2.14	Ruby/December 6, 2014	5 year
48	11.98505921	125.3593306	1.6	0.06	1.54	Low Pressure 2/January 9-10, 2017	2 year
49	11.9857208	125.358703	2.5	1.88	0.62	Yolanda/November 8, 2013	2 year
50	11.9857208	125.358703	2.2	1.88	0.32	Ruby/December 6, 2014	5 year
51	11.9857208	125.358703	1.6	1.88	-0.28	Low Pressure 2/January 9-10, 2017	2 year
52	11.9858529	125.359171	2.5	0.11	2.39	Yolanda/November 8, 2013	2 year
53	11.9858529	125.359171	2.2	0.11	2.09	Ruby/December 6, 2014	5 year
54	11.9858529	125.359171	1.6	0.11	1.49	Low Pressure 2/January 9-10, 2017	2 year
55	11.98628188	125.3596135	2.5	0.41	2.09	Yolanda/November 8, 2013	2 year
56	11.98628188	125.3596135	2.2	0.41	1.79	Ruby/December 6, 2014	5 year
57	11.98628188	125.3596135	1.6	0.41	1.19	Low Pressure 2/January 9-10, 2017	2 year
58	11.98634483	125.3585406	2.5	1.03	1.47	Yolanda/November 8, 2013	2 year
59	11.98634483	125.3585406	2.2	1.03	1.17	Ruby/December 6, 2014	5 year
60	11.98634483	125.3585406	1.6	1.03	0.57	Low Pressure 2/January 9-10, 2017	2 year
61	11.98641574	125.3591464	2.5	0.41	2.09	Yolanda/November 8, 2013	2 year
62	11.98641574	125.3591464	2.2	0.41	1.79	Ruby/December 6, 2014	5 year
63	11.98641574	125.3591464	1.6	0.41	1.19	Low Pressure 2/January 9-10, 2017	2 year
64	11.9867045	125.3595368	2.5	0.62	1.88	Yolanda/November 8, 2013	2 year
65	11.9867045	125.3595368	2.2	0.62	1.58	Ruby/December 6, 2014	5 year
66	11.9867045	125.3595368	1.6	0.62	0.98	Low Pressure 2/January 9-10, 2017	2 year
67	11.98690893	125.3590275	2.5	0.94	1.56	Yolanda/November 8, 2013	2 year
68	11.98690893	125.3590275	2.2	0.94	1.26	Ruby/December 6, 2014	5 year
69	11.98690893	125.3590275	1.6	0.94	0.66	Low Pressure 2/January 9-10, 2017	2 year
70	11.98608901	125.3603444	2.5	0.58	1.92	Yolanda/November 8, 2013	2 year
71	11.98608901	125.3603444	2.2	0.58	1.62	Ruby/December 6, 2014	5 year

72	11.98608901	125.3603444	1.6	0.58	1.02	Low Pressure 2/January 9-10, 2017	2 year
73	11.98682101	125.3601902	2.5	0.71	1.79	Yolanda/November 8, 2013	2 year
74	11.98682101	125.3601902	2.2	0.71	1.49	Ruby/December 6, 2014	5 year
75	11.98682101	125.3601902	1.6	0.71	0.89	Low Pressure 2/January 9-10, 2017	2 year
76	11.98731042	125.359289	2.5	0.90	1.60	Yolanda/November 8, 2013	2 year
77	11.98731042	125.359289	2.2	0.90	1.30	Ruby/December 6, 2014	5 year
78	11.98731042	125.359289	1.6	0.90	0.70	Low Pressure 2/January 9-10, 2017	2 year
79	11.98729198	125.3596859	2.5	0.89	1.61	Yolanda/November 8, 2013	2 year
80	11.98729198	125.3596859	2.2	0.89	1.31	Ruby/December 6, 2014	5 year
81	11.98729198	125.3596859	1.6	0.89	0.71	Low Pressure 2/January 9-10, 2017	2 year
82	11.98773279	125.3595867	2.5	1.32	1.18	Yolanda/November 8, 2013	2 year
83	11.98773279	125.3595867	2.2	1.32	0.88	Ruby/December 6, 2014	5 year
84	11.98773279	125.3595867	1.6	1.32	0.28	Low Pressure 2/January 9-10, 2017	2 year
85	11.98795047	125.3588424	2.5	0.95	1.55	Yolanda/November 8, 2013	2 year
86	11.98795047	125.3588424	2.2	0.95	1.25	Ruby/December 6, 2014	5 year
87	11.98795047	125.3588424	1.6	0.95	0.65	Low Pressure 2/January 9-10, 2017	2 year
88	11.98739961	125.3583851	2.5	5.49	-2.99	Yolanda/November 8, 2013	2 year
89	11.98739961	125.3583851	2.2	5.49	-3.29	Ruby/December 6, 2014	5 year
90	11.98739961	125.3583851	1.6	5.49	-3.89	Low Pressure 2/January 9-10, 2017	2 year
91	11.97149562	125.3647639	0	1.65	-1.65		
92	11.96240134	125.3583416	0	0.03	-0.03		
93	11.95963833	125.3562531	0	0.83	-0.83		
94	11.99518858	125.443352	0	0.03	-0.03		
95	11.99727961	125.4440567	0	0.26	-0.26		
96	11.99740408	125.4421973	0	0.03	-0.03		
97	11.99634679	125.4455984	0	0.32	-0.32		
98	11.99884971	125.4451495	0	0.11	-0.11		
99	12.00342212	125.3456137	3.4	4.24	-0.84	Yolanda/November 8, 2013	2 year
100	12.00342212	125.3456137	1.7	4.24	-2.54	Ruby/December 6, 2014	5 year
101	12.00342212	125.3456137	1.4	4.24	-2.84	Low Pressure 1/December 16-17, 2016	5 year
102	12.00407281	125.3461824	3.4	3.28	0.12	Yolanda/November 8, 2013	2 year
103	12.00407281	125.3461824	1.7	3.28	-1.58	Ruby/December 6, 2014	5 year
104	12.00407281	125.3461824	1.4	3.28	-1.88	Low Pressure 1/December 16-17, 2016	5 year
105	12.00842788	125.3503747	3.4	4.42	-1.02	Yolanda/November 8, 2013	2 year
106	12.00842788	125.3503747	1.7	4.42	-2.72	Ruby/December 6, 2014	5 year
107	12.00842788	125.3503747	1.4	4.42	-3.02	Low Pressure 1/December 16-17, 2016	5 year
108	12.00882141	125.3501172	3.4	2.73	0.67	Yolanda/November 8, 2013	2 year
109	12.00882141	125.3501172	1.7	2.73	-1.03	Ruby/December 6, 2014	5 year
110	12.00882141	125.3501172	1.4	2.73	-1.33	Low Pressure 1/December 16-17, 2016	5 year

111	12.00869568	125.3507738	3.4	2.85	0.55	Yolanda/November 8, 2013	2 year
112	12.00869568	125.3507738	1.7	2.85	-1.15	Ruby/December 6, 2014	5 year
113	12.00869568	125.3507738	1.4	2.85	-1.45	Low Pressure 1/December 16-17, 2016	5 year
114	12.00898142	125.351013	3.4	3.63	-0.23	Yolanda/November 8, 2013	2 year
115	12.00898142	125.351013	1.7	3.63	-1.93	Ruby/December 6, 2014	5 year
116	12.00898142	125.351013	1.4	3.63	-2.23	Low Pressure 1/December 16-17, 2016	5 year
117	11.9968212	125.3601406	3.4	3.86	-0.46	Yolanda/November 8, 2013	2 year
118	11.9968212	125.3601406	1.7	3.86	-2.16	Ruby/December 6, 2014	5 year
119	11.9968212	125.3601406	1.4	3.86	-2.46	Low Pressure 1/December 16-17, 2016	5 year
120	11.99690779	125.3595612	3.4	3.40	0.00	Yolanda/November 8, 2013	2 year
121	11.99690779	125.3595612	1.7	3.40	-1.70	Ruby/December 6, 2014	5 year
122	11.99690779	125.3595612	1.4	3.40	-2.00	Low Pressure 1/December 16-17, 2016	5 year
123	11.99744808	125.3593717	3.4	3.75	-0.35	Yolanda/November 8, 2013	2 year
124	11.99744808	125.3593717	1.7	3.75	-2.05	Ruby/December 6, 2014	5 year
125	11.99744808	125.3593717	1.4	3.75	-2.35	Low Pressure 1/December 16-17, 2016	5 year
126	11.99723829	125.3585554	3.4	3.29	0.11	Yolanda/November 8, 2013	2 year
127	11.99723829	125.3585554	1.7	3.29	-1.59	Ruby/December 6, 2014	5 year
128	11.99723829	125.3585554	1.4	3.29	-1.89	Low Pressure 1/December 16-17, 2016	5 year
129	11.99769787	125.3584954	3.4	3.40	0.00	Yolanda/November 8, 2013	2 year
130	11.99769787	125.3584954	1.7	3.40	-1.70	Ruby/December 6, 2014	5 year
131	11.99769787	125.3584954	1.4	3.40	-2.00	Low Pressure 1/December 16-17, 2016	5 year
132	11.99743509	125.3580136	3.4	3.01	0.39	Yolanda/November 8, 2013	2 year
133	11.99743509	125.3580136	1.7	3.01	-1.31	Ruby/December 6, 2014	5 year
134	11.99743509	125.3580136	1.4	3.01	-1.61	Low Pressure 1/December 16-17, 2016	5 year
135	11.99769736	125.3574789	3.4	2.88	0.52	Yolanda/November 8, 2013	2 year
136	11.99769736	125.3574789	1.7	2.88	-1.18	Ruby/December 6, 2014	5 year
137	11.99769736	125.3574789	1.4	2.88	-1.48	Low Pressure 1/December 16-17, 2016	5 year
138	11.99794672	125.3579251	3.4	2.87	0.53	Yolanda/November 8, 2013	2 year
139	11.99794672	125.3579251	1.7	2.87	-1.17	Ruby/December 6, 2014	5 year
140	11.99794672	125.3579251	1.4	2.87	-1.47	Low Pressure 1/December 16-17, 2016	5 year
141	11.99842952	125.357909	3.4	2.96	0.44	Yolanda/November 8, 2013	2 year
142	11.99842952	125.357909	1.7	2.96	-1.26	Ruby/December 6, 2014	5 year
143	11.99842952	125.357909	1.4	2.96	-1.56	Low Pressure 1/December 16-17, 2016	5 year
144	11.99528622	125.4495078	0	0.03	-0.03		
145	11.99543282	125.4503003	0	0.03	-0.03		
146	11.99587832	125.4503638	0	0.13	-0.13		
147	11.99612299	125.4503203	0	0.03	-0.03		



148	11.99611276	125.4506809	0	Not Covered On Map			
149	11.99717232	125.448296	0.5	0.04	0.46	Yolanda/November 8, 2013	2 year
150	11.99717232	125.448296	0.3	0.04	0.26	Ruby/December 6, 2014	5 year
151	11.99717232	125.448296	0.3	0.04	0.26	Low Pressure 1/December 16-17, 2016	5 year
152	11.99881626	125.4482921	0.5	0.04	0.46	Yolanda/November 8, 2013	2 year
153	11.99881626	125.4482921	0.3	0.04	0.26	Ruby/December 6, 2014	5 year
154	11.99881626	125.4482921	0.3	0.04	0.26	Low Pressure 1/December 16-17, 2016	5 year
155	11.99761279	125.4486931	0.5	0.03	0.47	Yolanda/November 8, 2013	2 year
156	11.99761279	125.4486931	0.3	0.03	0.27	Ruby/December 6, 2014	5 year
157	11.99761279	125.4486931	0.3	0.03	0.27	Low Pressure 1/December 16-17, 2016	5 year
158	11.99746703	125.4491647	0.5	0.03	0.47	Yolanda/November 8, 2013	2 year
159	11.99746703	125.4491647	0.3	0.03	0.27	Ruby/December 6, 2014	5 year
160	11.99746703	125.4491647	0.3	0.03	0.27	Low Pressure 1/December 16-17, 2016	5 year
161	11.99741883	125.4478844	0.5	0.09	0.41	Yolanda/November 8, 2013	2 year
162	11.99741883	125.4478844	0.3	0.09	0.21	Ruby/December 6, 2014	5 year
163	11.99741883	125.4478844	0.3	0.09	0.21	Low Pressure 1/December 16-17, 2016	5 year
164	11.99765068	125.4471354	0.5	0.10	0.40	Yolanda/November 8, 2013	2 year
165	11.99765068	125.4471354	0.3	0.10	0.20	Ruby/December 6, 2014	5 year
166	11.99765068	125.4471354	0.3	0.10	0.20	Low Pressure 1/December 16-17, 2016	5 year
167	11.99746979	125.4467769	0.5	0.05	0.45	Yolanda/November 8, 2013	2 year
168	11.99746979	125.4467769	0.3	0.05	0.25	Ruby/December 6, 2014	5 year
169	11.99746979	125.4467769	0.3	0.05	0.25	Low Pressure 1/December 16-17, 2016	5 year
170	11.9970973	125.4462066	0.5	0.19	0.31	Yolanda/November 8, 2013	2 year
171	11.9970973	125.4462066	0.3	0.19	0.11	Ruby/December 6, 2014	5 year
172	11.9970973	125.4462066	0.3	0.19	0.11	Low Pressure 1/December 16-17, 2016	5 year
173	11.99692061	125.4450528	0.5	0.55	-0.05	Yolanda/November 8, 2013	2 year
174	11.99692061	125.4450528	0.3	0.55	-0.25	Ruby/December 6, 2014	5 year
175	11.99692061	125.4450528	0.3	0.55	-0.25	Low Pressure 1/December 16-17, 2016	5 year
176	11.99773357	125.4460546	0.5	0.03	0.47	Yolanda/November 8, 2013	2 year
177	11.99773357	125.4460546	0.3	0.03	0.27	Ruby/December 6, 2014	5 year
178	11.99773357	125.4460546	0.3	0.03	0.27	Low Pressure 1/December 16-17, 2016	5 year
179	11.99786559	125.4479418	0.5	0.06	0.44	Yolanda/November 8, 2013	2 year
180	11.99786559	125.4479418	0.3	0.06	0.24	Ruby/December 6, 2014	5 year
181	11.99786559	125.4479418	0.3	0.06	0.24	Low Pressure 1/December 16-17, 2016	5 year
182	11.99876706	125.4458898	0.3	0.11	0.19	Yolanda/November 8, 2013	2 year
183	11.99876706	125.4458898	0.2	0.11	0.09	Ruby/December 6, 2014	5 year

184	11.99876706	125.4458898	0.1	0.11	-0.01	Low Pressure 1/December 16-17, 2016	5 year
185	11.99904978	125.4466452	0.3	0.10	0.20	Yolanda/November 8, 2013	2 year
186	11.99904978	125.4466452	0.2	0.10	0.10	Ruby/December 6, 2014	5 year
187	11.99904978	125.4466452	0.1	0.10	0.00	Low Pressure 1/December 16-17, 2016	5 year
188	11.99849063	125.4467404	0.3	0.14	0.16	Yolanda/November 8, 2013	2 year
189	11.99849063	125.4467404	0.2	0.14	0.06	Ruby/December 6, 2014	5 year
190	11.99849063	125.4467404	0.1	0.14	-0.04	Low Pressure 1/December 16-17, 2016	5 year
191	11.999318	125.4462466	0.3	0.10	0.20	Yolanda/November 8, 2013	2 year
192	11.999318	125.4462466	0.2	0.10	0.10	Ruby/December 6, 2014	5 year
193	11.999318	125.4462466	0.1	0.10	0.00	Low Pressure 1/December 16-17, 2016	5 year
194	11.99928607	125.4470548	0.3	0.09	0.21	Yolanda/November 8, 2013	2 year
195	11.99928607	125.4470548	0.2	0.09	0.11	Ruby/December 6, 2014	5 year
196	11.99928607	125.4470548	0.1	0.09	0.01	Low Pressure 1/December 16-17, 2016	5 year
197	11.99821662	125.4452652	0.3	0.29	0.01	Yolanda/November 8, 2013	2 year
198	11.99821662	125.4452652	0.2	0.29	-0.09	Ruby/December 6, 2014	5 year
199	11.99821662	125.4452652	0.1	0.29	-0.19	Low Pressure 1/December 16-17, 2016	5 year
200	11.99865432	125.4454795	0.3	0.13	0.17	Yolanda/November 8, 2013	2 year
201	11.99865432	125.4454795	0.2	0.13	0.07	Ruby/December 6, 2014	5 year
202	11.99865432	125.4454795	0.1	0.13	-0.03	Low Pressure 1/December 16-17, 2016	5 year
203	11.99917308	125.4475357	0.3	0.09	0.21	Yolanda/November 8, 2013	2 year
204	11.99917308	125.4475357	0.2	0.09	0.11	Ruby/December 6, 2014	5 year
205	11.99917308	125.4475357	0.1	0.09	0.01	Low Pressure 1/December 16-17, 2016	5 year
206	11.99882951	125.447417	0.3	0.09	0.21	Yolanda/November 8, 2013	2 year
207	11.99882951	125.447417	0.2	0.09	0.11	Ruby/December 6, 2014	5 year
208	11.99826339	125.44755	0.3	0.10	0.20	Yolanda/November 8, 2013	2 year
209	11.99826339	125.44755	0.2	0.10	0.10	Ruby/December 6, 2014	5 year
210	11.99883051	125.4479486	0.3	0.08	0.22	Yolanda/November 8, 2013	2 year
211	11.99883051	125.4479486	0.2	0.08	0.12	Ruby/December 6, 2014	5 year
212	11.99832927	125.4484611	0.3	0.05	0.25	Yolanda/November 8, 2013	2 year
213	11.99832927	125.4484611	0.2	0.05	0.15	Ruby/December 6, 2014	5 year
214	11.9994066	125.4480614	0.3	0.09	0.21	Yolanda/November 8, 2013	2 year
215	11.9994066	125.4480614	0.2	0.09	0.11	Ruby/December 6, 2014	5 year
216	11.99865801	125.4489901	0.3	0.03	0.27	Yolanda/November 8, 2013	2 year
217	11.99865801	125.4489901	0.2	0.03	0.17	Ruby/December 6, 2014	5 year
218	11.99936251	125.449181	0.3	Not Covered on Map		Yolanda/November 8, 2013	2 year
219	11.99936251	125.449181	0.2	Not Covered on Map		Ruby/December 6, 2014	5 year

220	11.99911407	125.4496654	0.3	Not Covered on Map		Yolanda/November 8, 2013	2 year
221	11.99911407	125.4496654	0.2	Not Covered on Map		Ruby/December 6, 2014	5 year
222	11.99964012	125.4475276	0.3	0.08	0.22	Yolanda/November 8, 2013	2 year
223	11.99964012	125.4475276	0.2	0.08	0.12	Ruby/December 6, 2014	5 year
224	11.99970064	125.4445026	0.3	0.08	0.22	Yolanda/November 8, 2013	2 year
225	11.99970064	125.4445026	0.2	0.08	0.12	Ruby/December 6, 2014	5 year
226	11.99977222	125.445051	0.3	0.10	0.20	Yolanda/November 8, 2013	2 year
227	11.99977222	125.445051	0.2	0.10	0.10	Ruby/December 6, 2014	5 year
228	12.00031084	125.4457677	0.3	0.08	0.22	Yolanda/November 8, 2013	2 year
229	12.00031084	125.4457677	0.2	0.08	0.12	Ruby/December 6, 2014	5 year
230	11.98135852	125.4323123	0	0.26	-0.26		
231	11.98105124	125.431995	0	0.28	-0.28		
232	11.98231188	125.4323047	0	0.26	-0.26		
233	11.98091302	125.4344394	0	0.05	-0.05		
234	11.98073717	125.4356454	0	0.09	-0.09		
235	11.98031128	125.4372601	0	0.19	-0.19		
236	11.98021699	125.4389911	0	0.19	-0.19		
237	11.98999389	125.443809	1	0.03	0.97	Low Pressure 1/December 16-17, 2016	5 year
238	11.98999389	125.443809	2.8	0.03	2.77	Ruby/December 6, 2014	5 year
239	11.98999389	125.443809	2.5	0.03	2.47	Yolanda/November 8, 2013	2 year
240	11.99027066	125.4441076	1	0.03	0.97	Low Pressure 1/December 16-17, 2016	5 year
241	11.99027066	125.4441076	2.8	0.03	2.77	Ruby/December 6, 2014	5 year
242	11.99027066	125.4441076	2.5	0.03	2.47	Yolanda/November 8, 2013	2 year
243	11.9894784	125.444139	1	0.03	0.97	Low Pressure 1/December 16-17, 2016	5 year
244	11.9894784	125.444139	2.8	0.03	2.77	Ruby/December 6, 2014	5 year
245	11.9894784	125.444139	2.5	0.03	2.47	Yolanda/November 8, 2013	2 year
246	11.99056864	125.4427351	0	0.06	-0.06		
247	11.99088623	125.443326	0	0.03	-0.03		
248	11.99098589	125.4437953	0	0.03	-0.03		
249	11.99157329	125.443244	0	0.19	-0.19		
250	11.96390589	125.4339067	0	Not Covered on Map			
251	11.99408887	125.4446396	0.4	0.50	-0.10	Ruby/December 6, 2014	5 year
252	11.99411913	125.445221	0.4	0.03	0.37	Ruby/December 6, 2014	5 year
253	11.99433169	125.4468024	0.4	0.03	0.37	Ruby/December 6, 2014	5 year
254	11.99438073	125.4471928	0.4	0.03	0.37	Ruby/December 6, 2014	5 year
255	11.99497727	125.4474123	0	0.03	-0.03		
256	11.9951149	125.4466774	0	0.04	-0.04		
257	11.99456421	125.4478853	0	0.03	-0.03		
258	11.99513988	125.4479957	0	0.03	-0.03		
259	11.99499068	125.4483291	0	0.03	-0.03		

260	11.99582694	125.4466076	0	0.55	-0.55		
261	11.99550793	125.4470549	0	0.05	-0.05		
262	11.99565017	125.4472245	0	0.18	-0.18		
263	11.99571194	125.4477315	0	0.06	-0.06		
264	11.99566014	125.4484389	0	0.05	-0.05		
265	11.99593029	125.4488855	0.3	0.05	0.25	Low Pressure 1/December 16-17, 2016	5 year
266	11.99593029	125.4488855	0.5	0.05	0.45	Ruby/December 6, 2014	5 year
267	11.99593029	125.4488855	4	0.05	3.95	Yolanda/November 8, 2013	2 year
268	11.99632944	125.4482897	0.3	0.12	0.18	Low Pressure 1/December 16-17, 2016	5 year
269	11.99632944	125.4482897	0.5	0.12	0.38	Ruby/December 6, 2014	5 year
270	11.99632944	125.4482897	4	0.12	3.88	Yolanda/November 8, 2013	2 year
271	11.99633002	125.4472596	0.3	0.37	-0.07	Low Pressure 1/December 16-17, 2016	5 year
272	11.99633002	125.4472596	0.5	0.37	0.13	Ruby/December 6, 2014	5 year
273	11.99633002	125.4472596	4	0.37	3.63	Yolanda/November 8, 2013	2 year
274	11.99657318	125.4475958	0.3	0.15	0.15	Low Pressure 1/December 16-17, 2016	5 year
275	11.99657318	125.4475958	0.5	0.15	0.35	Ruby/December 6, 2014	5 year
276	11.99657318	125.4475958	4	0.15	3.85	Yolanda/November 8, 2013	2 year
277	11.99686311	125.4473624	0.3	0.09	0.21	Low Pressure 1/December 16-17, 2016	5 year
278	11.99686311	125.4473624	0.5	0.09	0.41	Ruby/December 6, 2014	5 year
279	11.99686311	125.4473624	4	0.09	3.91	Yolanda/November 8, 2013	2 year
280	11.99690418	125.4488574	0.3	0.05	0.25	Low Pressure 1/December 16-17, 2016	5 year
281	11.99690418	125.4488574	0.5	0.05	0.45	Ruby/December 6, 2014	5 year
282	11.99690418	125.4488574	4	0.05	3.95	Yolanda/November 8, 2013	2 year
283	11.99686278	125.4493213	0.3	0.04	0.26	Low Pressure 1/December 16-17, 2016	5 year
284	11.99686278	125.4493213	0.5	0.04	0.46	Ruby/December 6, 2014	5 year
285	11.99686278	125.4493213	4	0.04	3.96	Yolanda/November 8, 2013	2 year
286	11.99567967	125.4495775	0.3	0.05	0.25	Low Pressure 1/December 16-17, 2016	5 year
287	11.99567967	125.4495775	0.5	0.05	0.45	Ruby/December 6, 2014	5 year
288	11.99567967	125.4495775	4	0.05	3.95	Yolanda/November 8, 2013	2 year
289	11.99641401	125.4496204	0.3	0.05	0.25	Low Pressure 1/December 16-17, 2016	5 year
290	11.99641401	125.4496204	0.5	0.05	0.45	Ruby/December 6, 2014	5 year
291	11.99641401	125.4496204	4	0.05	3.95	Yolanda/November 8, 2013	2 year
292	11.9962255	125.4497881	0.3	0.05	0.25	Low Pressure 1/December 16-17, 2016	5 year
293	11.9962255	125.4497881	0.5	0.05	0.45	Ruby/December 6, 2014	5 year
294	11.9962255	125.4497881	4	0.05	3.95	Yolanda/November 8, 2013	2 year
295	11.9758962	125.4142285	1	0.04	0.97	Low Pressure 1/December 16-17, 2016	5 year
296	11.9758962	125.4142285	1.64	0.04	1.61	Ruby/December 6, 2014	5 year
297	11.9758962	125.4142285	1.2	0.04	1.17	Yolanda/November 8, 2013	2 year



298	11.95403117	125.4257274	0.5	Not Covered on Map		Low Pressure 1/December 16-17, 2016	5 year
299	11.95486718	125.4253029	0.5	Not Covered on Map		Low Pressure 1/December 16-17, 2016	5 year
300	11.95500732	125.4244936	0.5	Not Covered on Map		Ruby/December 6, 2014	5 year
301	11.95500732	125.4244936	0.5			Low Pressure 1/December 16-17, 2016	2 year
302	11.95500732	125.4244936	0.6			Low Pressure 1/December 16-17, 2016	5 year
303	11.95512023	125.4239058	0.5	Not Covered on Map		Ruby/December 6, 2014	5 year
304	11.95512023	125.4239058	0.5			Low Pressure 1/December 16-17, 2016	2 year
305	11.95512023	125.4239058	0.3			Low Pressure 1/December 16-17, 2016	5 year
306	11.95569774	125.4240798	0.5	Not Covered on Map		Ruby/December 6, 2014	5 year
307	11.95569774	125.4240798	0.5			Low Pressure 1/December 16-17, 2016	2 year
308	11.95569774	125.4240798	0.3			Low Pressure 1/December 16-17, 2016	5 year
309	11.95570688	125.4257964	0	Not Covered on Map			
310	11.95646896	125.4261007	0.5	Not Covered on Map		Ruby/December 6, 2014	5 year
311	11.95646896	125.4261007	0.5			Low Pressure 1/December 16-17, 2016	2 year
312	11.95672067	125.4252696	0.4	Not Covered on Map		Ruby/December 6, 2014	5 year
313	11.95672067	125.4252696	0.5			Low Pressure 1/December 16-17, 2016	2 year
314	11.95643317	125.4244442	0	Not Covered on Map			
315	11.95710288	125.4256726	0.4	Not Covered on Map		Low Pressure 1/December 16-17, 2016	2 year
316	11.95747571	125.4260437	0.5	Not Covered on Map		Ruby/December 6, 2014	5 year
317	11.95747571	125.4260437	0.5			Low Pressure 1/December 16-17, 2016	2 year
318	11.95757638	125.424988	0	Not Covered on Map			
319	11.9581787	125.4252599	0	Not Covered on Map			
320	11.96374387	125.434869	0.3	Not Covered on Map		Ruby/December 6, 2014	5 year
321	11.96490526	125.4348077	0.2	Not Covered on Map		Ruby/December 6, 2014	5 year
322	11.96444417	125.4352428	0.4	Not Covered on Map		Ruby/December 6, 2014	5 year

323	11.96493887	125.4358903	0.3	Not Covered on Map		Ruby/December 6, 2014	5 year
324	11.96540181	125.4356353	0.3	Not Covered on Map		Ruby/December 6, 2014	5 year
325	11.96536216	125.4366549	0.4	Not Covered on Map		Ruby/December 6, 2014	5 year
326	11.96640738	125.436136	0.3	Not Covered on Map		Ruby/December 6, 2014	5 year
327	11.97800316	125.4423105	0.3	0.04	0.27	Yolanda/November 8, 2013	2 year
328	11.97800316	125.4423105	0.5	0.04	0.47	Ruby/December 6, 2014	5 year
329	11.97954392	125.4423253	0.3	0.36	-0.06	Yolanda/November 8, 2013	2 year
330	11.97954392	125.4423253	0.5	0.36	0.14	Ruby/December 6, 2014	5 year
331	11.98034699	125.4417602	0.3	0.29	0.01	Yolanda/November 8, 2013	2 year
332	11.98034699	125.4417602	0.5	0.29	0.21	Ruby/December 6, 2014	5 year
333	11.9815917	125.4417126	0.3	0.07	0.23	Yolanda/November 8, 2013	2 year
334	11.9815917	125.4417126	0.5	0.07	0.43	Ruby/December 6, 2014	5 year
335	11.98653476	125.4408677	0.4	0.10	0.30	Low Pressure 2/January 9-10, 2017	2 year
336	11.98741939	125.4412154	0.4	0.12	0.28	Low Pressure 2/January 9-10, 2017	2 year
337	11.98776984	125.4423224	0.3	0.10	0.20	Low Pressure 2/January 9-10, 2017	2 year
338	11.98806974	125.4418762	0.4	0.08	0.32	Low Pressure 2/January 9-10, 2017	2 year
339	11.98785449	125.4433327	0.5	0.05	0.45	Low Pressure 2/January 9-10, 2017	2 year
340	11.9882533	125.4437296	0.4	0.05	0.35	Low Pressure 2/January 9-10, 2017	2 year
341	11.98845942	125.4432169	0.2	0.08	0.12	Low Pressure 2/January 9-10, 2017	2 year
342	11.98856561	125.442418	0	0.08	-0.08		
343	11.98913491	125.4425977	0	0.08	-0.08		
344	11.9896675	125.4432334	0	0.05	-0.05		
345	11.98925788	125.4437052	0.2	0.06	0.14	Low Pressure 2/January 9-10, 2017	2 year
346	11.97970779	125.4437511	0.5	0.07	0.43	Ruby/December 6, 2014	5 year
347	11.97970779	125.4437511	0.3	0.07	0.23	Yolanda/November 8, 2013	2 year
348	11.98061689	125.4038024	0.2	0.06	0.14	Ruby/December 6, 2014	5 year
349	11.98061689	125.4038024	0.1	0.06	0.04	Yolanda/November 8, 2013	2 year
350	11.98061689	125.4038024	0.1	0.06	0.04	Low Pressure 1/December 16-17, 2016	5 year
351	11.980348	125.4043486	0.2	0.92	-0.72	Ruby/December 6, 2014	5 year
352	11.980348	125.4043486	0.1	0.92	-0.82	Yolanda/November 8, 2013	2 year
353	11.980348	125.4043486	0.1	0.92	-0.82	Low Pressure 1/December 16-17, 2016	5 year
354	11.97959304	125.4052328	0.2	0.17	0.03	Ruby/December 6, 2014	5 year
355	11.97959304	125.4052328	0.1	0.17	-0.07	Yolanda/November 8, 2013	2 year

356	11.97959304	125.4052328	0.1	0.17	-0.07	Low Pressure 1/December 16-17, 2016	5 year
357	11.97997928	125.4058321	0.2	0.27	-0.07	Ruby/December 6, 2014	5 year
358	11.97997928	125.4058321	0.1	0.27	-0.17	Yolanda/November 8, 2013	2 year
359	11.97997928	125.4058321	0.1	0.27	-0.17	Low Pressure 1/December 16-17, 2016	5 year
360	11.98039267	125.4061587	0.2	0.41	-0.21	Ruby/December 6, 2014	5 year
361	11.98039267	125.4061587	0.1	0.41	-0.31	Yolanda/November 8, 2013	2 year
362	11.98039267	125.4061587	0.1	0.41	-0.31	Low Pressure 1/December 16-17, 2016	5 year
363	11.99073862	125.3822359	0.1	0.03	0.07	Low Pressure 1/December 16-17, 2016	5 year
364	11.99073862	125.3822359	1.64	0.03	1.61	Ruby/December 6, 2014	5 year
365	11.99073862	125.3822359	1.2	0.03	1.17	Yolanda/November 8, 2013	2 year
366	11.9901513	125.3822213	0.1	0.03	0.07	Low Pressure 1/December 16-17, 2016	5 year
367	11.9901513	125.3822213	1.64	0.03	1.61	Ruby/December 6, 2014	5 year
368	11.9901513	125.3822213	1.2	0.03	1.17	Yolanda/November 8, 2013	2 year
369	11.98974763	125.3818901	0.1	0.03	0.07	Low Pressure 1/December 16-17, 2016	5 year
370	11.98974763	125.3818901	1.64	0.03	1.61	Ruby/December 6, 2014	5 year
371	11.98974763	125.3818901	1.2	0.03	1.17	Yolanda/November 8, 2013	2 year
372	11.98951411	125.3811036	0.1	0.03	0.07	Low Pressure 1/December 16-17, 2016	5 year
373	11.98951411	125.3811036	1.64	0.03	1.61	Ruby/December 6, 2014	5 year
374	11.98951411	125.3811036	1.2	0.03	1.17	Yolanda/November 8, 2013	2 year
375	11.98947631	125.3803344	0.1	0.20	-0.10	Low Pressure 1/December 16-17, 2016	5 year
376	11.98947631	125.3803344	1.64	0.20	1.44	Ruby/December 6, 2014	5 year
377	11.98947631	125.3803344	1.2	0.20	1.00	Yolanda/November 8, 2013	2 year
378	11.98900776	125.380639	0.1	0.03	0.07	Low Pressure 1/December 16-17, 2016	5 year
379	11.98900776	125.380639	1.64	0.03	1.61	Ruby/December 6, 2014	5 year
380	11.98900776	125.380639	1.2	0.03	1.17	Yolanda/November 8, 2013	2 year
381	11.99884074	125.4057181	0.1	1.19	-1.09	Ruby/December 6, 2014	5 year
382	11.99884074	125.4057181	0.2	1.19	-0.99	Yolanda/November 8, 2013	2 year
383	12.00149621	125.4001866	0.1	0.05	0.05	Ruby/December 6, 2014	5 year
384	12.00149621	125.4001866	0.2	0.05	0.15	Yolanda/November 8, 2013	2 year
385	12.00224061	125.4009947	0.1	0.51	-0.41	Ruby/December 6, 2014	5 year
386	12.00224061	125.4009947	0.2	0.51	-0.31	Yolanda/November 8, 2013	2 year
387	12.00347434	125.4037962	0.1	0.03	0.07	Ruby/December 6, 2014	5 year
388	12.00347434	125.4037962	0.2	0.03	0.17	Yolanda/November 8, 2013	2 year
389	12.00277244	125.4042696	0.1	0.06	0.04	Ruby/December 6, 2014	5 year
390	12.00277244	125.4042696	0.2	0.06	0.14	Yolanda/November 8, 2013	2 year
391	11.99639389	125.411682	0.1	0.03	0.07	Ruby/December 6, 2014	5 year
392	11.99639389	125.411682	0.2	0.03	0.17	Yolanda/November 8, 2013	2 year
393	11.99468398	125.4171555	2.6	0.17	2.43	Low Pressure 1/December 16-17, 2016	5 year
394	11.99468398	125.4171555	3	0.17	2.83	Ruby/December 6, 2014	5 year
395	11.99468398	125.4171555	2.8	0.17	2.63	Yolanda/November 8, 2013	2 year

396	11.99532746	125.4186781	2.6	0.71	1.89	Low Pressure 1/December 16-17, 2016	5 year
397	11.99532746	125.4186781	3	0.71	2.29	Ruby/December 6, 2014	5 year
398	11.99532746	125.4186781	2.8	0.71	2.09	Yolanda/November 8, 2013	2 year
399	11.99481122	125.4189425	2.6	0.52	2.08	Low Pressure 1/December 16-17, 2016	5 year
400	11.99481122	125.4189425	3	0.52	2.48	Ruby/December 6, 2014	5 year
401	11.99481122	125.4189425	2.8	0.52	2.28	Yolanda/November 8, 2013	2 year
402	11.99565344	125.4195728	2.6	0.27	2.33	Low Pressure 1/December 16-17, 2016	5 year
403	11.99565344	125.4195728	3	0.27	2.73	Ruby/December 6, 2014	5 year
404	11.99565344	125.4195728	2.8	0.27	2.53	Yolanda/November 8, 2013	2 year
405	11.99617948	125.4195272	2.6	0.23	2.37	Low Pressure 1/December 16-17, 2016	5 year
406	11.99617948	125.4195272	3	0.23	2.77	Ruby/December 6, 2014	5 year
407	11.99617948	125.4195272	2.8	0.23	2.57	Yolanda/November 8, 2013	2 year
408	11.99649749	125.4205572	2.6	0.06	2.54	Low Pressure 1/December 16-17, 2016	5 year
409	11.99649749	125.4205572	3	0.06	2.94	Ruby/December 6, 2014	5 year
410	11.99649749	125.4205572	2.8	0.06	2.74	Yolanda/November 8, 2013	2 year
411	11.99588042	125.4200516	2.6	0.08	2.52	Low Pressure 1/December 16-17, 2016	5 year
412	11.99588042	125.4200516	3	0.08	2.92	Ruby/December 6, 2014	5 year
413	11.99588042	125.4200516	2.8	0.08	2.72	Yolanda/November 8, 2013	2 year
414	11.99662138	125.4199541	2.6	0.03	2.57	Low Pressure 1/December 16-17, 2016	5 year
415	11.99662138	125.4199541	3	0.03	2.97	Ruby/December 6, 2014	5 year
416	11.99662138	125.4199541	2.8	0.03	2.77	Yolanda/November 8, 2013	2 year
417	11.99710149	125.4203276	2.6	0.03	2.57	Low Pressure 1/December 16-17, 2016	5 year
418	11.99710149	125.4203276	3	0.03	2.97	Ruby/December 6, 2014	5 year
419	11.99710149	125.4203276	2.8	0.03	2.77	Yolanda/November 8, 2013	2 year
420	11.99922882	125.4245638	2.6	0.11	2.49	Low Pressure 1/December 16-17, 2016	5 year
421	11.99922882	125.4245638	3	0.11	2.89	Ruby/December 6, 2014	5 year
422	11.99922882	125.4245638	2.8	0.11	2.69	Yolanda/November 8, 2013	2 year
423	12.00201019	125.429009	0.1	0.09	0.01	Low Pressure 1/December 16-17, 2016	5 year
424	12.00201019	125.429009	0.1	0.09	0.01	Ruby/December 6, 2014	5 year
425	12.00201019	125.429009	0.1	0.09	0.01	Yolanda/November 8, 2013	5 year
426	12.00165857	125.4297341	0.1	0.09	0.01	Low Pressure 1/December 16-17, 2016	5 year
427	12.00165857	125.4297341	0.1	0.09	0.01	Ruby/December 6, 2014	5 year
428	12.00165857	125.4297341	0.1	0.09	0.01	Yolanda/November 8, 2013	2 year
429	12.00500311	125.4381271	0.1	0.07	0.03	Low Pressure 1/December 16-17, 2016	5 year
430	12.00500311	125.4381271	0.1	0.07	0.03	Ruby/December 6, 2014	5 year
431	12.00500311	125.4381271	0.1	0.07	0.03	Yolanda/November 8, 2013	2 year
432	12.00849568	125.4373211	0.1	0.08	0.02	Low Pressure 1/December 16-17, 2016	5 year



433	12.00849568	125.4373211	0.1	0.08	0.02	Ruby/December 6, 2014	5 year
434	12.00849568	125.4373211	0.1	0.08	0.02	Yolanda/November 8, 2013	2 year
435	12.01004634	125.4375316	0.1	0.05	0.05	Low Pressure 1/December 16-17, 2016	5 year
436	12.01004634	125.4375316	0.1	0.05	0.05	Ruby/December 6, 2014	5 year
437	12.01004634	125.4375316	0.1	0.05	0.05	Yolanda/November 8, 2013	2 year
438	11.98235672	125.4330117	0	0.16	-0.16		
439	11.98183159	125.4334859	0	0.13	-0.13		
440	11.98167301	125.4327218	0	0.24	-0.24		
441	11.98144234	125.4330742	0	0.14	-0.14		
442	11.98112777	125.4334205	0	0.08	-0.08		
443	11.98185397	125.4322444	0	0.26	-0.26		



